

https://dspace.org/

Characterization of coir fibre composites reinforced with CNT, glass flakes and clay particles

Kuppen, Nalen

2015-04-10
http://hdl.handle.net/10539/18371

Downloaded from a DSpace repository. https://dspace.org/

CHARACTERIZATION OF COIR FIBRE COMPOSITES REINFORCED WITH CNT, GLASS FLAKES AND CLAY PARTICLES

NALEN KUPPEN

A research report submitted to the Faculty of Engineering and the Built Environment, University of the Witwatersrand, Johannesburg, in partial fulfilment of the requirements for the degree of Master of Science in Engineering.

Johannesburg, 2015

Contents

ABSTRACT 6
ACKNOWLEDGEMENTS 8
LIST OF FIGURES 9
LIST OF TABLES 14
1 INTRODUCTION 15
1.1 Background 15
1.2 Purpose and justification of the study 16
1.3 Scope of work 18
1.4 Objectives 19
1.5 Flowchart of the process 20
2 LITERATURE REVIEW 21
2.1 Composite background 21
2.2 Polymer 23
2.3 Nano composite 24
2.4 Hybrid composites 25
2.5 Composite constituent materials 27
2.5.1 Polymer 27
2.5.2 Natural fibres 28
2.5.3 Coconut Fibre (Coir Fibre) 32
2.5.4 Glass 35
2.5.5 Carbon Nano Tubes (CNT) 36
2.5.6 Clay 37
2.5.7 Additional research 37
2.6 Fabrication methods used in composite applications 42

2.7 Conclusion 43
3 METHODOLOGY 44
3.1 Materials 44
3.1.1 Coir fibre 44
3.1.2 Epoxy 45
3.1.3 CNT 45
3.1.4 Glass spheres 46
3.1.5 Clay 46
3.1.6 Chemicals 47
3.2 Chemical Treatment Procedure 47
3.2.1 Coir Fibre Treatment 47
3.2.2 Functionalization 49
3.3 Fabrication Procedure 53
3.3.1 Manufacturing of the coir mat 53
3.3.2 Composite mould 55
3.3.3 Vacuum Resin Transfer Moulding (VRTM) 58
3.4 Fibre and hybrid composites fabrication procedure 61
3.5 Particulate composites 67
3.6 Mechanical testing procedures 68
3.6.1 Tensile Testing Procedure 68
3.6.2 Flexural Testing Procedure 70
3.6.3 Impact Testing Procedure 73
3.7 Morphological Characterization 75
4 RESULTS AND DISCUSSION 76
4.1 Epoxy-coir composites 76

4.1.1 Tensile Testing Results 78
4.1.2 Flexural Testing Results 81
4.1.3 Impact Testing Results 84
4.2 Functionalization 85
4.2.1 Functionalization of MWCNT 85
4.2.2 Functionalization of Clay 91
4.3 Particulate composites 99
4.3.1 CNT composites 99
4.3.2 Glass composites 99
4.3.3 Clay composites 104
4.4 Hybrid composites 108
4.4.1 Hybrid CNT composites 108
4.4.2 Hybrid-glass composites 115
4.4.3 Hybrid-clay composites 121
4.5 Summary 128
5 CONCLUSION AND RECOMMENDATIONS 132
REFERENCES 133
Appendix A – Sample testing specimens 142
Appendix B – Sample fractured specimens 149
Appendix C – Results of mechanical testing 155

DECLARATION

I declare that this Research Report is my own unaided work. It is being submitted to the Degree of Master of Science in Engineering to the University of the Witwatersrand, Johannesburg. It has not been submitted before for any degree or examination to any other University.

……

Nalen Kuppen

…….. day of …….., ……

ABSTRACT

Hybrid composites are composite materials used when a material is required that has more than one property benefit from its constituent materials. The current research involves the fabrication of hybrid composite materials from a type of natural fibre being coconut/ coir fibre, using vacuum resin transfer moulding (VRTM). Epoxy resin was selected as the base matrix that would be used. The second reinforcements used to fabricate the hybrid composites were carbon nanotubes (CNT), clay and glass spheres. The coir fibre was treated with Sodium Hydroxide (NaOH) to improve its bonding properties by removing the cellulose and lignin found on the cell walls. Composite specimens were fabricated using epoxy and coir fibre at 7%, 10%, 15% and 20% volume fractions. These composite specimens were then exposed to mechanical tests such as tensile, flexural and impact tests which indicated that a 15% volume fraction of coir fibre showed the optimal mechanical properties. Due to the VRTM process being a controlled process the processing conditions had to be varied to ensure that good quality composite specimens were fabricated. Functionalization was done on both the CNT and clay particles. Acid functionalization of CNT was done using Nitric acid (HNO_3) and Sulphuric acid (H_2SO_4) with the optimal functionalization time of 12 hours being selected. Clay functionalization was done using 3-Aminopropyltriethoxysilane at different ratios with the optimum ratio of 1g clay : 2g silane being used. To confirm that the functionalization treatment was successful Fourier Transform Infrared Spectroscopy (FTIR), Raman analysis and the Transmission Electron Microscope (TEM) was used. Hybrid composites were then fabricated using the optimal coir volume fraction with the CNT, glass and clay reinforcements respectively. These composite specimens were then exposed to mechanical tests such as tensile, flexural and impact tests to observe the properties of the hybrid composites. The CNT hybrid composites proved to exhibit good mechanical properties at a 1.5% weight fraction followed by glass with an 8% weight fraction and finally clay at a 4% weight fraction. Epoxy-clay and epoxy-glass composites were fabricated to observe the difference in properties between hybrid composites and normal composites. From the results obtained for the epoxy-clay and epoxy-glass composites, a 0.5% weight fraction

of reinforcement exhibited the best mechanical properties amongst both reinforcements. These composite specimens did not show an increase in properties in comparison to the hybrid composites with an average of a 10% reduction in properties as compared to the hybrid composites. A few of the test specimens had undergone an SEM analysis to observe what occurred during the fabrication and testing processes. The SEM analysis had shown that the specimens fabricated where of good quality and conditions such as agglomeration, fibre pull out, voids as well as interfacial adhesion were observed.

ACKNOWLEDGEMENTS

The author graciously acknowledges the support from the school of Mechanical, Aeronautical and Industrial Engineering for the provision of resources and the guidance offered by the staff. He would also like to thank the school of Mechanical, Aeronautical and Industrial Engineering workshop staff for all of the assistance and support provided during the duration of the research.

The author would also like to thank his Project Supervisor Dr Jacob Muthu for all of his assistance, support and guidance.

The assistance from Pratley South Africa for the supply of the clay used in the current research is graciously acknowledged.

The author would also like to thank his mother and sister for their love, support and encouragement.

A very big thank you goes to the author's wife for her support, love encouragement and motivation throughout the entire research.

LIST OF FIGURES

Figure 1.1 : Flowchart indicating the scope of the current research 20

Figure 2.1 : A picture of nano fibrils shown with a strand of human hair [14] 25

Figure 2.2 : Representation of a natural vegetable fibre [25] 29

Figure 2.3 : Coir fibre..... 32

Figure 2.4 : SEM image of coir fibre 33

Figure 3.1 : Coir Fibre..... 44

Figure 3.2 : SEM image of the coir fibre structure 44

Figure 3.3 : SEM image of CNT..... 46

Figure 3.4 : SEM image of clay 47

Figure 3.5 : Treating of the fibres with the NaOH solution..... 49

Figure 3.6 : Flowchart of the fibre treatment process 49

Figure 3.7 : Representation of what occurs during CNT functionalization [49] .. 50

Figure 3.8 : Flowchart representation of the MWCNT functionalization process 51

Figure 3.9 : Flowchart representation of the clay functionalization process 52

Figure 3.10 : Pipe mat rig in horizontal position 53

Figure 3.11 : Flowchart representation of the mat manufacturing process..... 54

Figure 3.12 : Fabricated mat to be used for composite specimens 55

Figure 3.13 : Schematic representation of the first mould used..... 56

Figure 3.14 : Male mould piece indicating gasket and resin injection/ discharge locations 56

Figure 3.15 : Female mould piece containing the spoiled specimen 57

Figure 3.16 : Schematic of the second mould used..... 58

Figure 3.17 : Setup of the system..... 60

Figure 3.18 : Schematic of the system 60

Figure 3.19 : G-clamps used to hold the male mould section in place 62

Figure 3.20 : An example of a fabricated composite specimen fabricated 64

Figure 3.21 : Flowchart representation of the composite fabrication process 65

Figure 3.22 : Tensile testing specimens 69

Figure 3.23 : Flexural testing specimens..... 71

Figure 3.24 : Flexural testing of composite specimens..... 72

Figure 3.25 : Impact testing specimens..... 74

Figure 4.1 : SEM image of a raw coir fibre 77

Figure 4.2 : SEM image of coir fibre treated with a 10% w/v NaOH solution..... 78

Figure 4.3 : SEM image of coir fibre treated with a 20% w/v NaOH solution..... 78

Figure 4.4 : Tensile strength of coir specimens 79

Figure 4.5 : Elastic modulus of coir specimens 80

Figure 4.6 : SEM image of the 15% coir tensile specimen..... 81

Figure 4.7 : SEM image of the 20% coir tensile specimen..... 81

Figure 4.8 : Flexural strength of coir specimens..... 82

Figure 4.9 : Tangent modulus of coir specimens 83

Figure 4.10 : SEM image of the 15% coir flexural specimen..... 83

Figure 4.11 : SEM image of the 20% coir flexural specimen..... 84

Figure 4.12 : Fracture toughness of coir specimens..... 85

Figure 4.13 : TEM image of Pristine MWCNT 86

Figure 4.14 : TEM image of MWCNT after 12 hours of functionalization..... 87

Figure 4.15 : TEM image of MWCNT after 48 hours of functionalization..... 87

Figure 4.16 : Raman spectroscopy of 12 hour functionalized CNT 89

Figure 4.17 : Raman spectroscopy of 48 hour functionalized CNT 89

Figure 4.18 : FTIR spectroscopy of CNT functionalized for 12 hours..... 90

Figure 4.19 : FTIR spectroscopy of CNT functionalized for 48 hours 90
Figure 4.20 : TEM image of raw clay 92
Figure 4.21 : TEM image of functionalized clay (1g clay : 2g silane) 93
Figure 4.22 : Schematic representation of the functionalization process of clay.. 93
Figure 4.23 : Raman spectroscopy of 1g clay : 1g silane 94
Figure 4.24 : Raman spectroscopy of 1g clay : 2g silane 95
Figure 4.25 : Raman spectroscopy of 1g clay : 5g silane 95
Figure 4.26 : FTIR Spectroscopy of 1g clay : 1g silane 97
Figure 4.27 : FTIR Spectroscopy of 1g clay : 2g silane 97
Figure 4.28 : FTIR Spectroscopy of 1g clay : 5g silane 98
Figure 4.29 : Tensile strength of glass composite specimens 100
Figure 4.30 : SEM image of the 0.5% glass tensile specimen 100
Figure 4.31 : SEM image of the 2% glass tensile specimen 101
Figure 4.32 : Elastic modulus of glass composite specimens 101
Figure 4.33 : Flexural strength of glass specimens 102
Figure 4.34 : SEM image of the 2% glass flexural specimen 102
Figure 4.35 : Tangent modulus of glass specimens 103
Figure 4.36 : Fracture toughness of glass specimens 103
Figure 4.37 : Tensile strength of clay composite specimens 104
Figure 4.38 : SEM image of the 0.5% clay tensile specimen 105
Figure 4.39 : Elastic modulus of clay composite specimens 105
Figure 4.40 : Flexural strength of clay specimens 106
Figure 4.41 : SEM image of the 0.5% clay flexural specimen 106
Figure 4.42 : Tangent modulus of clay specimens 107
Figure 4.43 : Fracture toughness of clay specimens 107

Figure 4.44 : SEM image of the 2% clay impact specimens 108
Figure 4.45 : Tensile strength of hybrid-CNT composite specimens 109
Figure 4.46 : Elastic modulus of hybrid-CNT composite specimens 110
Figure 4.47 : SEM image of the hybrid-1.5% CNT tensile specimen 111
Figure 4.48 : SEM image of the hybrid-2% CNT tensile specimen 111
Figure 4.49 : Flexural strength of hybrid-CNT specimens 112
Figure 4.50 : Tangent modulus of hybrid-CNT specimens..... 113
Figure 4.51 : SEM image of the hybrid-1.5% CNT flexural specimen 113
Figure 4.52 : Fracture toughness of hybrid-CNT specimens 114
Figure 4.53 : SEM image of the hybrid-0.5% CNT impact specimen..... 114
Figure 4.54 : Tensile strength of glass composite specimens 116
Figure 4.55 : SEM image of the hybrid-8% glass tensile specimen 116
Figure 4.56 : SEM image of the hybrid-12% glass tensile specimen 117
Figure 4.57 : Elastic modulus of hybrid-glass composite specimens 117
Figure 4.58 : Flexural strength of hybrid-glass specimens 118
Figure 4.59 : SEM image of the hybrid-8% glass flexural specimen 119
Figure 4.60 : SEM image of a hybrid-12% glass flexural specimen 119
Figure 4.61 : Tangent modulus of hybrid-glass specimens..... 120
Figure 4.62 : Fracture toughness of hybrid-glass specimens 121
Figure 4.63 : Tensile strength of hybrid-clay composite specimens..... 122
Figure 4.64 : SEM image of the hybrid-4% clay tensile specimen..... 123
Figure 4.65 : SEM image of the hybrid-5% clay tensile specimen..... 123
Figure 4.66 : Elastic modulus of clay composite specimens 124
Figure 4.67 : Flexural strength of clay specimens 125
Figure 4.68 : SEM image of the hybrid-5% clay flexural specimen..... 125

Figure 4.69 : Tangent modulus of clay specimens..... 126

Figure 4.70 : Fracture toughness of hybrid-clay specimens 126

Figure 4.71 : SEM image of the hybrid-0.1% clay impact specimen 127

Figure 4.72 : SEM image of the hybrid-4% clay impact specimen 127

Figure 4.73 : Tensile strength of hybrid-composite specimens 128

Figure 4.74 : Elastic modulus of hybrid-composite specimens 129

Figure 4.75 : Flexural strength of hybrid-composites..... 130

Figure 4.76 : Tangent modulus of hybrid-composites 130

Figure 4.77 : Fracture toughness of hybrid-composites..... 131

LIST OF TABLES

Table 2.1 : Properties of two commonly used thermosetting polymers..... 27

Table 2.1 : Properties of a few types of natural fibres [18, 23-24] 30

Table 2.2 : Mechanical properties of unidirectional aligned continuous fibre vs. randomly oriented short fibre composites in a polyester matrix [18, 23-24]..... 31

Table 3.1 : Properties of the coir fibre used..... 45

Table 3.2 : Properties of the epoxy resin used 45

Table 3.3 : Properties of the glass spheres used..... 46

Table 3.4 : Properties of the clay used 47

1 INTRODUCTION

1.1 Background

Over the years there has been a growing need for materials with improved mechanical properties such as tensile strength, elastic modulus, flexural strength, impact resistance, etc. Combined with the improved mechanical properties, there is also a need for improved physical properties such as a reduction in weight, corrosion resistance and being aesthetically pleasing. Most materials are not able to achieve good mechanical and physical properties simultaneously. The only way to obtain materials capable of having many improved properties, is by the combination of more than one material and is termed a composite material. A composite is a combination of two or more constituents to form a material with one or more significant properties superior to those of its components [1].

Composites consist of a matrix and reinforcement. The properties of composites can be influenced by many variables such as the in-situ component properties, reinforcement types, weight fraction of reinforcement and their geometry. Composites are commonly classified by the type of matrix used such as polymer, metal, carbon, ceramic or by their reinforcement types such as conventional or natural fibres, carbon and metal based nano-particles, which can be in different forms such as continuous fibres, discontinuous fibres, whiskers or particles [2].

Composites reinforced with fibres are anisotropic which indicate that their properties vary depending on the direction of the fibres. Fibre reinforced composites such as the polymer, metal and ceramic matrix composites do not exhibit plastic behaviour like metals, and these materials are sensitive to the formation of stress concentration areas [2].

Many different methods can be used to fabricate composites which include hand layup, open moulding, resin transfer moulding, vacuum resin transfer moulding, compression moulding, injection moulding and pultrusion. The choice of fabrication method is dependent on the materials of construction used to fabricate

the composite with the vacuum resin transfer moulding (VRTM) process being the most suitable method used for the fabrication of fibre composite materials [3].

Composite materials have a large range of applications which include the aerospace industry, internal combustion engines, machine components, automobiles, mechanical components, pressure vessels, marine structures, sports and leisure equipment, and many more [1-3].

1.2 Purpose and justification of the study

The uses of fibres as reinforcements with extraordinary properties have been largely responsible for the revolutionary improvements in composite materials as compared to conventional materials. The most common types of fibres used include glass, carbon, ceramic and organic fibres [4]. Glass fibre-reinforced plastic (FRP) composites are widely used in a wide variety of sectors. The use of fibre composites has grown over the years due to its most crucial property being its high strength to weight ratio. Glass fibres are widely used to reinforce plastics due to their low cost and fairly good mechanical properties [5].

Over the recent years attempts have been made to use natural fibre composites in place of glass composites due to their desirable properties which include low density, low cost, renewability and good mechanical properties. Natural fibres are abundantly available and environmentally friendly which makes them much more beneficial in comparison to glass fibres. Manufacturing sectors such as the automobile, packaging and construction sectors have been pressurized to utilize natural fibres in place of the traditional petroleum based fibres such as glass, carbon and aramid [6].

The major drawback in using natural fibres is that they are hydrophilic, and thus have poor resistance to water absorption. Water absorption leads to swelling of the fibres which tends to form voids and micro cracks at the fibre-matrix interface region and hence reduces the mechanical properties of the composite. To overcome this, both chemical and physical treatments are used to reduce the hydrophilic nature of the fibres and thus produce better composites [6]. Another

issue in using natural fibre composites is the fibre matrix adhesion, as the role of the matrix in a fibre reinforced composite is to transfer the load to the stiff fibres through the matrix-fibre interface. Poor adhesion at this interface means that the full capabilities of the composite cannot be achieved which leaves it vulnerable to failure, thus reducing its life span [1].

Natural fibre composites suffer from low modulus, low strength and relatively poor moisture resistance as compared to synthetic/ glass fibre reinforced composites [7]. Due to the reduced properties of natural fibre composites the current researcher wanted to investigate what would be the properties of a natural fibre hybrid composite. Previous researchers found that the hybridization of natural fibre with stronger and more corrosion resistant synthetic fibre such as glass or carbon fibre improved the strength, stiffness and moisture resistance of a composite [7-8]. With a hybrid composite being fabricated it was decided that a natural fibre with average to low properties should be used to ascertain if a suitable composite can be fabricated from a lower grade of natural fibre. Researchers noted that the performance of coir as a reinforcement is unsatisfactory and not comparable with other natural fibres [5, 8]. The structural characteristics and chemical composition of coir fibre makes the tensile strength and elastic modulus relatively low amongst natural fibres therefore also making coir fibre not suitable as natural fibre reinforcement [5]. Due to researchers not finding the use of coir fibre as a suitable composite reinforcement it was decided that coir fibre shall be the natural fibre used as one of the reinforcement types for the composite. Coir fibres are cheap and readily available natural fibres which are not brittle like glass fibres, they are amenable to chemical modification, non-toxic and possess no waste disposal problems. This is due to various factors such as the low cellulose content, high microfibrillar angle and their large and variable diameter [8]. There are numerous studies that discuss the mechanical properties of synthetic composite materials but only a few references are available on the mechanical properties of coir fibre composites [7]. This could be due to the reduced mechanical properties that researchers obtained with natural fibre composites.

To fabricate the hybrid composite additional reinforcement materials would need to be added to observe the properties obtained in comparison to the epoxy-coir composites. These additional reinforcements would not be in fibre form but would be particles. Glass has been used as a composite reinforcement for many years thus it was decided by the current researcher to fabricate hybrid composites that make use of glass flakes to observe the mechanical properties of these composites. Clay is an abundantly available material that has been used as a composite reinforcement for many years and thus was the second type of reinforcement selected. Many researchers have studied the use of carbon nanotubes (CNT) by creating various composite materials, however not much information is available on CNT hybrid composites using natural fibres. The current researcher decided to undertake research comparing glass, clay and CNT to observe the different mechanical properties of micro reinforcing particles which are glass and clay and nano particles being CNT to determine which reinforcement would be able to produce an optimum hybrid composite, if possible.

1.3 Scope of work

The scope of work for the current research is to observe the mechanical properties of coir fibre hybrid composites manufactured via vacuum resin transfer moulding (VRTM). This research is to first obtain which is the optimum volume fraction of coir fibre that can be added to an epoxy matrix to generate the best mechanical properties. Hybrid composites using the optimal coir fibre volume fraction are then to be manufactured using CNT, glass and clay to observe what weight fraction of reinforcement would generate the best mechanical properties in a hybrid composite, if possible.

1.4 Objectives

The main objective of the current research is to develop the best hybrid coir fibre composite material with improved mechanical properties (tensile, flexural and impact) amongst the second reinforcement types selected (CNT, glass and clay).

In order to achieve this objective the following is required:

- Determine what Sodium Hydroxide (NaOH) solution concentration should be used on the coir fibres to remove the lignin and cellulose on the fibres which would enable good bonding within the composite.
- The coir fibre is to be embedded in the composite in a mat form, suitable non-woven, uniformly distributed coir fibre mats need to be fabricated.
- In order for good bonding to take place between the second reinforcement types functionalization of both the CNT and clay particles needs to be done. To determine if the functionalization of the particles are successful they would undergo TEM, Raman, and FTIR analysis.
- To fabricate good composite test specimens a VRTM process needs to be set up and tested.
- Evaluate what optimum volume fraction of coir fibre would produce the best mechanical properties after being subjected to tensile, flexural and impact tests.
- Evaluate what optimum volume fraction of glass and clay would produce the best mechanical properties in an epoxy composite after being subjected to tensile, flexural and impact tests.
- Evaluate what optimum volume fraction of CNT, glass and clay would produce the best mechanical properties in a hybrid composite after being subjected to tensile, flexural and impact tests.

The results from the investigation is to be compared and analysed

A schematic representation of the proposed method is shown Figure 1.1.

1.5 Flowchart of the process

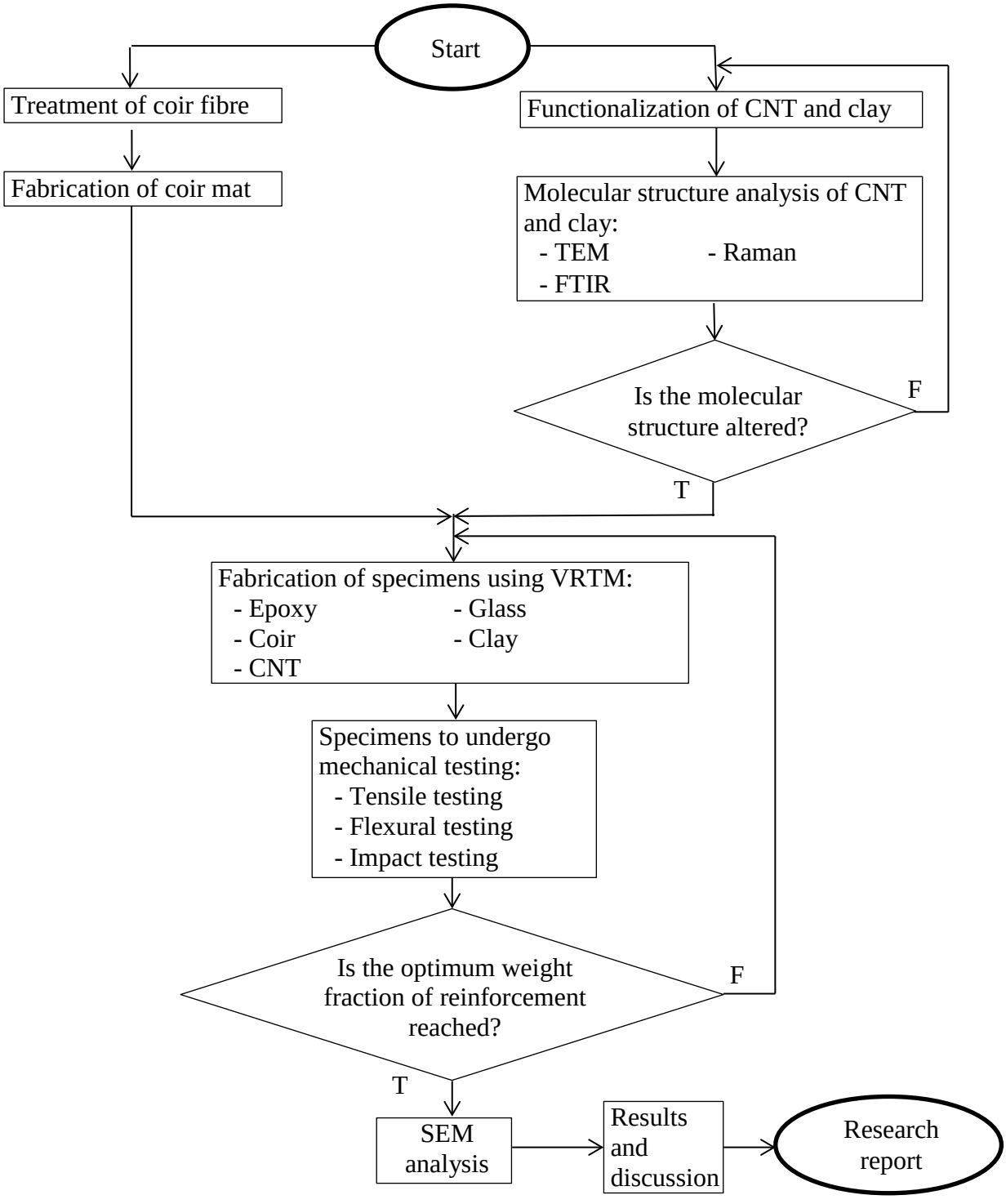


Figure 1.1 : Flowchart indicating the scope of the current research

2 LITERATURE REVIEW

2.1 Composite background

The use of composite materials dates back to as early as 1500BC when Egyptian and Mesopotamian settlers used a mixture of mud and straw for building purposes. Composite materials were also used as hunting tools such as composite bows, which comprised of wood, bone and animal glue that were pressed and wrapped. Before the development of plastics, natural resins obtained from plants and animals were the only source for glues and binding agents. The development of plastics begun in the early 1900's with vinyl, polystyrene, phenolic and polyester being developed. The use of these plastics increased over the years for general applications however they were not suitable for structural applications due to their low strength properties. The advancement of plastics in conjunction with certain reinforcement materials resulted in composite materials being suitable for certain structural applications. As the years progressed the use of composite materials grew with the development of new materials and processes, which also resulted in the discovery of new types of composite materials. Glass fibres being the most popular type of reinforcement, were developed in the 1930's which led to the beginning of a new era within the composite field and had found itself in many areas of use ranging from cars, boats, tanks, aeroplane structures and many more [1-3, 9-10].

Composite materials can now be found in a wide variety of applications from tools, automobile parts, aircrafts, ships, structural members, armour protection, sporting equipment, and many more [1, 3, 12]. The main benefit of using composite materials is that they are lightweight in comparison to other materials such as steels and concrete. They have high strength per unit weight especially if structural fibres are used and also exhibit good corrosion and chemical resistance properties. Some composites exhibit good elastic properties and are used for non-conductive applications [3].

Currently most of the conventional composites in use today are composed of synthetic materials, however the world is continuously evolving to offer

advantages to the environment such as the reduced dependence on non-renewable energy/ material sources, lower pollutant emissions, enhanced energy recovery and the extended biodegradability life of the materials. This is when the use of natural fibres as reinforcement materials becomes very relevant and important as they offer benefits of the properties mentioned above as well as good mechanical properties, [10]. The most common types of natural fibres used are jute, kenaf, flax, hemp and bamboo due to their good mechanical properties in comparison to the other types of natural fibres. Natural fibres are cheaper than the popular glass fibres but their major drawback is their lower mechanical properties in comparison to glass fibres [4-6].

A composite comprises of a matrix and a reinforcement material and can thus be classified on either the type of matrix or reinforcement used or a combination of them both. Composites are divided into groups based on the type of matrix which is used, being either ceramic, metal, carbon or polymer matrix composites. Composites that are defined based on the type of reinforcement used are known as either particulate, whisker, chopped fibre or fibre reinforced composites [14]. There are various types of fibre composites available such as glass, carbon, ceramic e.g. boron and even high tenacity aramid polymeric fibres e.g. kevlar [13, 15-16]. Fibre reinforced composites can be further subdivided according to the configuration of the reinforcement. Fibres aligned in one direction are known as uni-axial fibre composites, fibres arranged in layers are laminar composites and fibres knitted or woven in three dimensional shapes are known as three dimensional composites, [13, 14, 16].

The main parameters which affect the mechanical properties of composites are the reinforcement length, ratio of matrix to reinforcement, orientation of the reinforcement and interfacial adhesion between the reinforcement and the matrix. A good interfacial bond is required for effective load transfer from the matrix to the reinforcement which would enable maximum utilization of the properties in the constituents being achieved. A composite has three segments which are susceptible to failure, the reinforcement, matrix and the interface between these two, a failure in anyone of these segments would initiate failure in another. As

mentioned above, an important factor to be considered when fabricating composites is the volume or weight fraction of the reinforcement used. The best composite is produced when the optimum fraction of reinforcement is used which is usually determined by experimental or theoretical analysis [3, 12].

2.2 Polymer

As mentioned there are a few types of matrices which can be used to fabricate composite materials. Polymer matrices are the most popular and commonly used matrices with applications that can be found almost anywhere. A polymer is a molecule which consists of two or more molecules of monomers which have two distinctive features, they have carbon-carbon double bonds and side groups [9, 12]. Polymers are fabricated from long organic molecules made up of Carbon and Hydrogen atoms that are covalently bonded to form a solid material, various bonding arrangements are used to produce the different types of polymers with their unique properties. Polymers can behave either elastically, viscously or viscoelastically which is a combination of both [9, 12]. Polymers are divided into three main categories: thermosetting polymers, thermoplastic polymers and elastomers with the former two being the most commonly used in composite applications.

Thermosetting polymers are commonly known as thermosets. These plastics are usually set, cured or hardened into a permanent shape and are thus non-recyclable. Curing of a thermoset occurs with heat/ UV light and once cured an irreversible cross linking of the polymer takes place with the polymer permanently set once cooled. Some examples of thermosetting polymers are polyester, polyurethanes, epoxy and duroplast [2, 9, 12]. Thermoplastic polymers can be softened to a flow-able state upon heating, they can then be shaped into useful objects and retain their shape upon cooling. These plastics can be repeatedly shaped by heating of the plastic. Some examples of thermoplastic polymers are high density polyethylene (HDPE), polypropylene (PP), poly vinyl chloride (PVC) and nylon [2, 9, 12].

2.3 Nano composite

The word nano is derived from the Greek word for dwarf. It is also the prefix for units in the order of 10^{-9}. Nano science is the study of extremely small particles which are measured in nanometres (nm). A nano composite is a multiphase solid material where one of the phases has dimensions less than 100nm. Nano composites also refer to materials with structures that have nano scale distances between the different phases that make up the material [6, 13]. Nano composites have exceptionally high surface to volume ratios of the reinforcing phase or exceptionally high aspect ratios.

Figure 2.1 shows a picture of nano fibres which are approximately 1000 times smaller in diameter in comparison to human hair. These fibres are also generally 10 to 100 times smaller in diameter than conventional fibres. Zander [13] found that adding nano reinforcements to epoxy resin has the ability to enhance the properties and overcome the limitations of the matrix by utilizing the unique properties of the nano scale reinforcement. Nano reinforcements as opposed to conventional reinforcements have improved the mechanical and thermal properties at much lower reinforcement levels, usually between 0.1–5 percent. Due to the exceptionally high surface area of nano fillers, the inter-phase region between the matrix and the reinforcement forms a considerable portion of the composite. This is effective in yielding high performance composites as good dispersion of the reinforcement is achieved and the properties of the nano scale composites are better than those of the matrix. It had also been noted that the nano particle-matrix adhesion is crucial for proper stress transfer from the matrix to the reinforcement [6, 14-15].

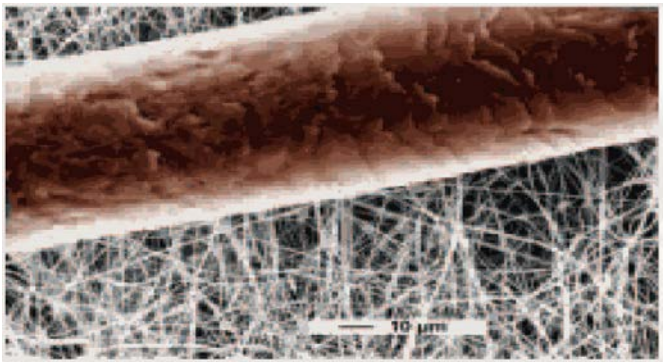


Figure 2.1 : A picture of nano fibrils shown with a strand of human hair [14]

The advantages of using nanocomposites are improved mechanical properties, decreased permeability to gases, water and hydrocarbons, improved surface appearance, thermal stability and flame retardancy. There are also a few drawbacks in using nanocomposites which include reduced toughness, impact performance, the insolubility of nano particles in solvents and particle agglomeration.

2.4 Hybrid composites

A hybrid composite is a material formed by combining two or more different types of reinforcements in one matrix. The level of mixing of these components can be on a small scale or on a large scale depending on the properties required. Hybridization is performed to fabricate a new material that possesses all of the advantages of its constituent materials without their disadvantages, in certain instances the advantage of one constituent complements what is lacking in the other [17, 20]. Due to this the hybridization of two types of reinforcements with different properties offers advantages over the use of either of the reinforcements independently in a matrix.

Inorganic polymer hybrid materials have attracted the interest of researchers due to these materials combining the advantages of an organic polymer matrix, which include process-ability, flexibility and functional groups, as well as the advantages of inorganic particles, such as their mechanical strength and elastic modulus [18]. Researchers found that the combination of the intrinsic mechanical properties of

both reinforcement materials increases the structural properties of the hybrid composite in terms of the impact, strength and stiffness properties [19-20].

The properties of a hybrid fibre composite is influenced by the fibre content, length of the fibres used, fibre orientation, extent to which the fibres intermingle with the other reinforcement and bonding of the reinforcements to the matrix. It has also been found that the strength of the hybrid composite is dependent on the failure strain of the individual fibres [20].

Hybrid composites are usually fabricated using the following processes [17]:

- Interply or tow-by-tow :- Where two or more constituent types of fibres are mixed in a regular or random manner
- Sandwich Hybrids :- One material being sandwiched between two layers of another
- Interply or laminated :- Alternate layers of the two or more materials are stacked in a regular manner
- Intimately mixed hybrids :- The fibres present are made to mix as randomly as possible to prevent over concentration of any one type of material

Thwe et al. [7] looked at hybrid composites fabricated from natural fibre with stronger and more corrosion-resistant synthetic fibre, such as glass or carbon fibre and noted an improvement in the stiffness, strength and moisture resistance of the composite. This provides an indication as to how hybrid composites are able to provide an advantage over standard composite materials with the advantages of one type of fibre being able to complement what is lacking in the other resulting in a much stronger material.

There is a large number of studies involving hybrid composites with glass fibres to improve the composite properties [7], however there are not many referenced reports available to date which involve hybrid composites using natural fibres that detail the mechanical properties of these composites [7].

2.5 Composite constituent materials

2.5.1 Polymer

As mentioned in section 2.1 there are generally four different types of matrices which can be used to fabricate a composite material. Polymer matrices being one of them, have a wide range of properties and have found their way into many of the items used in everyday life. With there being two common types of polymers, the use of either type is dependent on the application. For the fabrication of hybrid fibre composites it is beneficial to use a thermosetting polymer as compared to a thermoplastic polymer. This is due to the fact that thermosetting resins while in liquid state can infiltrate the gaps between fibres and then harden at room temperature whereas thermosetting polymers requires heating of the polymer in order to bring the polymer to a liquid state which would then damage the fibres and not provide adequate infiltration. The mechanical properties of the two commonly used thermosetting polymer composite matrices can be seen in Table 2.1 [3, 12].

Table 2.1 : Properties of two commonly used thermosetting polymers

Polymer	Density (g/cm3)	Modulus (GPa)	Tensile Strength (MPa)	Elongation to break (%)
Epoxy	1.1-1.4	3-6	35-100	1-6
Polyester	1.2-1.5	2-4.5	40-90	2

An epoxy is the result of a reaction between an epoxide (resin) and polyamine (hardener), and is also known as a two part polymer. Once the two parts are combined there is a working time (pot life) during which the epoxy can be used which varies between the different types of epoxies, [35]. By varying the temperature of the liquid epoxy mixture, the pot life and curing time of the epoxy can be varied. Another method to increase the pot life of epoxy is to spread out the epoxy mixture rather than to keep it concentrated, which minimizes the contact area of the epoxy particles. Epoxy polymers are low density polymers which are mechanically strong, chemically resistant, good adhesives, fairly heat resistant, possess good insulation properties and are durable [20].

Cui et al. [14] noted that epoxy resins once cured are brittle, have poor fatigue properties and heat and impact resistance which tend to restrict their corresponding applications. Additives can be added to epoxies to make them less brittle but generally at the loss or reduction of other positive properties of the epoxy. Epoxy resins are the polymer matrix used most often with reinforcing fibres for advanced composite applications as they show considerable adhesion to the embedded fibre, [15]. A few studies were reviewed which made use of epoxy resins reinforced with rubber which showed an increase in the fracture toughness but a decrease in the elastic modulus and strength indicating that not all properties can be increased simultaneously [15]. Shen et al. [21] defined epoxy resin to be the most common class of thermosetting resin to be used in various applications due to their high tensile strength and modulus, low shrinkage upon curing, good chemical and corrosion resistance, high adhesion and dimensional stability.

Due to the higher tensile strength and modulus of the epoxy polymer in comparison to polyester and the results obtained by the researchers above it was selected as the matrix that would be used to fabricate the hybrid composites

2.5.2 Natural fibres

Natural fibres can be defined as substances produced by plants or animals which can be spun into filaments, threads or rope. When these elements are woven, knitted, matted or bonded they form fabrics that are beneficial to society. Natural fibres can be divided into two categories, plant and animal fibres [22]. Plant fibres can be found in various different types such as abaca, coir, cotton, flax, hemp, jute, ramie and sisal. Plant fibres are classified into three categories depending on the part of the plant from which they are extracted, bast or stem fibres (jute, mesta, banana), leaf fibres (sisal, pineapple, screw pine, etc.) seed fibres (cotton, coir, old palm, etc.) [23-24]. These fibres can be considered as naturally occurring composites consisting mainly of cellulose fibres embedded in a lignin/ resin matrix. Whether the natural fibres are extracted from barks, stems or leaves the cellulose fibres are aligned along the length of the fibre which results in high tensile and flexural strengths of the fibres [17]. Figure 2.2 is a

representation of a natural vegetable fibre indicating how the fibres are embedded in the lignin and cellulose matrix. It is observed that in some types of plant fibres there is more than one wall which contains the fibres.

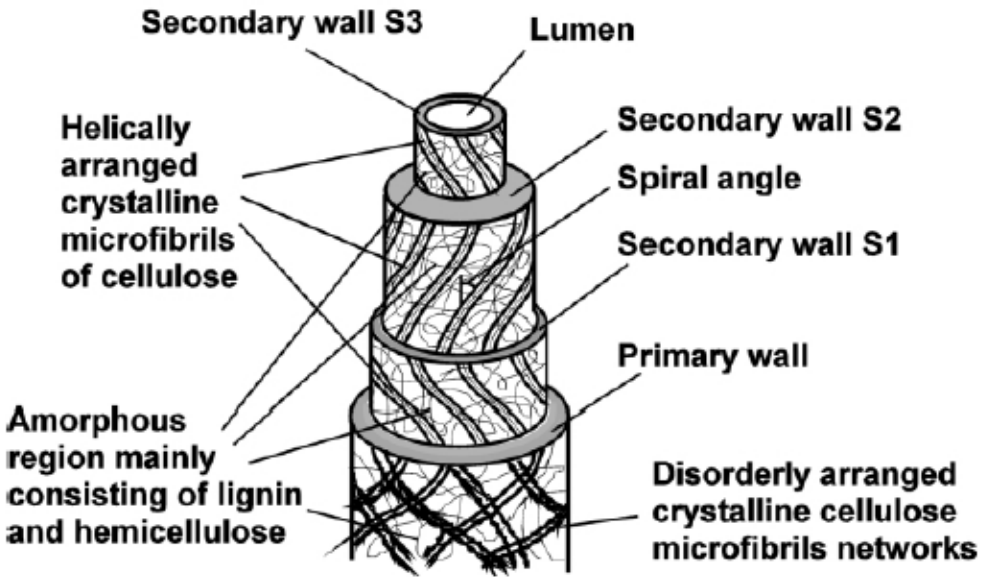


Figure 2.2 : Representation of a natural vegetable fibre [25]

Natural fibres are abundantly available in developing countries such as India, Sri Lanka and some African countries but they are not optimally utilized. These fibres are generally used for the fabrication of many basic items such as rope, yarn, mats, fillers for mattresses, cloth and many more [26].

The main reason for the increasing popularity of natural fibre composites is the availability and consistent quality of a wide range of fibres with them being environmentally friendly. The strongest plant based natural fibres are jute, kenaf, flax, hemp and bamboo which have been the subject of many studies. These fibres approach and sometimes even exceed the specific mechanical properties of synthetic fibres [26, 22].

Advantages and disadvantages of natural fibres:

Advantages:

- High strength and stiffness per weight
- Low cost
- Renewable resource

Disadvantages:

- Lower durability
- Moisture absorption
- Lower strength properties, particularly impact strength

Table 2.1 shows the different properties between a few natural fibres. It can be seen that coir fibres have a larger diameter as compared to the other materials and the lowest density, making them the lightest materials. However the lignin content of coir fibre is relatively high and thus the fibres have to be treated prior to use to ensure that a large amount of the lignin is removed to enable proper bonding to take place [18, 23-24].

Table 2.1 : Properties of a few types of natural fibres [18, 23-24]

Property	**Jute**	**Banana**	**Sisal**	**Pineapple**	**Coir (Coconut fibre)**
Width or Diameter (mm)	-	80-250	50-200	20-80	100-450
Density (g/ cc)	1.3	1.35	1.45	1.44	1.15
Cellulose/ Lignin Content (%)	61 /12	65 /5	67 /12	81 /12	43 /45
Elastic modulus (GPa)	-	8-20	9-16	34-82	4-6
Elongation (%)	1-1.2	1.0-3.5	3-7	0.8-1.6	15-40

Table 2.2 shows the mechanical properties of coir fibres together with sisal and banana fibres. It can be seen that in the case of either unidirectional or chopped random fibres, coir fibres are the weakest among these natural fibres.

Table 2.2 : Mechanical properties of unidirectional aligned continuous fibre vs. randomly oriented short fibre composites in a polyester matrix [18, 23-24]

Fibre (wt.%)	Tensile strength (MPa)	Young's Modulus (GPa)	Flexural Strength (MPa)	Flexural Modulus (GPa)	Impact Strength (kJm^{-2})
Unidirectional					
Sisal (40)	129	8.5	192	7.5	98
Banana (30)	121	8	-	-	52
Coir (30)	45	4	56	4	44
Chopped Random					
Sisal (25)	34.5	1.9	86.4	-	30
Banana (25)	43.5	2.3	92	-	10
Coir (25)	14	1.4	31.2	-	11

One of the major problems identified with natural fibres when using them to fabricate composites is their poor compatibility when using hydrophobic polymers. Studies in the use of natural fibres show that moisture absorption of natural fibre causes degradation of the mechanical properties of the natural fibre composites when compared to synthetic fibre reinforced composites. It was noted that the tensile, flexural strength and stiffness of natural fibre composites were improved with pre-treatment of the fibres [1]. Pre-treatments of the natural fibre surface can clean the fibre surface, stop the moisture absorption process (hydrophilic nature), increase the surface roughness and chemically modify the surface to improve bonding between the matrix and the fibres. With natural fibres bearing hydroxyl groups from both cellulose and lignin it makes them amenable to chemical modification which may activate these groups or introduce new parts which can bond to the matrix. There are various treatment processes which can be used on natural fibres, some of them include isocyante, acetylation, silane, peroxide and mercerization (e.g. NaOH) treatments [26, 28-30].

2.5.3 Coconut Fibre (Coir Fibre)

Coconuts being a tropical fruit have many purposes from their use in various cuisines to the fabrication of mats and ropes. A coconut comprises of the coconut husk (excocarp) which is made up of the waterproof outer skin (epicarp) and fibrous zone (mesocarp), the inside of the coconut is where the seed is housed. Covering the seed is an external leathery skin and a 5-8 cm thick intermediate layer of fibrous pulp. The very versatile type of natural fibre extracted from the mesocarp or husk of the coconut fruit which grows between the husk of the coconut and its outer shell is known as coir [31]. Figure 2.3 and Figure 2.4 show an actual and SEM representation of coir fibres respectively.



Figure 2.3 : Coir fibre

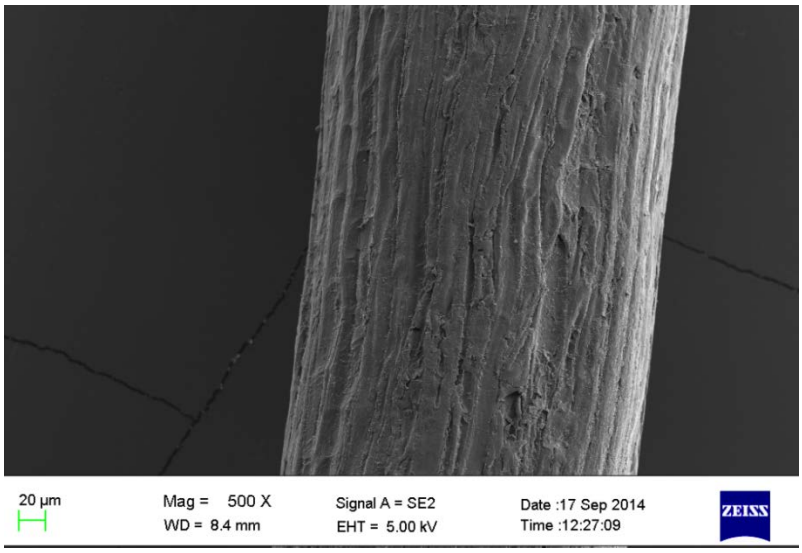


Figure 2.4 : SEM image of coir fibre

Coir fibres come in two different forms, brown or white fibres. These are characterized based on the stage of the fruit when the fibres are extracted. White coir is extracted from the husks of a coconut which is not fully ripened about 6-12 months on the tree. Brown fibres are extracted from the husks of a coconut which is fully ripened, these fibres are stronger in comparison to white fibres [29]. Individual coir fibres are narrow and hollow with thick walls made of cellulose. Coir fibres are generally golden in colour due to the fact that as the fibres harden they change colour because of the lignin deposits found on their walls. The lignin deposits are responsible for the colour, harshness and relative brittleness of the fibres. Mature brown fibres contain more lignin and less cellulose than fibres such as flax and cotton [29]. Coir fibres range in length from 10-30 cm, 20-30 cm fibres are called bristle fibres and the shorter fibres are called mattress fibres. Mature coconut husks are made up of 66% of dust and pith and 33% of coir fibre, of the 33% of coir fibre being produced 33% are bristle fibres and 66% are mattress and shorter fibres. As an example a 300g coconut is able to yield about 80-90 g of fibre [31]. Coconut trees flower monthly with the fruits taking a year to ripen thus each tree usually contains fruits at 12 stages of maturity. Harvesting usually takes place on a 45-60 day cycle and a single tree is able to produce around 50-100 coconuts per year [31].

Properties of coir fibre [29]:

- They can provide padding against extreme temperatures and sound
- These fibres are resistant to moisture growth
- Their shape remains unaffected over long periods of time

Table 2.3 shows the properties for coir fibre as discovered by various researchers, however it can be seen that the properties of coir fibre varies from one researcher to the next. This can be due to a number of factors as these fibres are natural fibres formed in environmental conditions which vary between locations.

Table 2.3 : Properties of coir fibre, data obtained from a number of different researchers [28-31]

Diameter (mm)	**Length (mm)**	**Tensile Strength (MPa)**	**Elongation (%)**	**Elastic modulus (GPa)**	**Density (kg/m^3)**
0.40 - 0.10	60 - 25	15 - 327	75.00	-	-
0.21	-	107	37.70	2.80	1104-1370
0.30	-	69	-	2.00	1140
-	-	51	17.60	-	1000
0.27 ± 0.073	50 ± 10	142 ± 36	24.00	2 ± 0.3	-
0.11 - 0.53	-	108 - 252	13.70	2.5 - 4.5	670-1000
0.12 ± 0.005	-	137 ± 11	-	-	870
-	-	500	-	-	1150
-	-	175	30.00	-	1200
0.10 - 0.40	-	174	10 – 25	16 - 26	-
0.10 - 0.40	50 - 250	100 - 130	10 – 26	19 - 26	145 - 280
0.10 - 0.45	-	106 -175	17 – 47	-	1150

Coir fibres are usually bleached first before use, once done they have numerous uses such as brushes, doormats, sacks, twine, fish nets, marine ropes, and many more. Pads of curled brown coir fibre are usually made by needle felting (a machining technique that mats the fibres together) which are shaped to cut and fill mattresses, car seats and for erosion prevention.

Rout et al. [30] studied the growing environmental awareness throughout the world in the use of materials which are compatible with the environment. The advantages of natural fibres over the more common reinforcements such as glass fibres, talc and micra were looked at. With natural fibres possessing qualities such as good strength, low cost, low density, good thermal properties, enhanced energy recovery and biodegradability these reinforcements look promising for composite materials of the future [30]. Researchers have found that the use of coir as a reinforcement material is not very good and is not comparable with other natural fibres due to its low cellulose content, 36-43 %, and high lignin content 41-45 %. To curb the compatibility issues, alkali treatment of the coir fibres prior to dispersion into the composite material were looked at. Rout et al. [30] found that a NaOH treatment of the fibres resulted in an increase of the strength properties in the composite materials.

2.5.4 Glass

Hollow glass microspheres are used as reinforcements in composite materials due to their unusual and useful characteristics such as low density, high stiffness, low thermal and electrical conductivity and high compressive strength. The addition of HGM proved to enhance the properties of composites according to Patankar et al. [32]. An important point to note when using HGM is that if they are not anchored properly in the matrix they can act as dispersed voids causing a reduction in the mechanical properties.

2.5.5 Carbon Nano Tubes (CNT)

Carbon nano tubes (CNT) can be described as being molecular scale tubes (cylinders) of graphitic carbon (graphene) with outstanding properties. The simplest Carbon nanotube is composed of a single sheet of a honeycomb network of Carbon atoms called graphene, rolled up seamlessly into a tubular form which is closed at each end [15, 33-34]. The diameter of a nanotube is in the range of a few billions of a meter with its length being up to a few micrometers (μm) and forms part of the fullerene structural family.

CNT can be broken up into two basic types, Single wall carbon nanotubes (SWCNT) and multiwall carbon nanotubes (MWCNT). SWNT are made up of one cylindrical graphene sheet with a diameter ranging from 0.4-200 nm and a length in the range of 20-1000 nm. The structure of a SWCNT can be conceptualized by wrapping a one atom thick layer of graphite into seamless cylinder. MWCNT consists of multiple layers of graphite rolled in a tubular shape with their diameters ranging from 1.4-200 nm and lengths from 1μm to several μm. The exact structure of a nanotube depends on the different angles and curvatures in which a graphene sheet can be rolled into a tube and is determined by a vector which breaks up CNT into zigzag, armchair and chiral forms [34-36].

CNT exhibit novel properties such as outstanding mechanical, electrical, thermal and chemical properties which can be used in a wide variety of applications from catalytic applications, optics, nano-electronics, composite materials, conductive polymers and gas sensors. CNT can be used to create better pressure sensitive conductors, longer lasting batteries, transparent conductor technologies, biomolecule markers for cancer detection, nerve cell signal carrying and stimulation and ultra-capacitors. Due to their strength and flexibility they could be beneficial in society and could be used to revolutionize various fields [34-36].

Carbon nanotubes are excellent candidates for multi-functional nano-reinforcing a variety of polymer materials because of their high strength (approx. 100 times stronger than steel), high thermal conductivity (twice as high as diamond)

excellent electrical capacity (1000 times higher than copper) and good thermal stability [15]. A small amount of CNT (<1 wt.%) added to a matrix system can increase electric, thermal and mechanical properties of a composite without compromising the weight or process ability of the composite [15].

2.5.6 Clay

A natural zeolite is a type of clay that contains hydrated aluminosilicates with symmetrically stacked alumina and silicate tetrahedral particles. Clay contains open and stable three dimensional structures with a negative charge that is neutralized by cations such as sodium and potassium. Their capabilities of ion exchange, acidity, porosity and high surface area have enabled their use as builders in detergents, fillers in the paper industry, catalysts in the petrochemical industry and absorbents for metal removal in waste water treatment [37]. Montmorillonite is a type of clay which is recognized as an appropriate choice for manufacturing high performance polymer-clay composites. This naturally occurring clay possesses a nano-scale layered structure. Montmorillonite (MMT) consists of approximately 1nm thick aluminosilicate layers surface substitutes with metal cations and stacked in 10μm sized multilayer stacks [38, 39]. To render a polymer-MMT composite the layered MMT has to be dispersed finely and uniformly in the polymer matrices. MMT does not exhibit affinity to organic polymers because of its hydrophilic nature therefore it is frequently modified with the addition of certain organic surfactants to improve its compatibility with the organic polymers prior to the mixing procedure [40].

2.5.7 Additional research

Romli et al. [41] found that the optimum strength of coir epoxy composites had been obtained with a 3-15% wt. fraction of coir fibres, any addition of fibres above this resulted in a reduction of the composite strength.

Epoxy-clay composites have become popular over the years due to increased properties that result in terms of stiffness, strength, fire resistance, dimensional stability and shrinkage [42].

Polymer-clay mineral composites can be classified into three different types: [42]

- conventional micro composites where stacks of silicate layers are dispersed on a micro scale inside the matrix
- intercalated composites in which some polymeric chains are able to insert between the platelets maintaining a long range order
- exfoliated composites in which the platelets are not ordered but are separately and homogeneously dispersed into the matrix as single platelets

In many cases a mixture of intercalated and exfoliated structures are obtained. The best properties are achieved when the clay mineral platelets are exfoliated and well dispersed. Phonthammachai et al. [43] found that the dilemma in using clay is the low exfoliation and poor interfacial interaction between the resin and clay due to the hydrophilic nature of the clay. In order to achieve good dispersion of clay minerals in the polymer it is often necessary to modify them in order to make them more compatible to the polymer [38]. Gianni et al. [38] studied the use of silanes to functionalize clay and had noted that the -OH reactive sites of the clay structures become exposed upon functionalization. Silva et al. [39] investigated the grafting reaction of hydrophobic groups onto the clay surfaces which was performed through a reaction between the silane coupling agent and the reactive silanol groups, structural defects located at the interlayer and external surface of the treated clay were noted.

Park et al. [44] achieved a high degree of exfoliation of the clay particles when using an amino silane to functionalize the clay particles. This resulted in an increase in the mechanical properties of the composites [40, 42-43]. It has been mentioned previously that in order to produce a good quality clay composite proper dispersion of the clay particles is imperative. Researchers looked at different methods of dispersing clay particles in the polymer matrix. They found that mechanical stirring and ultra-sonication proved to be the most convenient and efficient methods of dispersing the particles into the matrix [43, 45]. Upon dispersing of the clay particles using the methods mentioned above it was found that the composites produced had improved mechanical properties. Alternative

dispersion methods tried by other researchers are the solution induced intercalation method and in situ polymerization which proved to be unsuccessful by causing a reduction in the mechanical properties [46].

The optimum weight fraction of clay to be used in composites varies among researchers and is dependent on a few factors which include different material grades, environmental conditions and variables in processing of the composites. It was discovered that a 5% weight fraction of clay resulted in the best mechanical properties of a composite, any weight fraction greater than this resulted in a decrease in the properties [6, 47-48]. Silani et al. [49] found that a 0.1-10 % weight fraction of clay provided an alteration of the properties of the clay composite with the optimum weight fraction being 2%. It was found that the addition of clay in an epoxy-clay composite reduces the ductility of the composite due to the barrier effect of clays which results in crack propagation [50]. Yasmin et al. [51] found that as the clay content increases so does the strain to failure rate. They conducted tests on two different grades of clay and found that up to a 2% weight fraction of clay they both exhibited the same properties. Higher than a 2% weight fraction one type of clay produced enhanced properties, until a 5% weight fraction, over this weight fraction the properties of the composite decreased. Mohan et al. [47] noted that a large amount of research had not been conducted on the mechanical properties of epoxy-clay composites which is due to the increase in resin viscosity upon addition of the clay [45-46, 52-54].

High strength composites are important materials for aircrafts, space shuttles and many other applications due to the fact that they possess high strength, light weight and multi-functional features. Zou et al. [35] noted that CNT reinforced epoxy systems hold the promise of delivering high performance composites. CNT has great potential as a reinforcement due to their high surface to volume ratio and has found to positively alter the mechanical properties of composite materials [36]. Zou et al. [35] showed that although CNT's have extraordinary mechanical properties there are two main problems evident when using CNT as a composite reinforcement. Due to the nature of the nano-scale effect, CNT's tend to hold together due to the high van der Waals forces present, with bundles and ropes

formed in the matrix, thus homogenous dispersions are hardly obtained [35, 55]. Because of the atomically smooth surface of the CNT's, lack of interfacial bonding limits the ability of load transferring from the polymer to the CNT [36]. Cui et al. [14] found that in order to take full advantage of the properties of CNT the above two limitations must be removed. The most effective method to overcome these limitations is to prepare CNT reinforced composites by chemical functionalization of the CNT first. Donsheng Mao [56] reviewed studies involving the use of CNT's without any surface modification which showed an increase in the elastic modulus of the composite at relatively low nanotube concentration, <1% by weight which indicates the potential of CNT as reinforcing materials especially if the surface modification of CNT is optimized [56].

Surface functionalization of carbon nanotubes plays an essential role for improving the solubility and dispersion of the nanotubes in solutions for the design of new materials. Functional groups attached on the carbon surface were found to be responsible for the various physio-chemical and catalytic properties of the material. The oxygen containing functional groups could be introduced by mechanical, chemical and electrochemical routes. It is found that the amount and type of oxygen containing functional groups depends on the treatment methods used [35]. There are numerous methods which can be used to functionalize CNT. Acid treatment of MWNT is the easier and controllable way for laboratory and industrial functionalization which removes the graphitic and metal catalytic particles and thus creates a higher number of oxidation sites on the CNT [53-54]. A common acid treatment used involves a mixture of HNO_3 and H_2SO_4 [51, 56]. Zou et al. [35] noted that a very strong acid treatment would cut off the CNT's length and limit its application as a high performance filler due to the acid solution causing an introduction of a number of oxygenated acidic surface groups onto the surface [35, 53]. The use of different solvents to disperse CNT results in different degrees of changes in the curing properties of the epoxy resin even after the solvents are completely removed [36]. Dongsheng Mao [56] researched traditional methods such as sonication, high shear mixing, stirring and surfactants which are often used in a laboratory to disperse CNT and have noted

improvement in the properties by using these methods. It was noted that a longer sonication time can result in better dispersion state of the particles, however extended exposure to high ultrasonic energy introduced defects in the CNT's which adversely affected the mechanical properties of the composite [56]. Contrary to the results of the researchers mentioned above Yudianti et al. [34] showed that the homogenous dispersion of CNT was relatively difficult to achieve. They found that most of the techniques used to disperse CNT such as ultra-sonication, addition of surfactant and chemical modification of the nanotube surface served as a susceptible way to break down the CNT structure [34]. This indicates that depending on the processing methods and conditions different researchers can produce different results. A longer functionalization period for the MWCNT resulted in cutting of the CNT after HNO_3/ H_2SO_4 treatment whereas the MWCNT functionalised in a shorter period were easily dispersed in the epoxy. MWCNT tends to aggregate when the MWCNT content reaches a certain percentage of the composite which indicates the maximum tensile strength for the composite [57]. Part of the research undertaken by Kim et al. [36] showed that an increase in the CNT concentration resulted in a smaller heat of reaction, with an increase in the degree of dispersion leading to an increase in the Young's modulus. The degree of dispersion of CNT is observed by optical methods such as optical microscope, SEM and TEM and had shown that these methods made it possible to observe individual particles and assess the degree of dispersion easily [35-36].

Dongsheng Mao [56] found that the mechanical properties of their CNT composites increased from a 0.5% weight fraction to a 1.5% weight fraction of CNT which produced the best mechanical properties. A 2% and higher weight fraction of CNT caused a reduction in the mechanical properties of the composite. Zhou et al. [15] found that the modulus of the composites in their research increased with increasing un-functionalized CNT up to the 0.33% weight fraction. A 0.33% weight fraction of CNT proved to be the best composite as it showed the greatest strength enhancement with a 28% increase in strength. The strength of the composite decreased on the addition of a 0.4% weight fraction of CNT due to

the non-uniform dispersion of CNT. Cui et al. [14] discovered that the tensile strength of pristine epoxy-MWCNT composites achieved maximum value at relatively low content of MWCNT [48-49]. As part of their research they have reviewed that some researchers have proclaimed that the Young's modulus of a CNT composite increased by 100% by the addition of 1% CNT. They concluded that the variation in the extent of improvement may be due to factors such as the state of dispersion and orientation of the CNT particles as well as the interface between the particles and the matrix [36]. Samples with a low concentration of CNT exhibited larger modulus than samples with higher concentrations based on the dispersion of the CNT [36]. The performance of a functionalized MWNT epoxy nano composites is as good as or even better than a DWNT reinforced epoxy composite [56].

2.6 Fabrication methods used in composite applications

There are various methods which can be used to fabricate composite materials, however the most suitable method is dependent on the type of constituents used and the shape of the composite to be fabricated. Some of the composite fabrication methods used are press moulding, pultrusion moulding, wet lay-up, compression moulding and vacuum bag moulding just to name a few. The type of fabrication method selected for the current research is vacuum resin transfer moulding (VRTM).

This process was selected as a hybrid composite is to be fabricated with the use of coir fibre reinforcement which would be highly beneficial for the matrix to infuse properly with the reinforcement. It is a closed mould low-pressure process that allows the fabrication of composites ranging in complexity from simple low performance to complex high performance articles in small and large sizes. The process involves a two sided mould which fits together to produce a mould cavity. One of the main features of using VRTM is that the reinforcement material is placed into the mould cavity prior to the introduction of the matrix material. A vacuum pump is used to pull the matrix into the mould and simultaneously reducing the amount of air bubbles formed within the composite.

Some of the benefits of using the VRTM process is that a better fibre to resin ratio can be achieved, less resin is wasted, there is also a very consistent use of resin with unlimited set up time as the system is set up and tested prior to any of the matrix being introduced. VRTM is also a much cleaner process as there are no brushes or rollers required which generally produce splashing of material. The major complication in using the VRTM process is that if the system is not set up properly and air tight then the composites produced are not usable. The trial and error method is usually used to solve this issue which does take time.

2.7 Conclusion

It was noted by the researcher that there are not many journal references available for natural fibre hybrid composites. Coir natural fibres are abundantly available and the full potential of this material still remains untapped with regards to composite applications. Due to the reduced properties of coir fibre in comparison to the other types of natural fibres these composites need to be additionally enhanced which could enable them to be used for more applications. The three popular reinforcements used in polymer composites are glass, clay and over the past few years, CNT. The fabrication of hybrid composites with the three popular polymer reinforcements using coir fibre is to be undertaken to observe if a polymer-coir fibre composite can have enhanced properties by the fabrication of a hybrid composite.

3 METHODOLOGY

3.1 Materials

3.1.1 Coir fibre

The coir fibre used for the current research had been procured from the Coir Institute of South Africa which had come rolled up in a mat separated by plastic meshing which enabled the coir fibre to be easily removed. The coir fibre was un-cleaned with all of the peat still present on the mat, a representation of the mat can be seen in Figure 3.1. Figure 3.2 shows an SEM image of the coir fibre with Table 3.1 indicating some of the properties of the fibre used.



Figure 3.1 : Coir Fibre



Figure 3.2 : SEM image of the coir fibre structure

Table 3.1 : Properties of the coir fibre used

Property	Quantity
Density (kg/m^3)	670
Tensile strength (MPa)	108
Elastic modulus (GPa)	2.5

3.1.2 Epoxy

The matrix used for this research project was Epolam MY which was supplied by AMT composites, South Africa, LH 956 is the corresponding hardener for this epoxy. Some of the features of this epoxy are that it has good wetting properties, good dimensional stability and good mechanical properties. Additional mechanical properties can be found in Table 3.2.

Table 3.2 : Properties of the epoxy resin used

Property	Quantity
Specific gravity (S.G)	1.05 +/- 0.02
Tensile strength (MPa)	40 +/- 5
Flexural strength (MPa)	70 +/- 6
Flexural modulus of elasticity (MPa)	200 +/- 22
De-mould time at room temperature (hrs.)	20-24

3.1.3 CNT

The multi-walled carbon nanotubes (MWCNT) used for this research was obtained from Sigma Alrich. The diameter of these tubes range from 110-170 nm and have a length between 5-9 micrometers (μm) with purity greater than 90%. Figure 3.3 shows an SEM image of the CNT indicting the tubes.

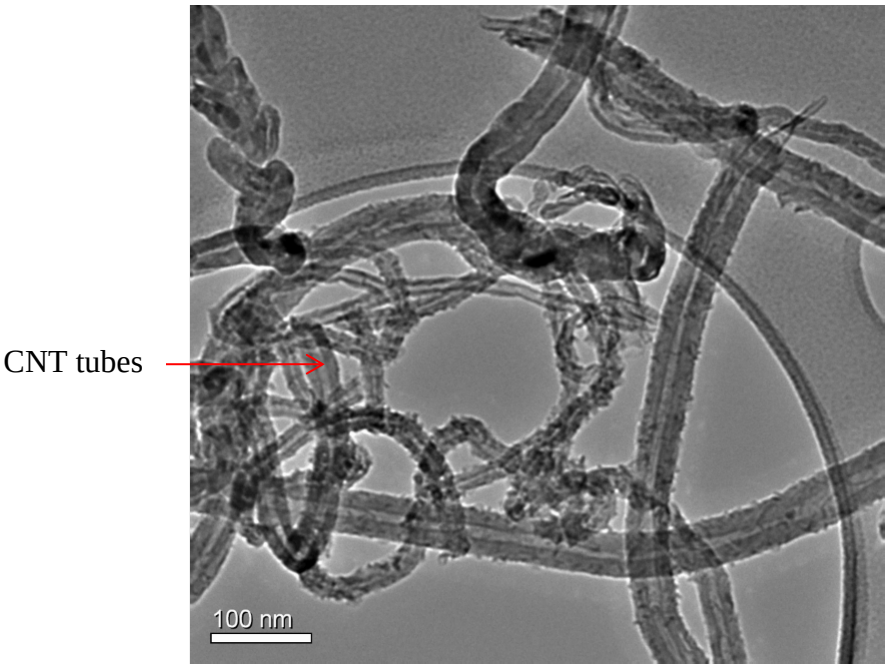


Figure 3.3 : SEM image of CNT

3.1.4 Glass spheres

Glass spheres were obtained from Sigma Alrich. The average size of the particles ranges from 9-13 µm with some of their basic properties listed in Table 3.3.

Table 3.3 : Properties of the glass spheres used

Property	**Quantity**
Density (kg/m^3)	1050-1150
Appearance	Powder
Colour	White
Physical form	Hollow, spherical nor-porous glass beads

3.1.5 Clay

The clay used in this research is known as Clinoptilolite which is a type of Montmorillonite clay, this material was donated by Pratley South Africa for research purposes. Clinoptilolite has the following formula $(MgCaNa_2K_2)_{2.5}(AlO_2)_{30}21H_2)$ and possesses properties listed in Table 3.4. Figure 3.4 showing an SEM image of the clay indicating the clay platelets.

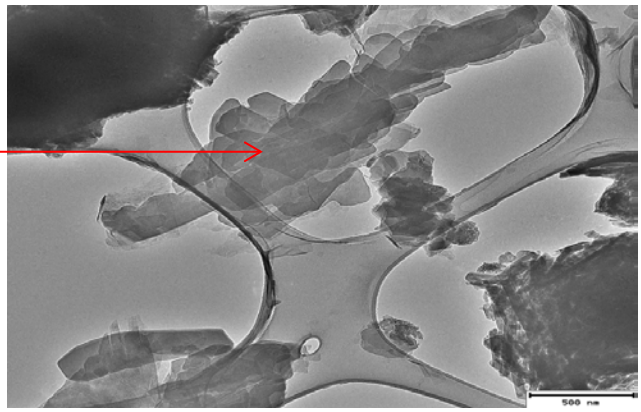


Figure 3.4 : SEM image of clay

Table 3.4 : Properties of the clay used

Property	Quantity
Density (g/cm^3)	2.2
Thermal stability	Up to 700°C
Colour	White
Hardness (MOH)	3.5-4.0

3.1.6 Chemicals

A few chemicals were used for the treatment of the reinforcements and the coir fibres which included Sulphuric Acid, Nitric Acid, Sodium Hydroxide, Acetone and 3-aminopropyltriethoxysilane. The mould release agent used for the fabrication of specimens was ram wax which was obtained from AMT composites.

3.2 Chemical Treatment Procedure

3.2.1 Coir Fibre Treatment

The coir fibre had to first be cleaned prior to treatment to remove all of the unwanted pith and peat found on the fibres. This process was done by hand with the aid of a steel wire brush to ensure that all of the fibres were separated and the unwanted material removed. As mentioned by Rout et al. [30] coir fibre needs to be treated with Sodium Hydroxide (NaOH) prior to use to ensure that the lignin and cellulose is removed from the fibres so that they can add to the properties of

the composite. Experimentation was done with the treatment of fibres using 10% and 20% NaOH solutions over two different time periods being 1 and 2 hours. The 10% NaOH solution was prepared using 2000 ml of NaOH with 200g of NaOH pellets which were mixed by hand until the NaOH pellets dissolved producing a 10% w/v solution of NaOH. The 20% NaOH solution was prepared using 2000 ml of distilled water with 400g of NaOH pellets producing a 20% w/v solution of NaOH.

An observation of the fibres showed that both the 10% and 20% volume fraction of NaOH solution impacted change to the coir fibre upon treatment. The fibres which were treated for 2 hours reduced the colour of the coir fibres from brown to yellow as well as caused the fibres to fray and thus would not be used further. Due to this it was decided that the 10% fibre treatment over 1 hour had been selected as the treatment method to be used for the current research.

A 10% NaOH solution was then prepared using distilled water, the coir fibres were completely immersed in the solution and left for an hour, Figure 3.5. The solution was then drained and the fibres washed thoroughly with distilled water, which was a minimum of 5 times, to reduce the alkalinity of the solution to a neutral pH. The fibres were dried in an oven for 2 hours at 70°C and then left to dry overnight. Figure 3.6 is a flowchart representation of the fibre treatment process used.



Figure 3.5 : Treating of the fibres with the NaOH solution

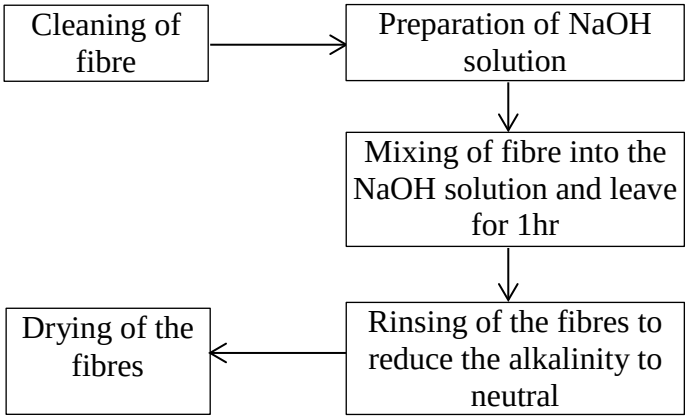


Figure 3.6 : Flowchart of the fibre treatment process

Although the fibres were cleaned prior to the treatment, they needed to be cleaned once again upon completion of the treatment as black clumps formed on the fibres. These clumps are due to the agglomeration of pith and the removal of both lignin and cellulose from the fibres. It is imperative that all of the unwanted material is removed from the fibres to ensure that only the fibres are used in the composites. The fumes emitted from the H_2O-NaOH mixture are strong and one should not linger at the top of the mixture or inhale any vapours, a gas mask should be used during this procedure.

3.2.2 Functionalization

Surface modification or functionalization of the CNT and clay used in the current research was crucial to ensure that these materials have functional groups created

on their surface to improve dispersion and the chemical interaction between materials. Functionalization of the materials was performed by chemical treatment. Functionalization of the glass spheres had not been performed as glass cannot be chemically treated.

Functionalization of MWCNT

Research reports indicate that the common method of functionalizing CNT is by using either HNO_3 or H_2SO_4 [42, 49, 56]. Dongsheng Mao [56] made use of a combination of HNO_3 and H_2SO_4 at a ratio of 3:1 which had resulted in the production of strong composite materials when tested. Cui et al. [14] made use of acid functionalization together with amino functionalization with the acid functionalization resulting in increased properties of the composite material. Due to this it was decided that acid functionalization is to be done on the MWCNT particles which would result in COOH bonding taking place on the particles. Figure 3.7 is a representation of what is to occur during the functionalization process of CNT.

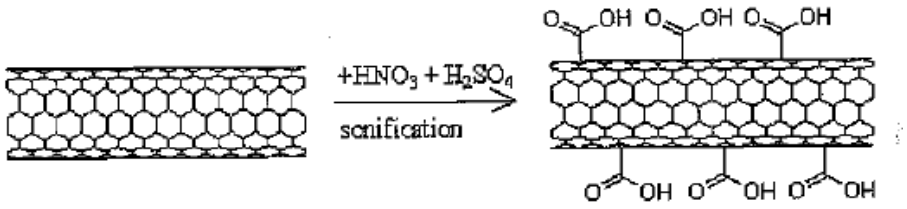


Figure 3.7 : Representation of what occurs during CNT functionalization [49]

5g of MWCNT had been weighed on the laboratory scale and decanted into a beaker. A ratio of 300ml of 98% concentrated sulphuric and 100 ml of 55% concentrated nitric acid was added to the beaker. The beaker was then put into an ultrasonicator at 40°C for 12 hours. Upon completion of the sonication a sufficient amount of distilled water was added to the mixture to dilute and wash away all of the acid from the particles. The MWCNT particles were removed from the mixture using vacuum filtration. This process was continued until the acidity of the solution reached a neutral pH. The mixture was then filtered and dried in a vacuum oven for 2 hours at 85°C. Figure 3.8 is a flowchart representation of the functionalization process used for the MWCNT.

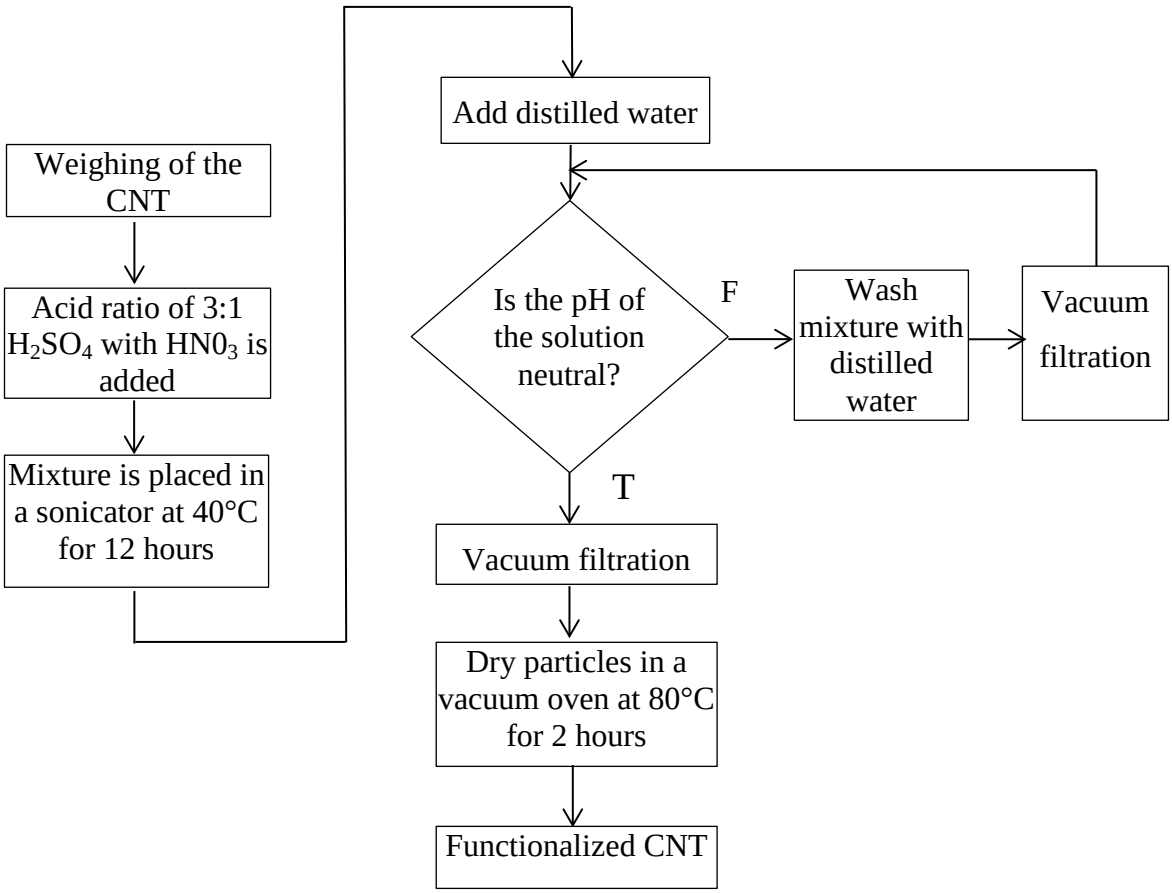


Figure 3.8 : Flowchart representation of the MWCNT functionalization process

Functionalization of CNT was done with two strong acids, extreme care needed to be exercised when handling of these acids, acid proof gloves were used to prevent any acid from spilling onto any part of the hands. Proper neutralization of the acid solution needs to be done prior to filtration, as prolonged exposure of the CNT to acid will damage the CNT.

Functionalization of clay

With clay being an organophillic material it needed to undergo a functionalization treatment method which would allow it to bond to both the epoxy and the natural fibres. Shanmugharaj et al. [42] made use of a silane treatment for the functionalization of clay and it was noted that the treatment of clay with 3-Aminopropyltriethoxysilane resulted in an improvement of their particles over a

30 minute period. Due to this it was decided by the researcher to use a 3-Aminopropyltriethoxysilane treatment on the clay particles for 30 minutes.

1g of clay was mixed with 100ml of distilled water. This solution was mixed using a magnetic stirrer at constant stirring under very low revolutions for 30 minutes. A solution of 3-Aminopropyltriethoxysilane was prepared using distilled water at a ratio of 2g : 100ml respectively and stirred using a magnetic stirrer. The ratio of clay to silane used was 1g clay : 2g silane. The silane mixture had then been added to the clay mixture under constant stirring for 30 minutes. The mixture was filtered and dried in an oven for 1.5 hours. Figure 3.9 shows a flowchart representation of the functionalization process used for the clay particles.

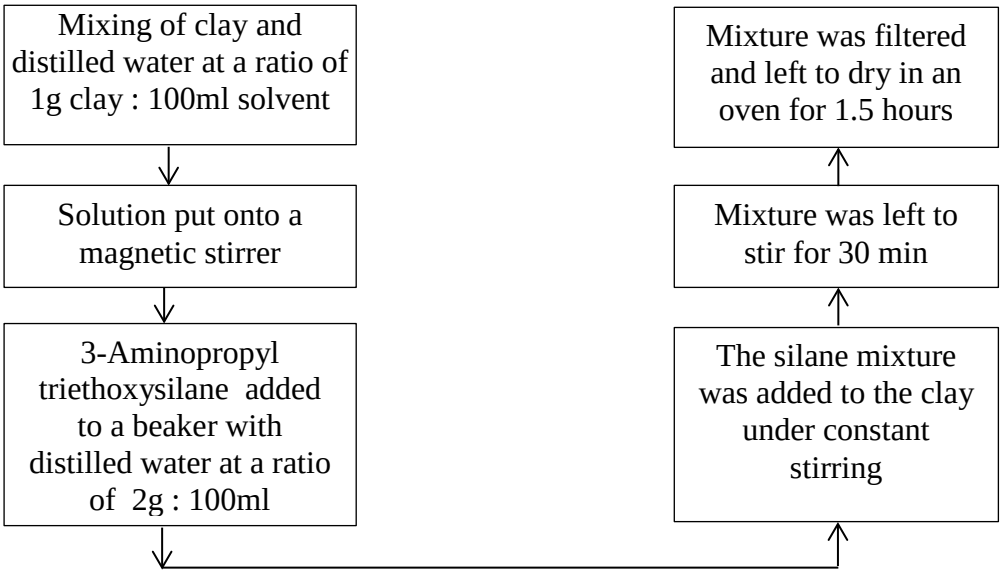


Figure 3.9 : Flowchart representation of the clay functionalization process

Functionalization of clay was done using 3-Aminopropyltriethoxysilane which gives off a very strong odour which requires the use of a breathing mask when using this chemical.

3.3 Fabrication Procedure

3.3.1 Manufacturing of the coir mat

A pipe mat manufacturing rig was used to manufacture the coir fibre mat that was used to fabricate the composite specimens. Figure 3.10 shows a representation of the mat rig used to fabricate the coir fibre mat in the horizontal position. A closed end fitted with a water nozzle is on the left and an open end on the right which is able to accommodate the pipe sieve. The bottom right corner of Figure 3.10 shows the pipe sieve in which the coir mat was fabricated. This process uses the concept of turbulence both inside and at the inlet of a pipe to randomly disperse fibres to achieve a randomly distributed non-woven mat.



Figure 3.10 : Pipe mat rig in horizontal position

The volume fractions used in the current research was 7%, 10%, 15% and 20% of coir fibre. The following equation was used to obtain the mass of the coir fibre required, [53] :-

$$Wf = \frac{(Vf\ x\ pf)}{((Vf\ x\ pf)+((1-Vf)\ x\ pm))} \qquad 3.1$$

where:- Wf – weight fraction

Vf – volume fraction of fibre

pf – density of fibre, pm – density of matrix

The equation above generated masses of 10g, 15g, 23g and 31g for the corresponding volume fractions of 7%, 10%, 15% and 20% of coir fibre respectively. The quantity of fibre to be used was then measured on the laboratory scale for the relevant specimens. Figure 3.11 is a flowchart representation of the process that was undertaken to fabricate the coir fibre mat used.

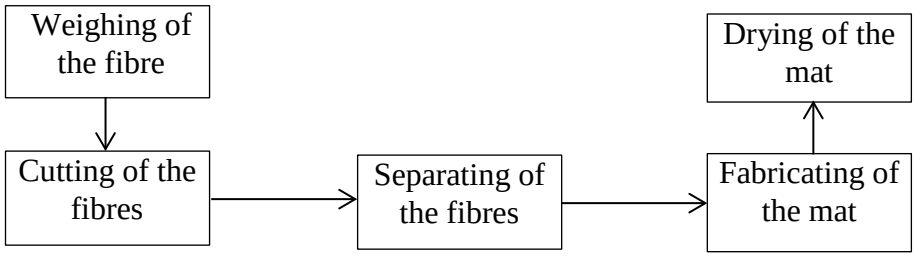


Figure 3.11 : Flowchart representation of the mat manufacturing process

Once the fibres were weighed they were untangled and cut into strips which ranged from 2.5-3 cm in length. The fibres were then separated and put into a container which had been filled with water that allowed the fibres to disperse easily. This procedure prevented clumping of the fibres during the fabrication process. The mat manufacturing rig was setup with water being allowed to enter the bottom of the pipe via the hose connection point. This was done only when the pipe was in the vertical position as in this position the inlet water flow is similar to a fountain and thus creates vortices within the pipe which allows mixing of the fibres to take place. The fibres were then dropped into the pipe when the pipe was less than an eighth full of water. The pipe sieve was then fitted to the exit section of the pipe fastened with a bolt and continued to be filled with water until water began to exit the sieve end of the pipe. The water was turned off and the pipe flipped by 180 degrees, so that all of the water escaped from the pipe through the sieve under gravity. The hose connection was removed immediately, preventing a vacuum from forming. When the water from within the pipe was discharged the pipe had to be perpendicular to the ground as any lateral gravity component would affect the fibre distribution. The pipe was allowed to drain and the sieve end removed containing the randomly distributed fabricated mat. The mat was dried in the oven for 2 hours at 70°C and then left to dry overnight. The

dried mat was then pressed using mild pressure overnight, and then cut into the required square shape as shown in Figure 3.12.



Figure 3.12 : Fabricated mat to be used for composite specimens

The pipe from the mat manufacturing rig needed to be cleaned of all products deposited within by other users prior to use. The sieve has to be fitted as soon as the fibres have been dropped into the pipe to ensure that no fibres are lost when the pipe does over flow, as any loss of fibres resulted in a lower mass of the mat. Care had to be exercised when fitting the sieve into the pipe to prevent the sieve from slipping into the pipe, if the sieve does fall into the pipe it was very difficult to have it removed. The pipe has to be discharged vertically as soon as possible, if this was not done then the mat produced was not evenly distributed.

3.3.2 Composite mould

With vacuum resin transfer moulding being the chosen process to be used for this research a suitable mould had to be constructed to conduct the fabrication of the composite specimens. An initial test mould was fabricated which comprised of two parts, a male and a female mould piece fabricated from carbon steel, a schematic representation of this mould can be seen in Figure 3.13.

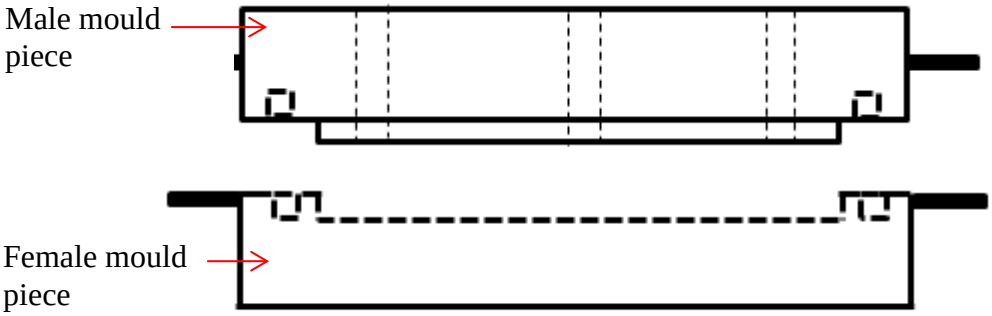


Figure 3.13 : Schematic representation of the first mould used

In conducting test runs with this mould it was noted that a few modifications needed to be made to the mould as suitable composite specimens could not be fabricated. Figure 3.14 shows the male piece of the carbon steel mould that had been used with the relevant labels.

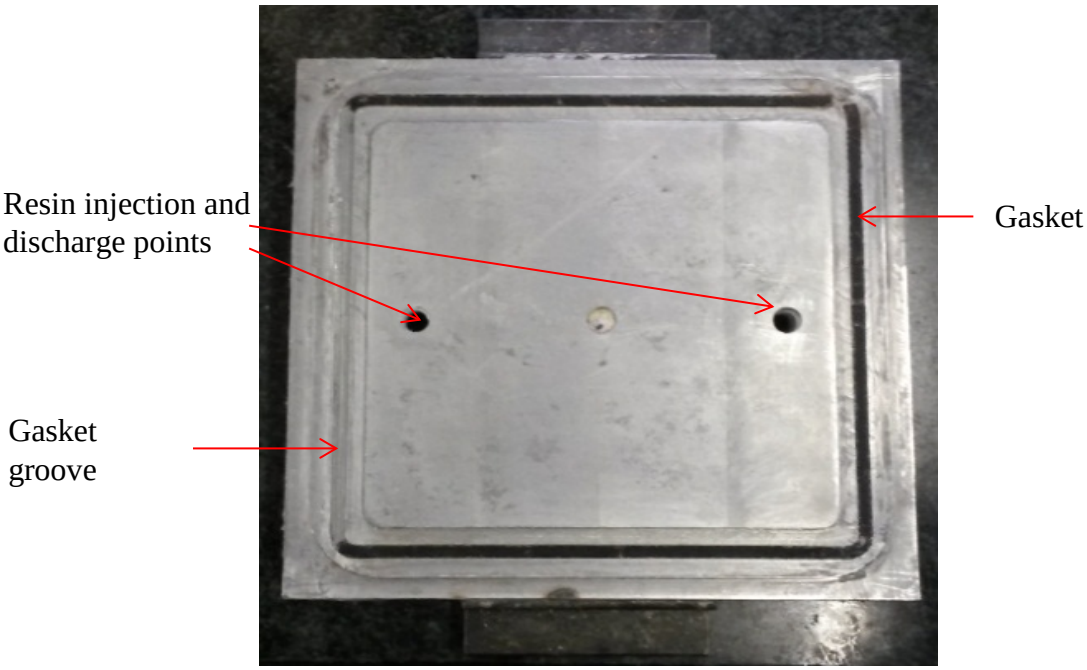


Figure 3.14 : Male mould piece indicating gasket and resin injection/ discharge locations

A test run was done and it was noticed that the mould never filled up completely and thus produced an incomplete specimen. A solution to this was the use of a secondary reservoir also called a resin trap, which was fitted just after the exit port from the mould, however this also did not improve the quality of the specimens.

Removal of the specimens fabricated from this method was a problem, as the design of the mould did not facilitate easy specimen removal. A hammer and a sharp pointed tool or screwdriver needed to be used to remove the specimen. This removal process always resulted in damage to the end points of the specimen. In some instances the specimen cracked causing the specimen to be disregarded. The initial mould was designed with three holes located at the top of the mould, two of the holes are for resin feed into the mould and the other hole was for the vacuum suction line, Figure 3.14.

After running the process and being unable to fabricate good specimens the configuration of the holes was changed to a diagonal orientation which did improve the resin transfer process. The location of the feed and discharge holes in the diagonal orientation were experimented to find the best position of these points to fill the mould properly. The best configuration of the feed and discharge points was when the corner holes of the diagonal were used, one for the resin feed line and the other for the vacuum line with the middle hole sealed off. Figure 3.15, shows an example of the initial mould design being half filled with resin. Due to the composite specimens produced not being of good quality another mould design had been looked at.

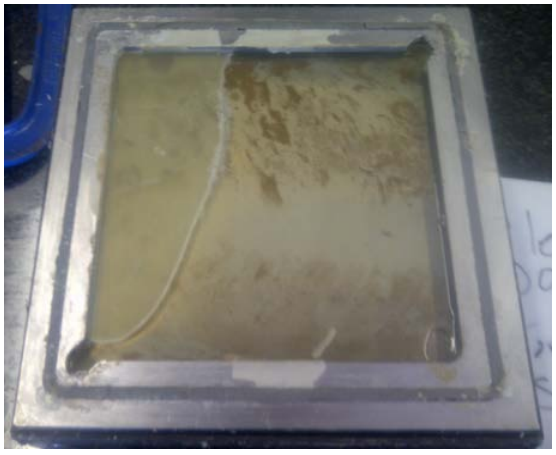


Figure 3.15 : Female mould piece containing the spoiled specimen

A second mould was then fabricated which comprised of three parts two male mould pieces and a single female mould piece, Figure 3.16.

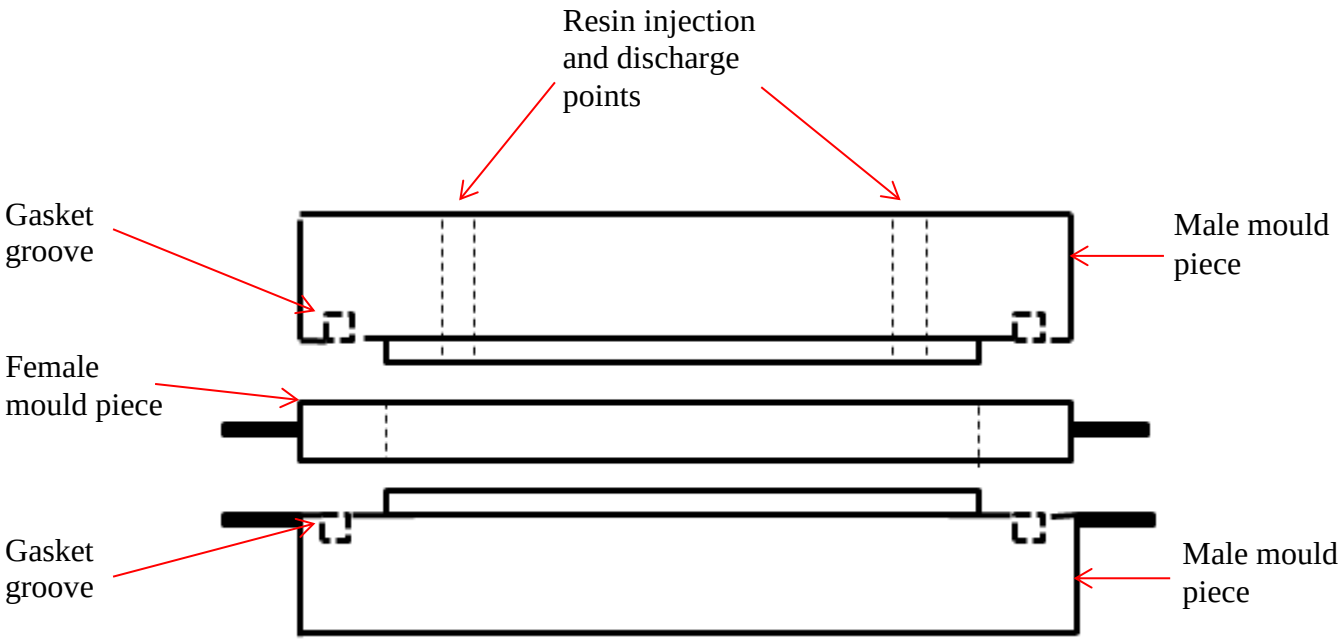


Figure 3.16 : Schematic of the second mould used

Due to the errors that were occurring in the fabrication process it was decided that if one could see what was occurring within the mould a solution could be found. The top piece of the new mould was fabricated from High Density Polyethylene (HDPE) plastic which enabled viewing the flow of resin into the mould. The second male mould piece was located at the bottom of the mould forming the base of the mould which had still been fabricated from steel. The centre mould piece, female component, can then be easily removed containing the composite specimen.

3.3.3 Vacuum Resin Transfer Moulding (VRTM)

With the mould design corrected and being able to produce good quality specimens the remainder of the equipment required for the VRTM process needed to be assembled. Swagelok fittings were used to interconnect the various 6 mm steel pipes used within the setup. A large reservoir was used to prevent the resin from being pulled directly to the vacuum pump causing damage to the vacuum pump. The reservoir also provided the ability of measuring the vacuum pressure in the system with the use of a 100kPa Wika pressure gauge. A resin trap was used to ensure that the mould filled up completely with resin as the resin would collect in the resin trap before flowing to the larger reservoir as shown in Figure

3.19. Ball valves were used in the system to control the flow of either resin or air within the mould. A needle/ throttling valve was used to set the vacuum pressure within the system. The mould was elevated by placing it on a fabricated stand to make working with the mould much easier. The sandwiched mould design had two grooves cut in for the fitment of a gasket to ensure that a good vacuum is held within the mould shown in Figure 3.14. Figure 3.17 and 3.18 shows an actual and schematic representation of the VRTM process respectively.

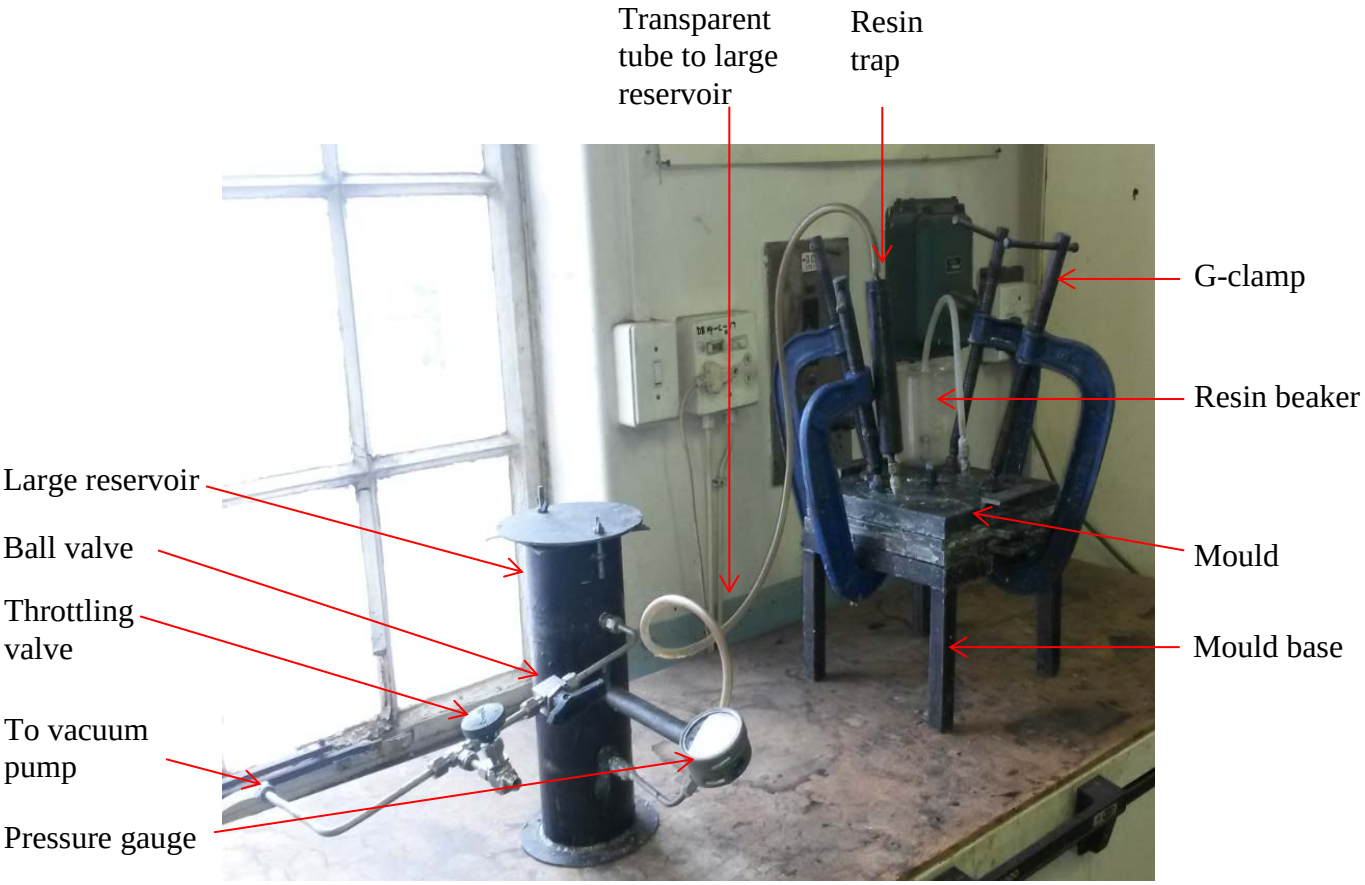


Figure 3.17 : Setup of the system

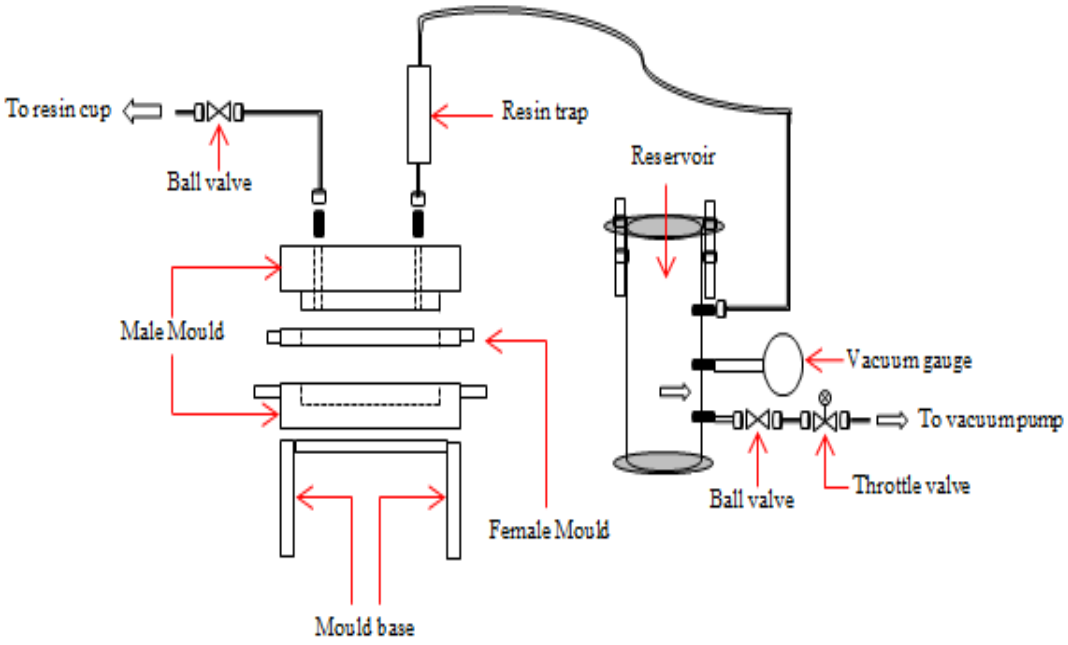


Figure 3.18 : Schematic of the system

All parts of the mould had to be cleaned properly prior to each use to ensure that it did not contain any materials from previous experiments. Once the mould was cleaned the sealing gasket was inspected to ensure that it was suitable for use and can ensure a proper seal, this was done by ensuring that the gasket has a slight ridge above the mould. All of the valves, fittings and pipes needed to be inspected to ensure that they were clean and were able to transport the polymer. The base of the mould was placed on the mould stand with a layer of ram wax applied to the surface of the base mould piece. A thin layer of silicone had been applied on the gasket to ensure that proper sealing takes place. If the mould was not sealed properly then a bad specimen was produced, due to the air leaks that would be present. The female mould section was coated with wax before placing on top of the base male mould section and pressed down. A further layer of wax was put within the mould as some of the wax does rub off while handling the pieces. A layer of wax was then applied to the internal surface of the top male mould piece. With all of the components making up the VRTM system connected the process was run with various vacuum pressures to obtain a suitable pressure set point. It was noted that the vacuum set point pressure required to fabricate a plain epoxy specimen was 30 kPa. If the system was not set at the pressure set point then the specimens produced were unacceptable for use as they contained voids.

3.4 Fibre and hybrid composites fabrication procedure

Fibre composites

All components that were to be used in the VRTM process had to be cleaned before use. This included the mould which was cleaned using acetone, a scraper as well as sandpaper. All tubes and fittings had to be cleaned and blown using an air line. Once this was done the fittings were fastened to the top mould piece, in some instances this was not possible due to the holes being blocked with resin. The injection and discharge holes were then drilled and tapped to thread the holes. A layer of wax was applied to the base of the mould. Coir mats had then been fitted into the mould depending on the volume fraction of the composite being fabricated. The volume fractions of fibre used was 7%, 10%, 15% and 20%

corresponding to mass fractions of 10g, 15g, 23g and 31g. The top mould piece was prepped for use by applying a layer of silicone on the gasket for sealing. The mould was designed to be used by placing the top mould section on top of the sandwiched plate with the weight of the top mould piece to hold the composite material in place during fabrication. However it was observed that the top mould piece was lifting during the filling of the mould. To prevent this from occurring g-clamps were used to clamp the top mould piece as shown in Figure 3.19.



Figure 3.19 : G-clamps used to hold the male mould section in place

The large reservoir designed for the system was assembled which contained three different holes. One was for a pressure gauge to measure the vacuum pressure in the system, the second hole connects to the discharge point located at the top of the mould and the third hole connects to the vacuum pump via a throttling/ needle valve and ball valve to seal the system as shown in Figure 3.20. A combination of transparent and steel pipes were used to connect the mould to the reservoir. The vacuum pump was started with the resin feed hose sealed and was allowed to run until it reached its running capacity. With the resin feed hose sealed the valve at the reservoir was closed, which blocked off the vacuum pump and sealed the system. The system was tested to ensure that it held a vacuum. This process was continued and the mould adjusted until the system showed evidence of no leaks. Once this was achieved the throttle valve was adjusted so that the pressure in the system reached the pressure set-point being 20kPa for the coir fibre composites, which was obtained after numerous trial runs. Once the pressure in the system

reaches the pressure set-point the system was left to run for a minute to ensure that the system stabilizes.

The volume of the mould used was 288 ml, to cater for losses that may occur 300ml of resin was mixed with 75ml of hardener. This was done by mechanical mixing for ten minutes. The mixture was then degassed and left to settle for approximately 5 minutes. The resin was allowed to enter the mould via the resin feed pipe which slowly got sucked up into the mould. The process was only stopped when the level of resin in the mixing cup showed that 300ml of the mixture had been sucked through the system. In some instances there was evidence of resin beginning to exit the small reservoir and moving towards the large reservoir which indicated that the process was complete. The pipes were then disconnected after two minutes of settling and the mould left to settle for five minutes before all of the fittings were removed.

The composite specimen was allowed to stand overnight for 8 hours to cure in the mould. Once 8 hours had elapsed the g-clamps were removed and the mould was split, the composite was then gently removed from the mould. Figure 3.20 shows an example of the composite specimens which was fabricated using the vacuum resin transfer moulding process mentioned above. Figure 3.21 is a flowchart representation of the fabrication process used.



Figure 3.20 : An example of a fabricated composite specimen fabricated

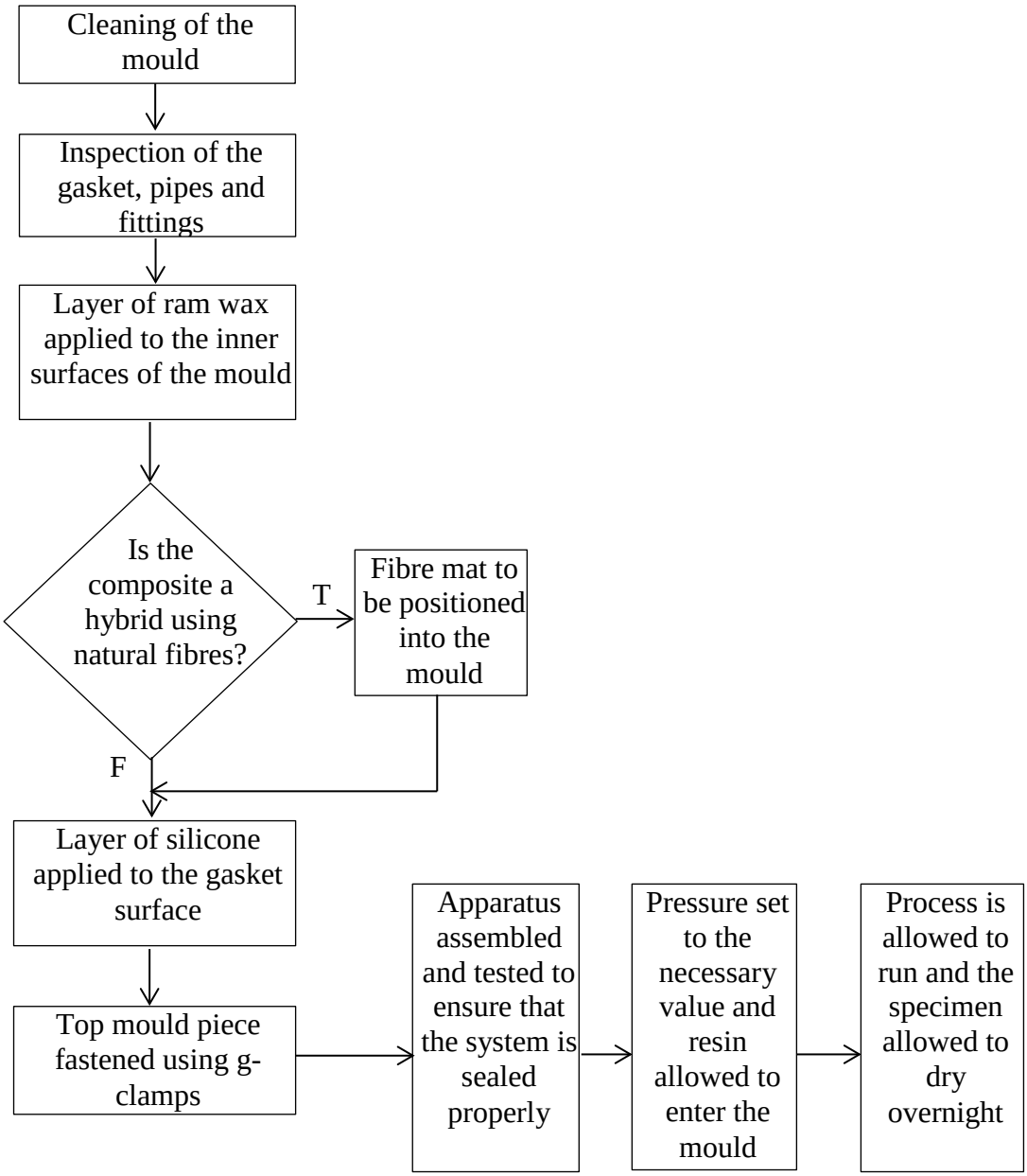


Figure 3.21 : Flowchart representation of the composite fabrication process

During the fabrication of the composite specimens using the VRTM process the researcher made a few observations as to what must be done to ensure that the process runs smoothly. The mould must be positioned properly prior to the tightening of the g-clamps as the mould can be damaged easily. If this is not done then chipping of the top mould piece could occur which would hinder proper sealing of the mould. The g-clamps must be tightened evenly to ensure that an even downward force distribution is exerted on the mould. A proper dry vacuum test must be run once the system is set up to ensure that the system is sealed. Due

to the repetitive use of the fittings they do not seal properly thus prior to use they need to be sealed off with silicone to ensure that no air gets sucked into the mould. Bends in the pipeline should be avoided, the mould was run with pipes containing a few bends which resulted in the formation of air bubbles in the mould.

Once the specimens were manufactured they needed to be cut into their various shapes in order for the relevant tests to be done. The composites laboratory has a Tensilkut cutting machine and a Tensilkut diamond cutting machine which assisted in the preparation of specimens as per the relevant ASTM standards.

Hybrid composites

The hybrid composites were fabricated using a similar process as described for the fibre composites. There were two modifications done for the hybrid fabrication process which included mixing of the resin with the MWCNT, glass or clay particles and the pressure set point was varied for the different weight fractions of reinforcement used. The hybrid composites were fabricated by mixing the resin and the reinforcement being either MWCNT, clay or glass with a magnetic stirrer for 45 minutes at ambient temperature. The hardener was added to the mixture and the entire mixture mechanically stirred for ten minutes. The mixture was then degassed and left to stand for 5 minutes and then used in the VRTM process as described above.

The weight fraction of the reinforcements used in the hybrid composites had been obtained by using the following equation, [58]:-

$$Wf = \frac{(Vre\ x\ pre)}{((Vre\ x\ pre)+\left(\left(1-(Vre+Vf)\right)\ x\ pr\right)+(Vf\ x\ pf))} \qquad 3.2$$

where:- Wf – weight fraction
Vre – volume of reinforcement
Vf – volume fraction of fibre
Vr – volume of resin

pf – density of fibre

pre – density of reinforcement

pr – density of resin

Four different weight fractions were used for the hybrid-CNT composites which were 0.1%, 0.5%, 1.5% and 2% which resulted in masses of 0.5g, 2.5g, 7.4g and 9.6g respectively. It was found that for the lower weight fractions the vacuum pressure had to be set to 15 kPa but for the 1.5% and 2% weight fractions the vacuum pressure was set to 9 kPa which ensured fabrication of good composite specimens. The weight fractions used for the hybrid-clay composites were 0.1%, 0.5%, 2%, 4%, 5% and 6% resulting in masses of 0.5g, 2.6g, 10.2g, 20g, 24.6g and 29.2g respectively. A vacuum pressure of 15 kPa was sufficient to fabricate the 0.1%, 0.5% and the 2% hybrid-clay composites however, for the 4%, 5% and 6% weight fractions the vacuum pressure was reduced to 7 kPa. For the hybrid-glass composites weight fractions of 0.1%, 0.5%, 2%, 4%, 8% and 12% were used with their respective masses being 0.3g, 1.3g, 5.2g, 10.5g, 20.8g and 31.2g as per the equation above. A vacuum pressure of 15 kPa was used for the 0.1%, 0.5% and 2% weight fractions with the 4%, 8% and 12% using a vacuum pressure of 9 kPa.

3.5 Particulate composites

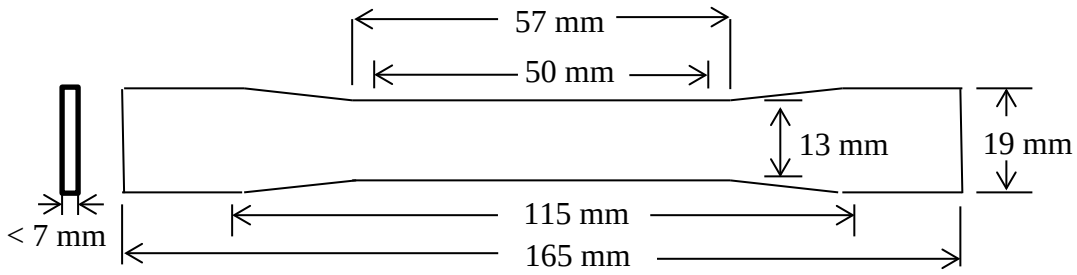
Epoxy-clay and epoxy-glass composites were fabricated to observe the difference in properties between hybrid composites and normal composites. Both the epoxy-clay and epoxy-glass composites were fabricated using 0.1%, 0.5% and 2% weight fractions of reinforcement. This resulted in masses of 0.24g, 1.19g and 4.75g for the respective weight fractions used for the epoxy-glass composite. The epoxy-clay composites had masses of 0.47g, 2.36g and 9.3g for their respective weight fractions. The process followed was the same as the process followed for the fibre composites but without the use of fibre. The vacuum pressure required to fabricate these specimens was 20kPa. Once fabricated these specimens were cut and prepared for testing using the laboratory equipment.

3.6 Mechanical testing procedures

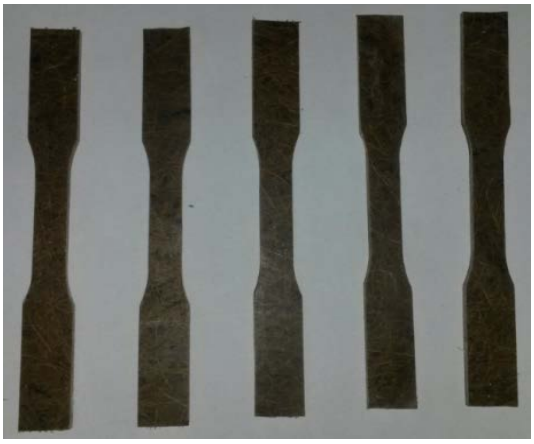
The composite specimens were subjected to mechanical testing to observe their respective properties to determine if the composite materials have enhanced properties or not. Three different types of tests were conducted on the specimens which include tensile, flexural and impact tests. The tensile tests were conducted as per ASTM D638 – 03 on a JJ Lloyd MX 100 testing machine. The cross head speed indicated in the standard shows a speed of 5 mm/min is to be used provided that the specimen can be tested over a 30 second period however the specimens failed in less than 10 seconds. Research conducted by Muthu et al. [59] showed that good results were obtained at a cross head speed of 1 mm/min. During the running of the experiments it was noted that the specimens failed over a 30 second period and thus all of the specimens were tested at a 1 mm/min cross head rate. Flexural testing of the specimens was conducted as per ASTM D790 – 03 on a Shimadzu Universal testing machine. The cross head speed used as stipulated in this standard is 2 mm/min with all of the specimens failing adequately as required in the standard. Impact testing of the specimens was conducted as per ASTM D256 – 03 on an Avery impact testing machine. All of the three standards used stipulates a minimum of 5 specimens to be tested for each composite material and thus was the standard followed for the current research.

3.6.1 Tensile Testing Procedure

Preparation of the specimens required to conduct the tensile tests was done using laboratory equipment. The diamond disc cutter was used which cut the specimens from the square specimen plate, 190mm x 190mm, to rectangular shaped specimens 20mm in width and 190mm in length. ASTM D638 indicates that all specimens need to be cut into dog bone specimens. The materials laboratory facility has a dog bone shaped mould which clamps a specimen and cuts it down to the required size using the diamond cutter. The 190mm long rectangles were then cut to the required specimen dimensions indicated on Figure 3.22(a) using the diamond cutter. Figure 3.22(b) shows a representation of the specimens after preparation for testing.



(a) Specimen dimensions for Tensile Testing



(b) Tensile testing specimens fabricated and prepared for testing

Figure 3.22 : Tensile testing specimens

Tensile tests were carried out using a JJ Lloyd testing machine. Various jaw grips were available for the machine and a suitable set of jaw grips had been selected which matched the requirements listed in ASTM D638. A 5kN load cell was used on the machine to conduct the tensile testing. The displacement of the specimen was measured using an external extensometer which is able to measure change in displacement over the 50mm gauge length. The experimental data was recorded using a Lloyd MX100K built-in data acquisition (encoder) system.

The width and thickness of each specimen was measured and recorded. The correct testing jig was fitted into the machine and the software program started. Once all of the relevant settings were entered into the Mat test program the program was ready for the test specimens which were positioned into the jig centrally. The extensometer was then clamped onto the gauge length portion of

the specimen and the machine reset. The program was started and run at a 1 mm/min cross head speed until the specimen failed. The data was saved immediately and the same process followed for the remaining specimens.

The formula used to calculate the tensile strength of the composites was obtained from ASTM D638:

$$\sigma = \frac{F}{(w\ x\ t)} \qquad 3.3$$

Where σ - tensile strength

F - applied load

w - width of specimen

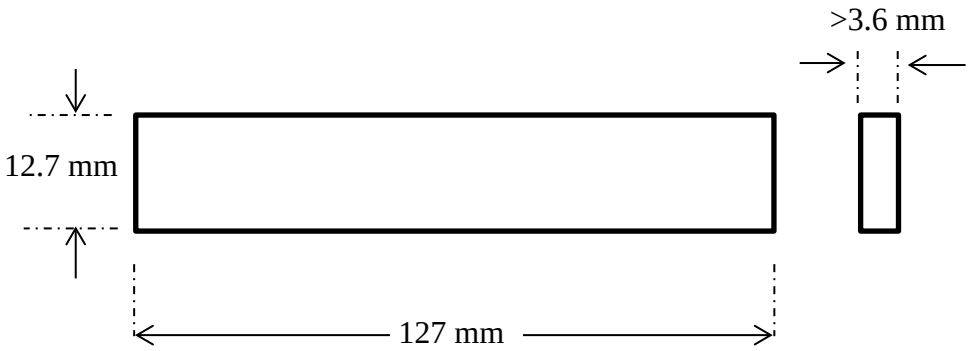
t - thickness of specimen

The equation used to calculate the elastic modulus of the specimens was E = ΔStress/ ΔStrain, which was calculated from the stress vs strain plot generated for each specimen.

The tensile testing process resulted in a few observations being made such as the specimens need to be properly aligned and tightened when fitted into the grips. The extensometer must be fitted the correct way around to get proper readings. The software must be reset before each use and once the test is complete the data must be saved immediately else there is a risk of a sample being tested and the data being overwritten.

3.6.2 Flexural Testing Procedure

Flexural testing of the specimens was done on a Shimadzu precision universal testing machine according to ASTM D790 standards. The specimens were cut as per the dimensions stipulated in ASTM D790 which is shown in Figure 3.23(a), using the band saw machine. Figure 3.23(b) is a representation of the specimens cut and prepared for testing.



(a) : Flexural testing specimen dimensions



(b) : Flexural testing specimens fabricated and prepared for testing

Figure 3.23 : Flexural testing specimens

The width and thickness of the specimens were measured. The flexural base jig, support span, was adjusted to allow for the specimens to fit in as per ASTM D790, with each end point being 63mm from the centre of the specimen. Figure 3.24 is a representation of the setup used for the flexural testing procedure. The Trapezium software program was then started and the program set up to begin the testing procedure. The machine has a built in encoder to capture the required data. The specimens were positioned in place with the loading nose placed at the central point of the specimen. The machine was reset and the program started and run at a cross head speed of 2 mm/ min until the specimen failed. Once the specimen failed the machine was returned to its starting position and reset with the same procedure followed for the remaining specimens.

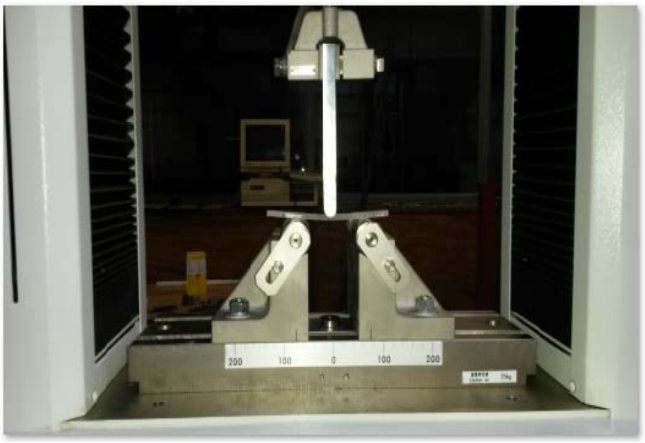


Figure 3.24 : Flexural testing of composite specimens

The equation used to calculate the flexural stress for the composite materials was obtained from ASTM D790:

$$\sigma f = \frac{3PL}{(2bd^2)} \qquad 3.4$$

Where σf = flexural strength

P – applied load

L – support span

b – width of specimen

d – depth of specimen

The equation used to calculate the tangent modulus of elasticity was obtained from ASTM D790:

$$E_B = \frac{(L^3 m)}{(4bd^3)} \qquad 3.5$$

Where E_B - tangent modulus of elasticity

L - support span

b – width of specimen

d – depth of specimen

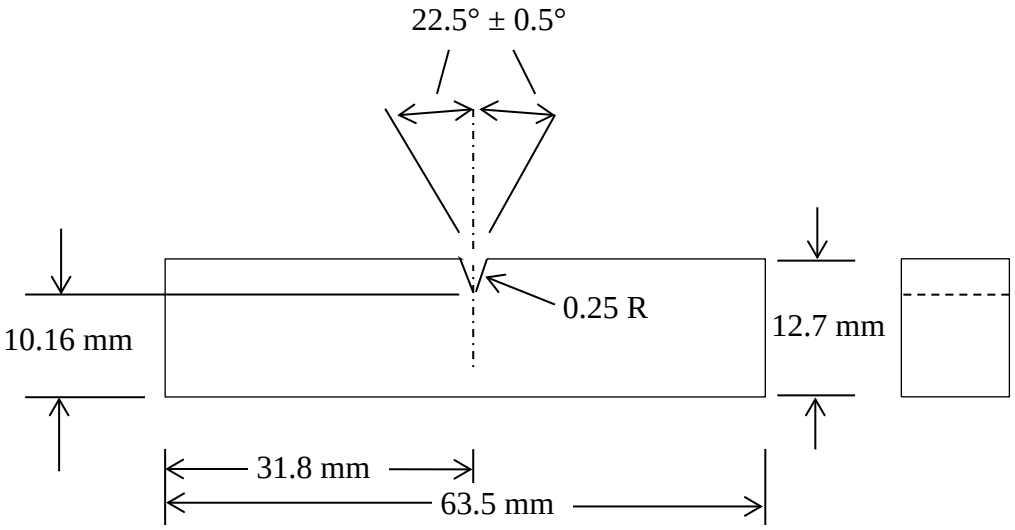
m - slope of the tangent line of the load-deflection curve

The flexural testing of the specimens resulted in a few precautions to be made which included that the sample must be properly aligned prior to running of the

test and the load bar should be brought as close as possible to the specimen, due to the slow rate of travel unnecessary time was wasted if the load bar had to free travel. Upon completion of the testing saving of the data was important to ensure that the test data was captured.

3.6.3 Impact Testing Procedure

Impact testing on the specimens was conducted on an Avery Impact testing machine. This machine comprises of a pendulum which when released swings onto a test specimen fixed at the bottom of the machine using the clamping device present on the machine. Upon impact of the pendulum with the specimen the dial indicator indicates the energy absorbed by the specimen. The specimen was cut to dimensions indicated in ASTM D256 standards, shown in Figure 3.25(a) using both the diamond cutting machine as well as a band saw machine. Figure 3.25(b) shows a representation of the specimens before being subjected to impact testing.



(a) : Specimen dimensions for Impact testing



(b) : Impact testing specimens fabricated and prepared for testing

Figure 3.25 : Impact testing specimens

The thickness and width of each specimen had been measured. The pendulum was clipped into its locking position and the dial indicator moved to the 4.2J position on the scale. The specimen was then fitted into the equipment base and clamped into position. The pendulum was released and allowed to impact with the specimen, the value at which the dial indicator stopped was recorded. The specimen was then released from the grips and the procedure repeated for all specimens thereafter.

The fracture toughness was calculated using the following equation :

$$K1c = Y1 \; x \; \sigma \; x \; \sqrt{(\Pi \; x \; c)} \qquad 3.6$$

Where : K1c – fracture toughness
Y1 – geometry factor
σ – stress (energy/ area)
c – crack length

When conducting the test it is important that the specimens slot easily into the specimen slot, if the specimen is held too tightly then incorrect readings will be obtained.

3.7 Morphological Characterization

Morphological characterisation of the CNT and clay particles was carried out using a FEI Technai T12 (80-120 kV) Transmission Electron Microscope (TEM). SEM for the current research was conducted on a Carl Zeiss Sigma FESEM equipped with an EDX detector for elemental analysis. Three different types of detectors were used SE2 - secondary electrode, NTSBS – back scatter detector and the SEI – Iulens depending on the type of image required. Before using the SEM the samples were coated with a 15nm layer of palladium in an Emitech K550X sputter coater. The specimens were then attached to 1cm diameter stubs with carbon tape. The Raman analysis was conducted on the 514.5nm line of an argon ion laser as the excitation source, and the instrument used was a Horiba Jobin-Yvon Lab RAM HR Raman spectrometer. The FTIR analysis was conducted on a Bruker Vector 22 FT-IR spectrometer using 64 sample scans and 32 background scans to obtain the results.

4 RESULTS AND DISCUSSION

Composite materials were fabricated using epoxy resin and coir fibre which had undergone tensile, flexural and impact tests as per ASTM D638, ASTM D790 and ASTM D256 standards respectively. This was done to determine what volume fraction of coir fibre would generate the best mechanical properties. Hybrid composites were then fabricated using three different reinforcement materials being CNT, glass and clay as the second reinforcement. Clay and glass were selected as they are some of the most common reinforcement materials used in composites and the mechanical properties of these reinforcements together with coir fibre was to be investigated. MWCNT was chosen as there is a lot of research conducted using CNT but not many on hybrid coir fibre composites, the mechanical properties of these composites was to be investigated. Functionalization treatments were conducted on the MWCNT and clay particles prior to use, this was done to enhance the bonding ability and dispersion of these particles in the composite. The functionalized particles were analysed using TEM, Raman and FTIR analysis methods to determine which treatment produced the best results for the particles. The optimum volume fraction of coir fibre was used to fabricate hybrid composites using MWCNT, glass and clay as the second reinforcement to obtain the optimum composite for the different weight fractions of the second reinforcement selected. The mechanical properties of the hybrid composites were reviewed to ascertain which reinforcement generated the best mechanical properties. Epoxy-clay and epoxy-glass composites were fabricated to observe the difference in mechanical properties in comparison to the respective hybrid composites.

4.1 Epoxy-coir composites

The fabrication of the coir composites required good bonding between the coir fibres and the epoxy matrix to produce good composites. As mentioned above coir fibres have high lignin and cellulose content which must be removed in order to achieve good bonding. Rout et al. [30] found that a sodium hydroxide (NaOH) treatment on the fibres aids in the removal of the lignin and cellulose to produce a good composite. For this research two different NaOH treatments were used, one

with a 10% w/v solution and the other a 20% w/v solution. Figure 4.1 shows an SEM image of a raw coir fibre strand. Here it can be seen that there is a large amount of cellulose and lignin which encased the fibre completely. Figure 4.2 shows an SEM image of the coir fibres treated with a 10% w/v NaOH solution. Here it can be seen that a lot of the cellulose and lignin was removed as the internal strands within the coir fibre have been exposed. Much more reactive sites can be seen which shows that good bonding can take place between the epoxy and the fibres. Figure 4.3 shows an SEM image for the coir fibres treated with a 20% w/v NaOH solution. Although the cellulose and lignin was removed from the fibre it can also been seen that the internal fibres were damaged due to the treatment. This can be noted by the broken fibres in Figure 4.3. These broken fibres would reduce the strength of the coir fibres and thus the chosen treatment for the coir fibres was a 10% w/v NaOH solution.

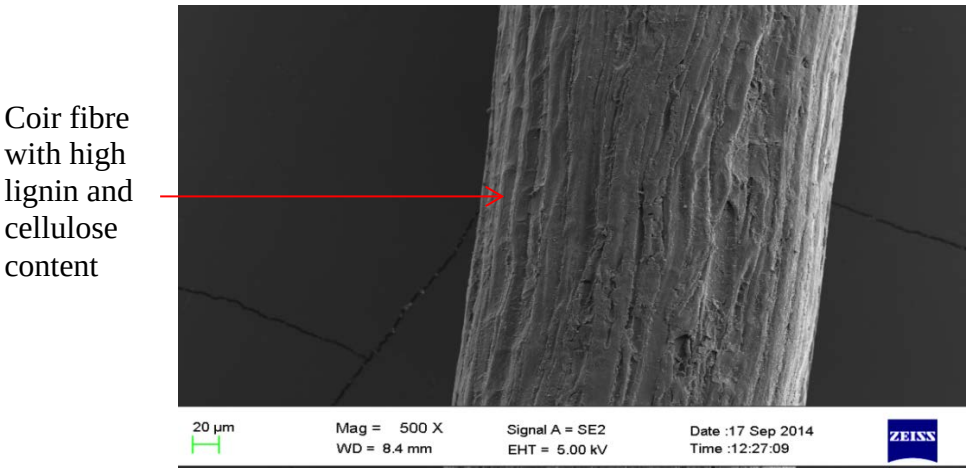


Figure 4.1 : SEM image of a raw coir fibre

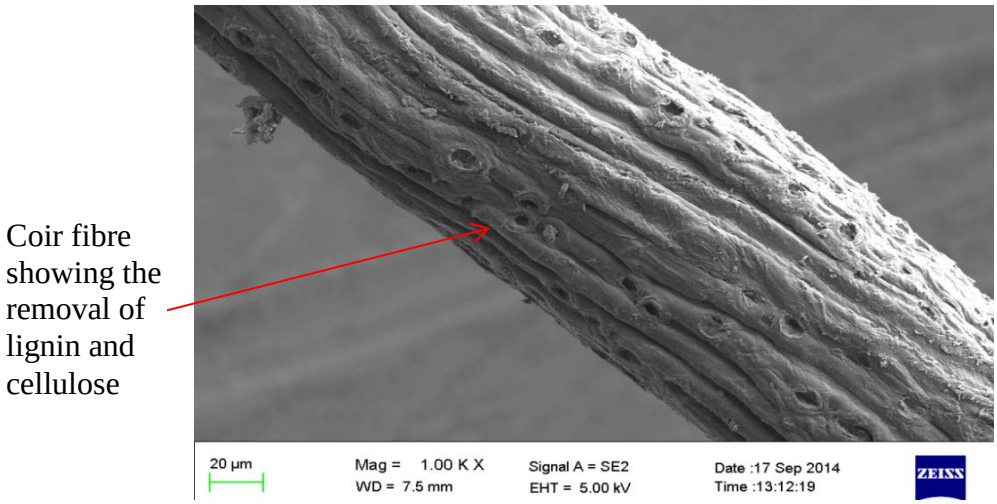


Figure 4.2 : SEM image of coir fibre treated with a 10% w/v NaOH solution

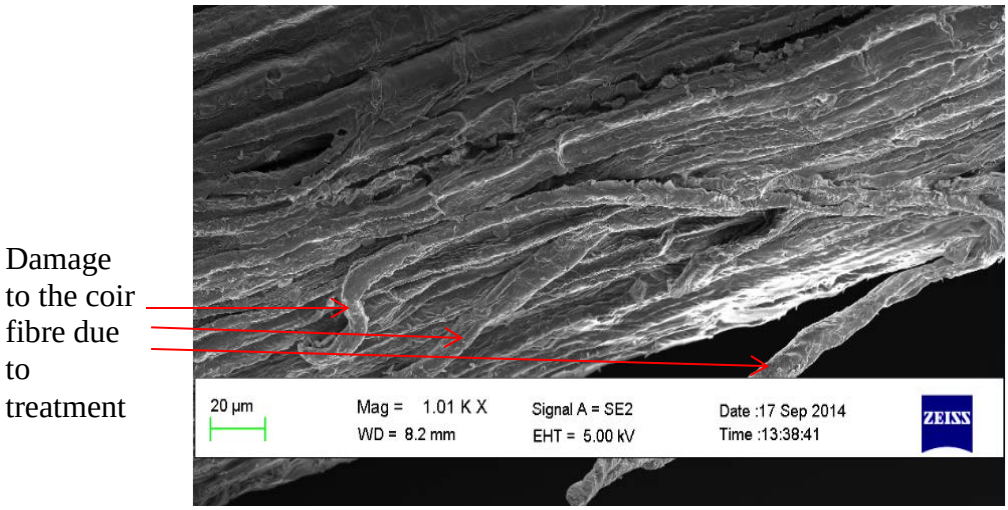


Figure 4.3 : SEM image of coir fibre treated with a 20% w/v NaOH solution

4.1.1 Tensile Testing Results

Tensile testing of the composites were conducted as per ASTM 638 on a JJ Lloyd testing machine with a minimum of five samples tested for the different volume fractions of coir fibre used. The specimens were fabricated with volume fractions of 7%, 10%, 15% and 20% of coir fibre and tested at a cross head speed of 1mm/min. The displacement of the specimens was measured using an external extensometer. Figure 4.4 shows the tensile strength of epoxy-coir composites in

comparison to plain epoxy. It can be seen that the addition of coir fibre to epoxy increased the tensile strength of the composite specimens. A 15% volume fraction of coir fibre shows the highest tensile strength among the composites tested being 28 MPa which is a 33% increase in strength in comparison to the plain epoxy composite with a tensile strength of 21 MPa.

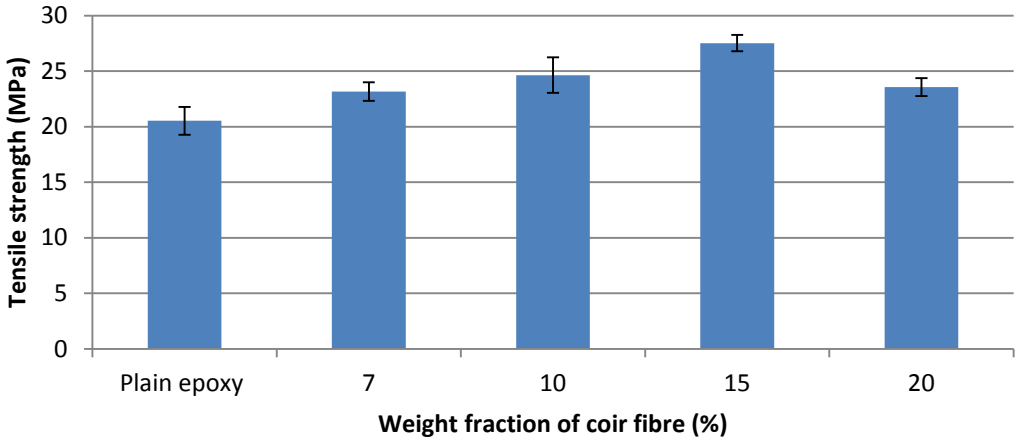


Figure 4.4 : Tensile strength of coir specimens

Figure 4.5 shows the elastic modulus of the coir fibre specimens and indicates that the elastic modulus obtained for the plain epoxy composite is 0.46 GPa. The 7% coir composite generated a 20% increase in the modulus in comparison to plain epoxy. As the volume fraction of coir fibre increased so did the modulus until the 15% volume fraction which produced the highest modulus of 0.68 GPa. A 20% weight fraction of fibre resulted in a drop in the elastic modulus from the 15% volume fraction by 13%, thus showing a decrease in the properties of this composite.

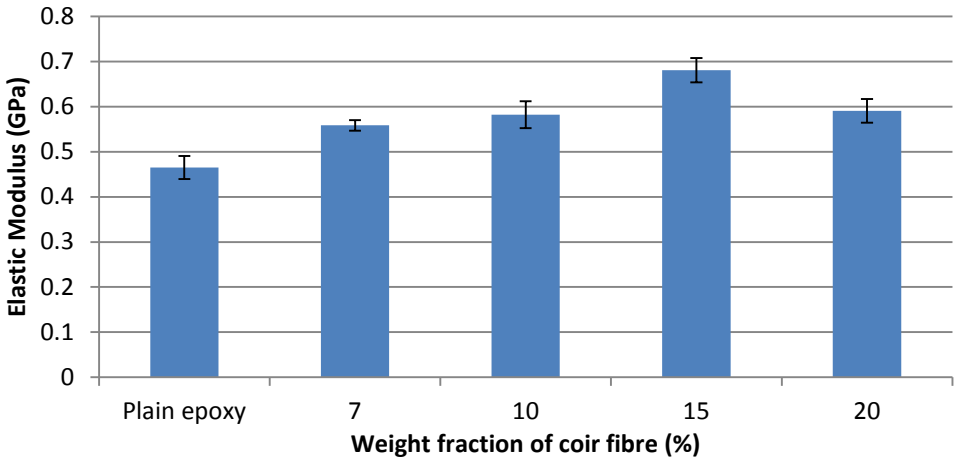


Figure 4.5 : Elastic modulus of coir specimens

Figures 4.6 and 4.7 show SEM images of the 15% and 20% coir composites. Since the fibres were pre-treated with the NaOH solution good bonding can be seen between the fibres and the matrix with no fibre pull out. This confirms that the surface treatment used on the fibres was successful. In Figure 4.7 it can be seen that there is a larger concentration of fibres which results in more bonding sites. Due to this the fibres bonded to each other rather than the matrix which reduced the strength of the composites. This also resulted in the 20% volume fraction of coir producing lower properties than the 15% volume fraction. Romli et al. [41] conducted research with epoxy-coir composites and had also found that a 15% volume fraction of coir produced the highest tensile strength amongst the tests conducted.

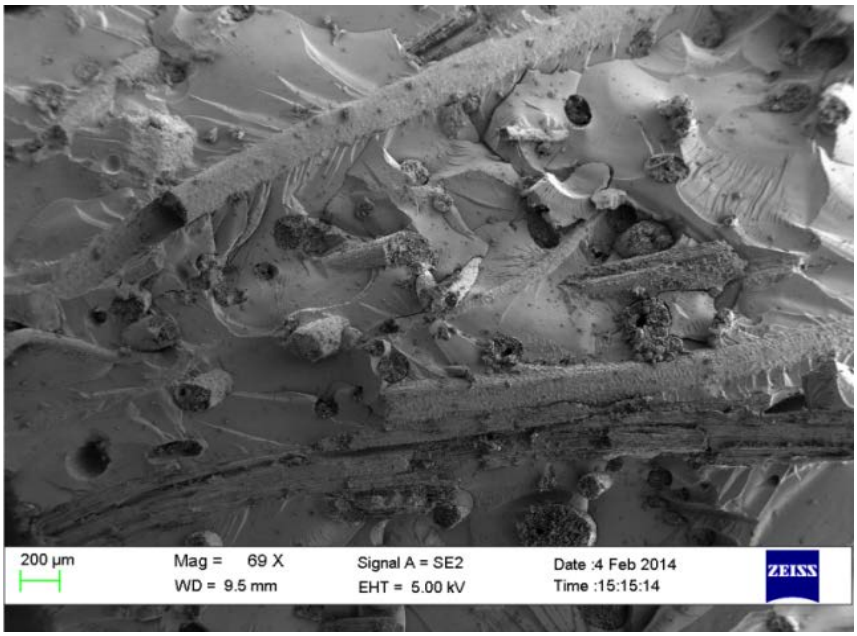


Figure 4.6 : SEM image of the 15% coir tensile specimen

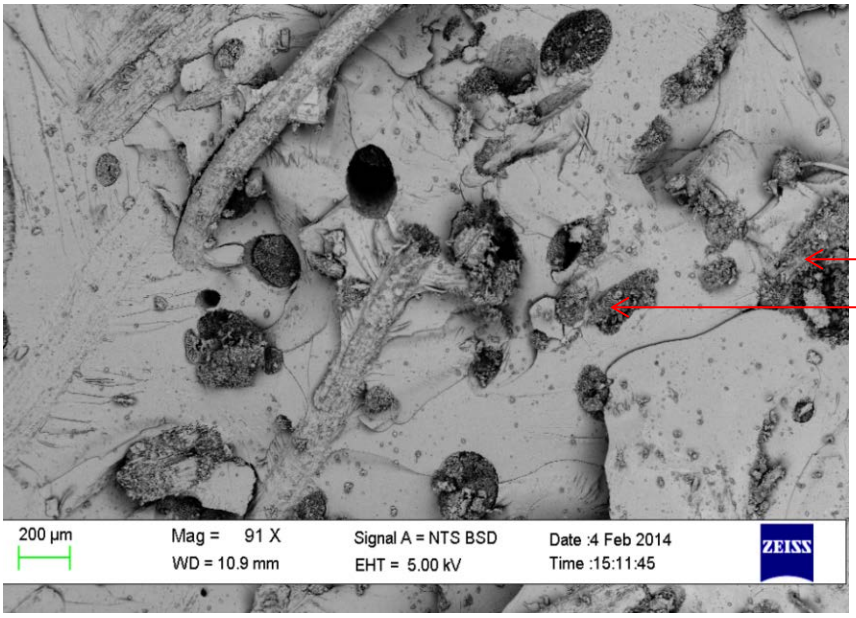


Figure 4.7 : SEM image of the 20% coir tensile specimen

4.1.2 Flexural Testing Results

Flexural testing of the specimens was performed to observe the resistance of the specimens to bending. The coir composites were compared to plain epoxy to determine the effect that the coir reinforcement has on the properties of the composite. Figure 4.8 shows the flexural stress obtained for the coir composites,

the 15% coir composite shows a 39% increase in flexural strength in comparison to plain epoxy with a value of 54 MPa. Even a volume fraction of 7% of coir shows a 2% increase in the flexural strength indicating that the flexural strength increased upon the addition of the coir fibre. A 20% addition of coir fibre reduced the flexural strength by 3% from the 15% coir fibre composite indicating that a 15% volume fraction of coir generates the highest flexural strength. Figure 4.10 shows an SEM image of the 15% composite specimen, it can be seen that there is good interfacial bond strength between the fibres and the matrix confirming that the fibre treatment was successful. The reduction in the properties of the 20% composite is due to the larger fibre quantity as shown in Figure 4.11. The larger quantity of fibres used reduced the ability of bonding between the matrix and the fibres from occurring thus reducing its properties.

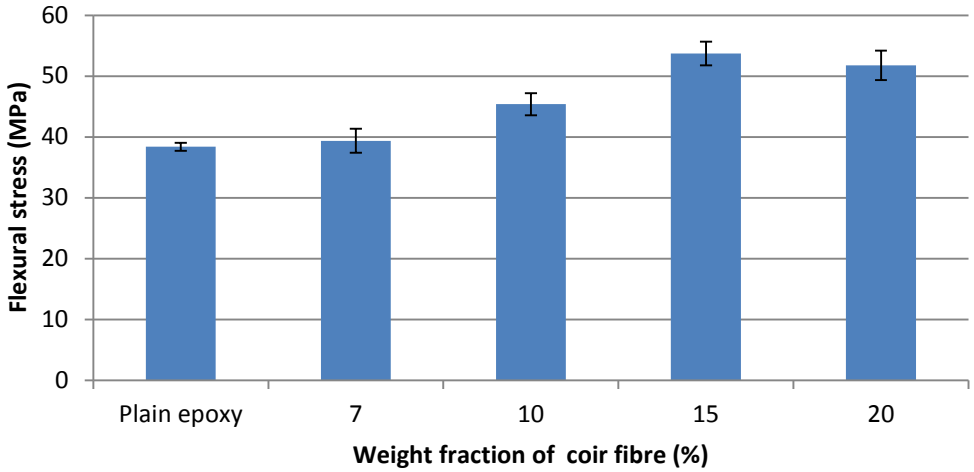


Figure 4.8 : Flexural strength of coir specimens

Tangent modulus is the ratio of stress to strain within the elastic limit of the flexural tests. The tangent modulus was calculated for the different volume fractions of coir fibre composites and is shown in Figure 4.9. The highest tangent modulus obtained for the composite specimens is for the 20% coir specimen which shows that the modulus increased as the volume fraction of coir fibre increased. Although the flexural strength was reduced at a 20% volume fraction of coir fibre, the tangent modulus of the specimen increased showing an increase in the stress-strain ratio of the composite. This increase in modulus is due to the

good bonding that had taken place between the matrix and the fibre due to the NaOH fibre treatment. Romli et al. [41] found that the highest flexural strength obtained for epoxy-coir composites is with the use of a 15% volume fraction of coir fibre.

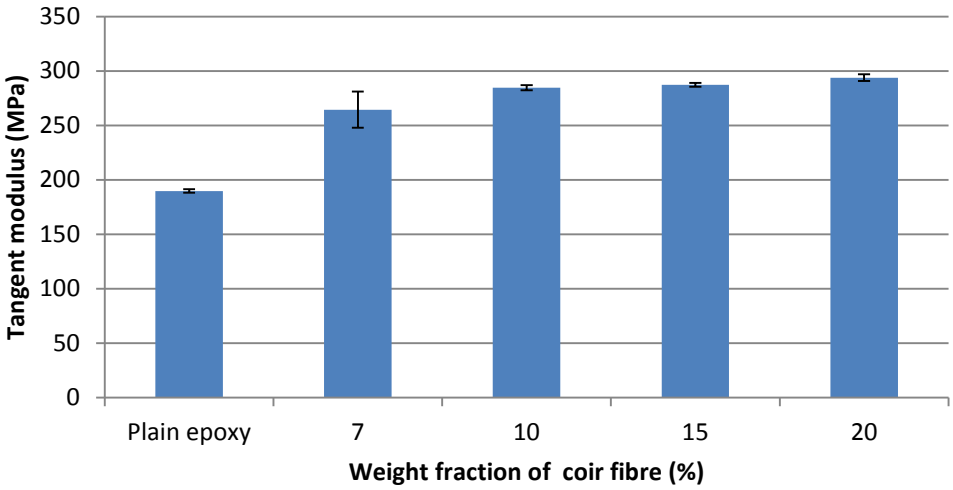


Figure 4.9 : Tangent modulus of coir specimens

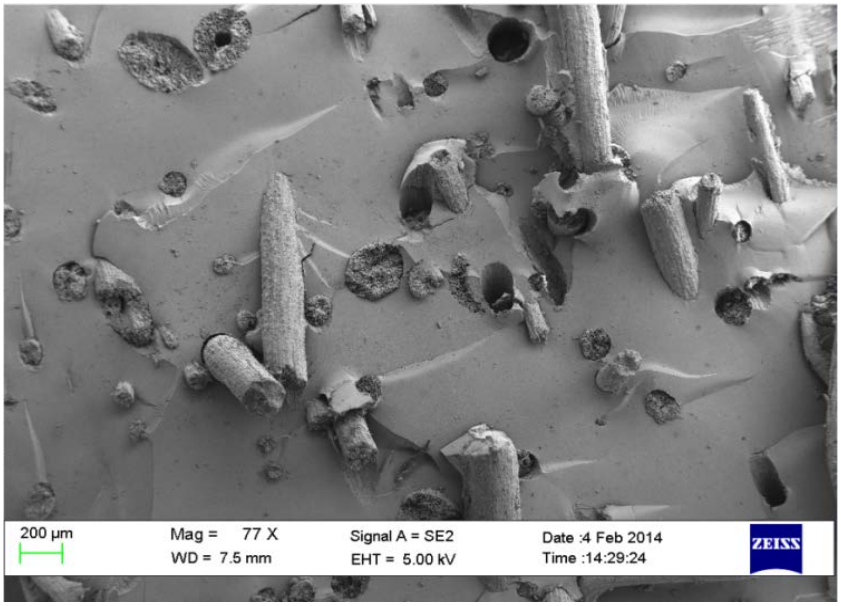


Figure 4.10 : SEM image of the 15% coir flexural specimen

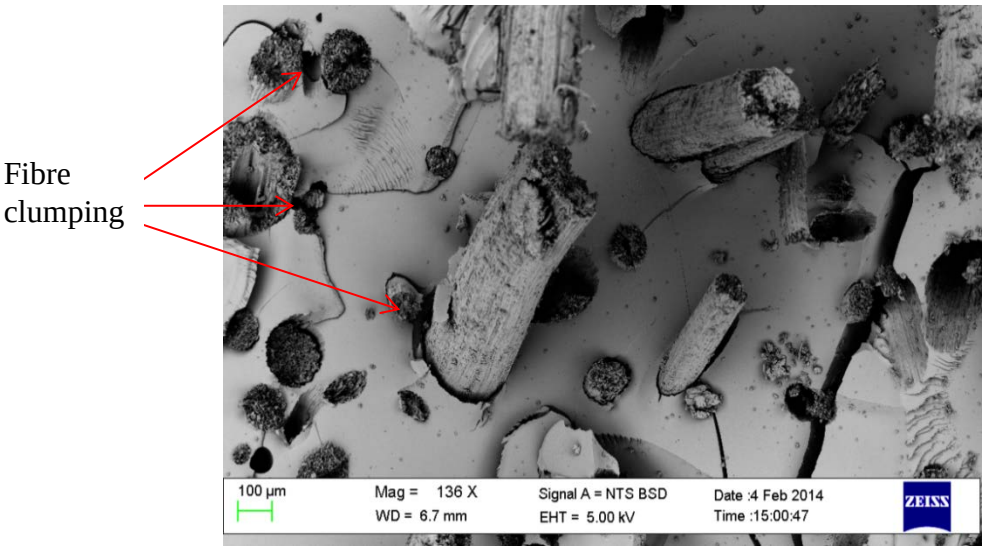


Figure 4.11 : SEM image of the 20% coir flexural specimen

4.1.3 Impact Testing Results

Impact tests were conducted for the coir composites, with volume fractions of 7%, 10%, 15% and 20% of coir fibre as per ASTM D256. The results shown in Figure 4.12 indicate that the 15% coir composite displays the highest fracture toughness of 0.0008126 MPa√m which is a 62% increase in comparison to plain epoxy, with a fracture toughness of 0.0005 MPa√m. A 6% reduction in fracture toughness was observed when the volume fraction of coir fibre was increased to 20% from 15%. The reduction in the fracture toughness of the 20% composite was due to the higher quantity of fibres used that resulted in reduced interfacial adhesion between the fibres and the matrix as indicated in Figures 4.7 and 4.11. Figures 4.7 and 4.11 also show that the load had not been effectively transferred from the matrix to the fibre which is shown by the matrix cracking that is also a result of the higher fibre volume.

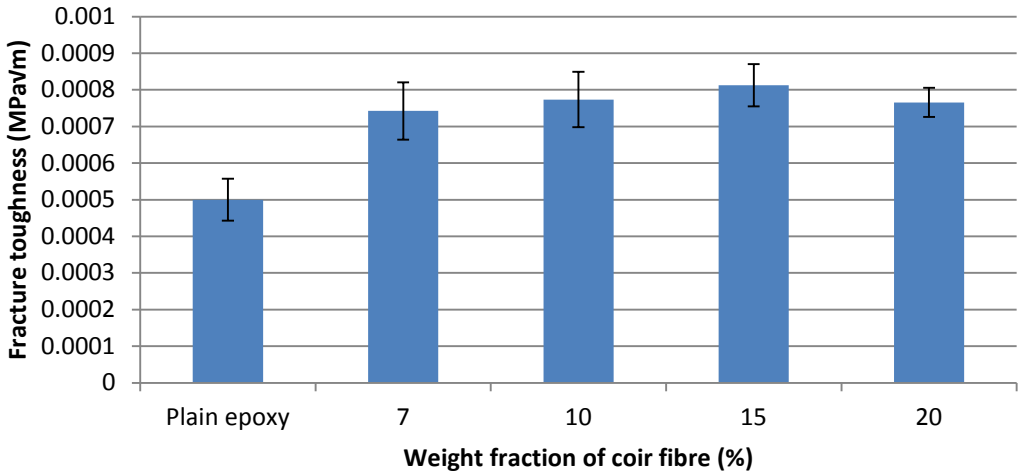


Figure 4.12 : Fracture toughness of coir specimens

All three of the mechanical tests conducted showed that the 15% volume fraction of coir fibre exhibited the best properties. It was then decided that the optimum volume fraction of coir fibre is 15% and would be used to fabricate the hybrid composites.

4.2 Functionalization

As mentioned in Chapter 3, surface modification or functionalization of the CNT and clay reinforcements used in the current research is crucial to ensure that these materials have functional groups created on their surface to improve dispersion and chemical interaction between materials. Chemical treatments were done to create OH and COOH functional groups on the materials which would assist in the dispersing and bonding of these materials to the matrix. The results of the functionalized reinforcements were analysed by three different analysing methods being TEM, Raman and FTIR.

4.2.1 Functionalization of MWCNT

Acid functionalization of the MWCNT particles was done using sulphuric acid and nitric acid over a 12 hour and 48 hour period to determine which treatment period would create the best functional groups on its surface without causing any damage to the MWCNT.

Figure 4.13 shows the TEM image of the pristine MWCNT particles, it can be seen that the tube structures are not clear with traces on amorphous carbon materials remaining on the tubes. Figure 4.14 shows the MWCNT which was functionalized for 12 hours, showing clean tube walls with no visible defects on the tube structure. Figure 4.15 shows the TEM structure for CNT particles treated over 48 hours, the tube structures for this sample were damaged due to the prolonged exposure of the MWCNT to the acid. The TEM analysis shows that a 48 hour functionalization treatment is not suitable and a 12 hour functionalization treatment is feasible.

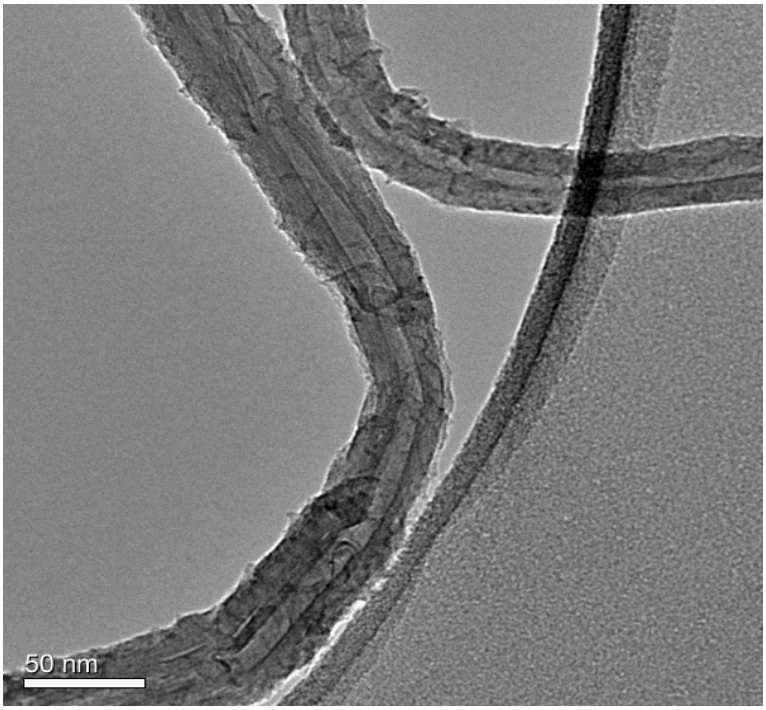


Figure 4.13 : TEM image of Pristine MWCNT

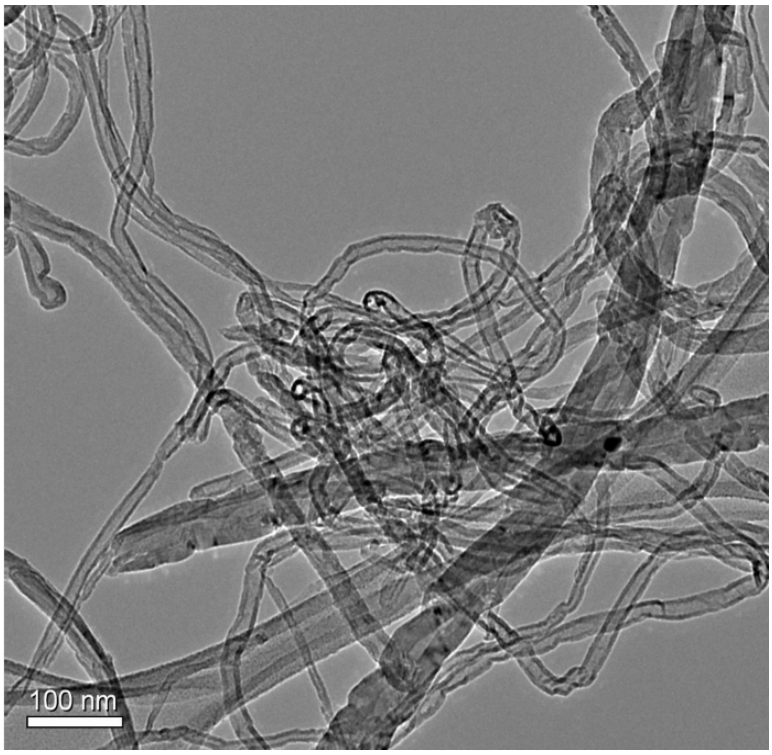


Figure 4.14 : TEM image of MWCNT after 12 hours of functionalization

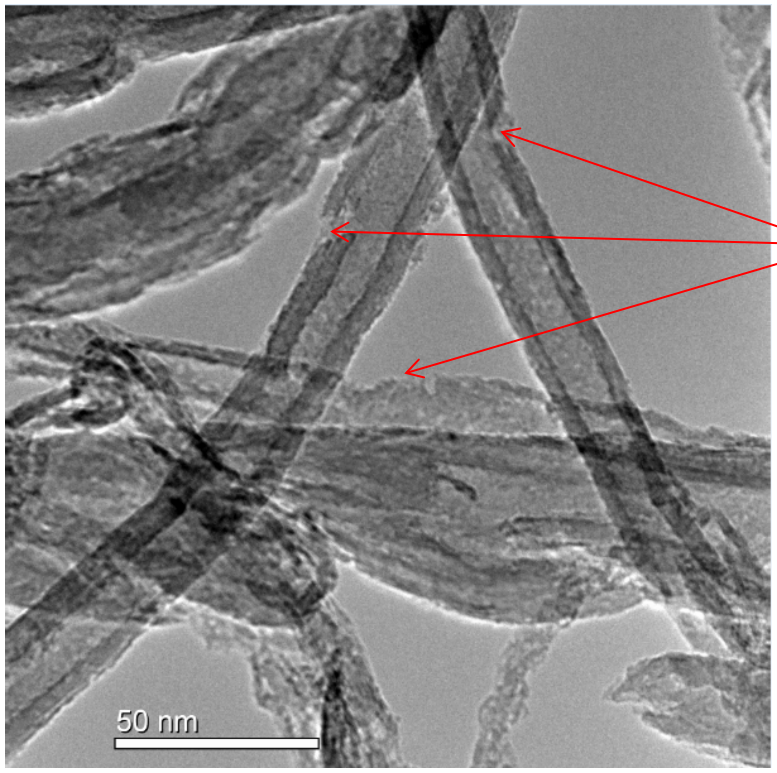


Figure 4.15 : TEM image of MWCNT after 48 hours of functionalization

The Raman spectrum of MWCNT is interpreted by the use of two different bands, the tangential G-band which runs from 1550 -1650 cm^{-1} and the disorder induced D-band which is found at approximately 1360 cm^{-1} [32, 50]. The D-band is due to defective sites in the hexagonal framework of the MWCNT such as the formation of carboxyl groups on the surface. The method used to detect defect introduction is the intensity ratio, (I_D/ I_G), which is a ratio of the D-band to G-band [60] with a higher ratio indicating a more crystalline material. Functional groups attach to the walls of the MWCNT to improve its crystallinity to a certain point before it reduces.

Figure 4.16 and 4.17 shows the Raman Spectroscopy for three different CNT samples, pristine CNT, CNT treated for 12 hours and CNT treated for 48 hours. The D-band is still less than the G-band for the treated samples however it is evident that the D-band has grown considerably from the plain CNT to the treated CNT samples. With the increasing D-band, there is also an increase in the G-band for the treated samples. The intensity ratio (I_D/ I_G) for plain CNT is calculated to be 0.08, for the treated CNT ratios of 0.44 and 0.32 for the 12 and 48 hour treatment were obtained respectively. Due to the intensity ratio being higher for the 12 hour functionalized CNT it was noted that this sample is more crystalline that the other samples. There are more functional groups, defective sites introduced thus functionalization is more successful in comparison to the 48 hour functionalized CNT.

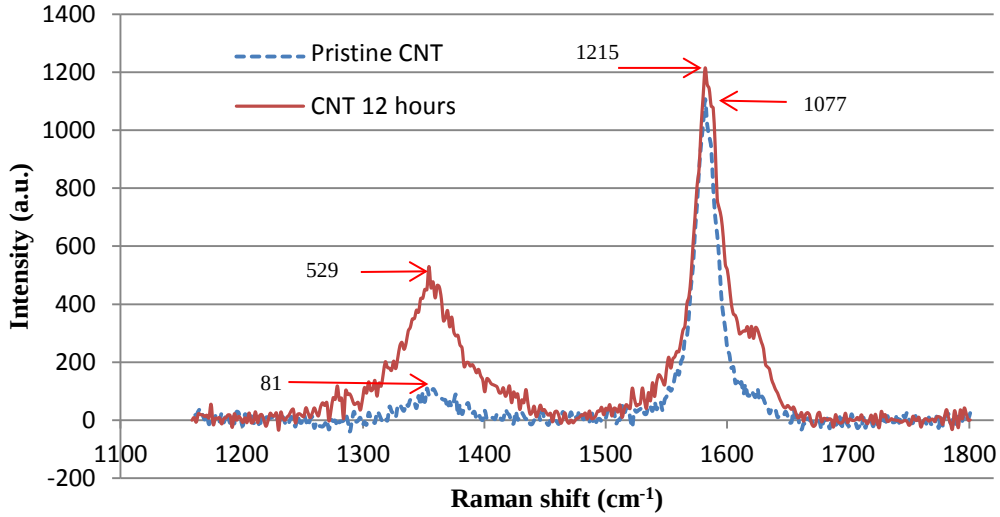


Figure 4.16 : Raman spectroscopy of 12 hour functionalized CNT

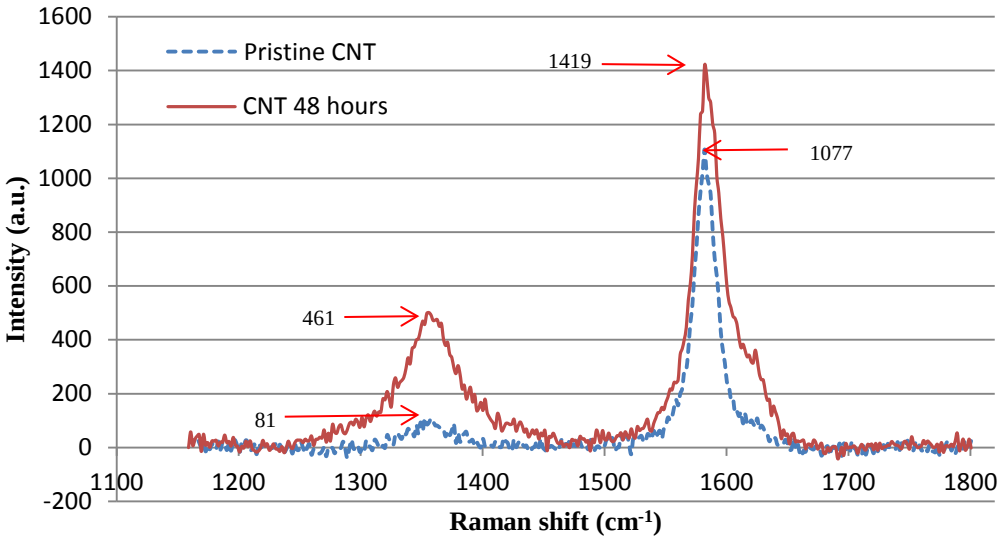


Figure 4.17 : Raman spectroscopy of 48 hour functionalized CNT

Figure 4.18 and 4.19 shows the FTIR spectroscopy of CNT treated for 12 hours and 48 hours respectively compared with that of pristine CNT. For the 12 hour functionalization treatment it can be noted that there is a considerable difference from the pristine CNT, it appears as though the pristine CNT is amplified to produce the FTIR plot of the 12 hour treated CNT. The FTIR plot of the 48 hour treated CNT did show partial amplification from the pristine CNT but only at certain specific points such as between 702 cm^{-1} and 1776 cm^{-1} and a slight increase between 2740 cm^{-1} and 3994 cm^{-1}. An amplification can be seem at the

991 cm^{-1} which is less than the value obtained for the 12 hour treated CNT, this further indicates that the 12 hour treatment process impacted more change to the CNT.

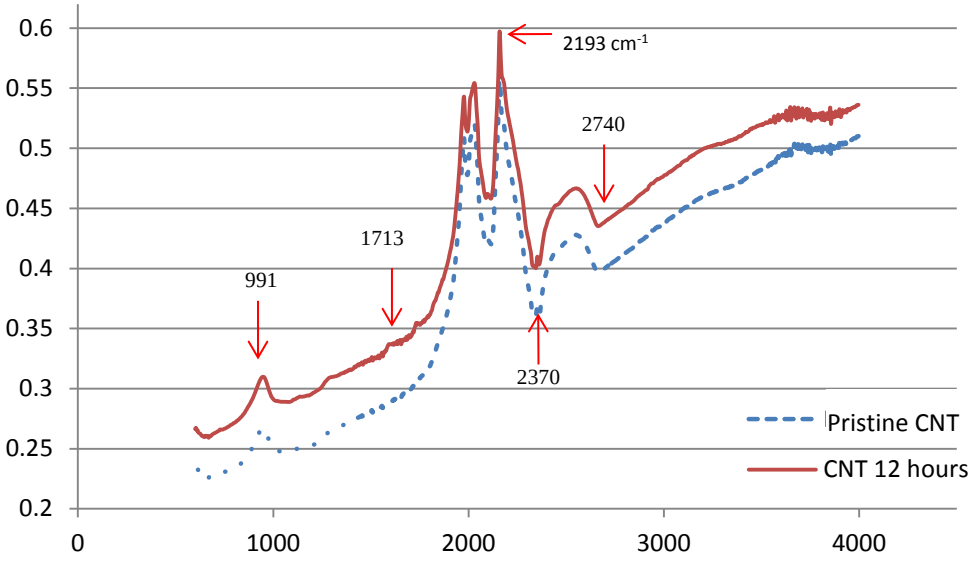


Figure 4.18 : FTIR spectroscopy of CNT functionalized for 12 hours

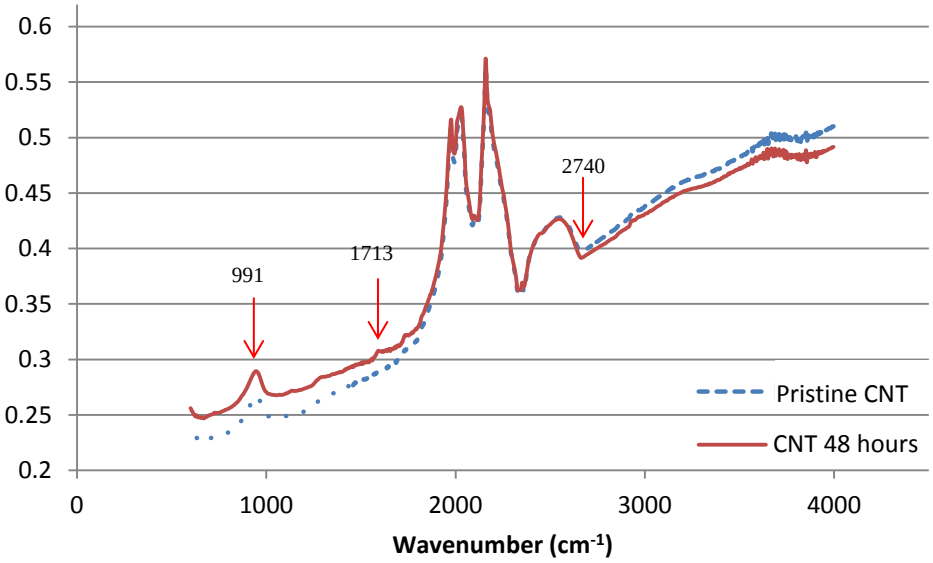


Figure 4.19 : FTIR spectroscopy of CNT functionalized for 48 hours

Osorio et al. [60] stated that FTIR is used to identify the presence or absence of functional groups on treated samples. Damian et al. [61] found that peaks between 1800 cm^{-1} and 2200 cm^{-1} indicate stretching vibrations of C-H and O-H bonds, which can be related to hydroxyl and carboxylic groups with additional C-H stretching vibrations noted between 2200-2860 cm^{-1}. Acid treatment of CNT results in a peak at 1713 cm^{-1} which corresponds to C-O stretching indicating the introduction of carboxylic groups (COOH) due to surface oxidation [50]. Figures 4.18 and 4.19 show peaks at similar wave numbers found by Osorio et al. [60] and Damian et al. [61] indicating that functional groups are found at the respective points. However it can be seen that the 12 hour treated CNT had more amplified peaks at these values in comparison to the 48 hour treatment and thus proved to be more successful.

From the conclusions made from researchers and the results above the 12 hour functionalization treatment proved to be superior to the 48 hour treatment and thus was the treatment used.

4.2.2 Functionalization of Clay

Clay particles were functionalized by using 3-Aminopropyltriethoxysilane over a 30 minute period. Functionalization of the clay particles is done to have functional groups created on their surface to improve dispersion and chemical interaction between the matrix and the clay. The silane used aids in the formation of OH reactive sites on the surface of the clay which gives clay the ability to be used in composites. Three different treatments were experimented on the clay to establish which method creates the best amount of functional groups on the clay. The treatments used were 1g clay : 1g silane, 1g clay : 2g silane and 1g clay : 5g silane, these treatments were then analysed by using TEM, Raman and FTIR analysis.

Figure 4.20 shows a TEM analysis of raw clay where a large number of orderly stacked clay platelets can be seen. Due to the clay platelets all being bunched up these platelets would not mix easily with the matrix thus reducing the properties

of the composite. Upon functionalization of the clay particles the agglomerated clay platelets shifted from their ordered structure shown in Figure 4.21. With the platelets being separated they would be able to be dispersed easily and better bonding would occur. Due to this it was decided that the 3-Aminopropyltriethoxysilane functionalization treatment would be beneficial and would enhance the strength of the composite when used. Figure 4.22(a-d) is a schematic representation of what occurred during the functionalization process and the Figure 4.22(e) shows what would occur with the functionalized particles within the composite.

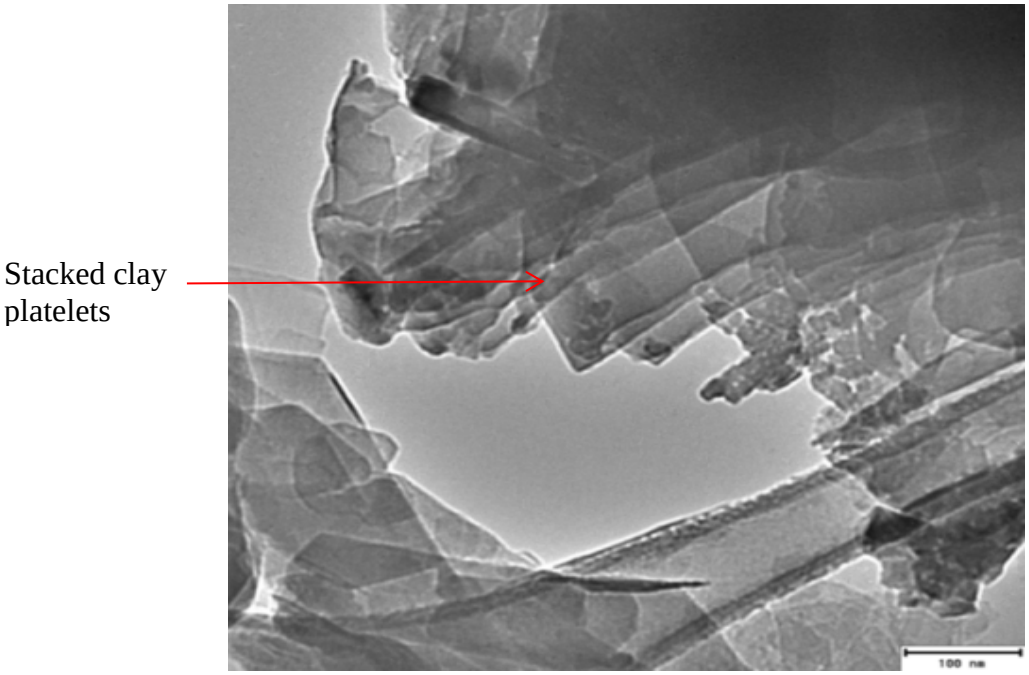


Figure 4.20 : TEM image of raw clay

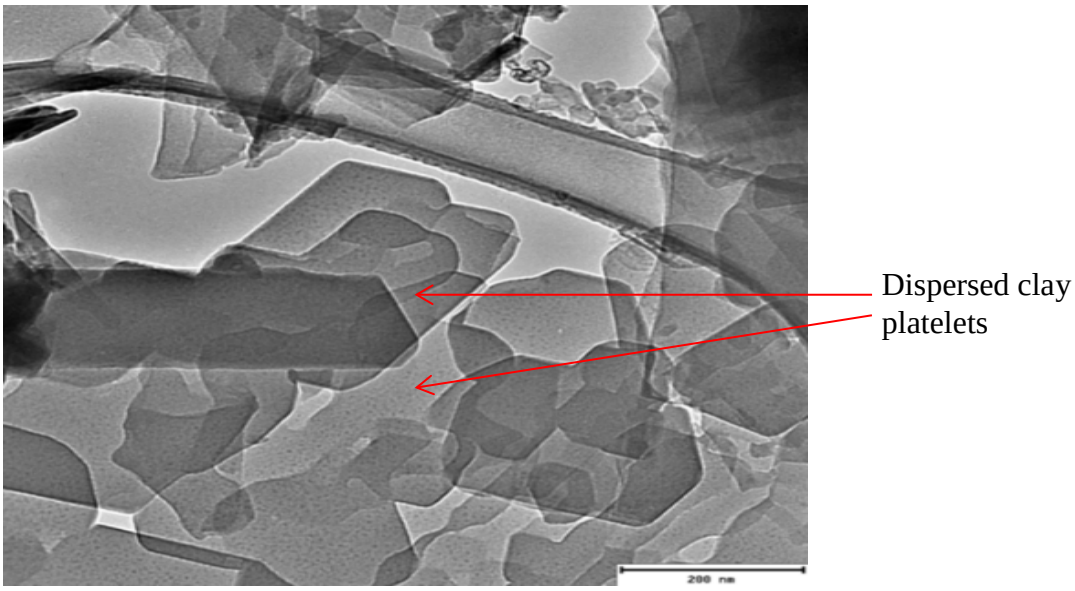


Figure 4.21 : TEM image of functionalized clay (1g clay : 2g silane)

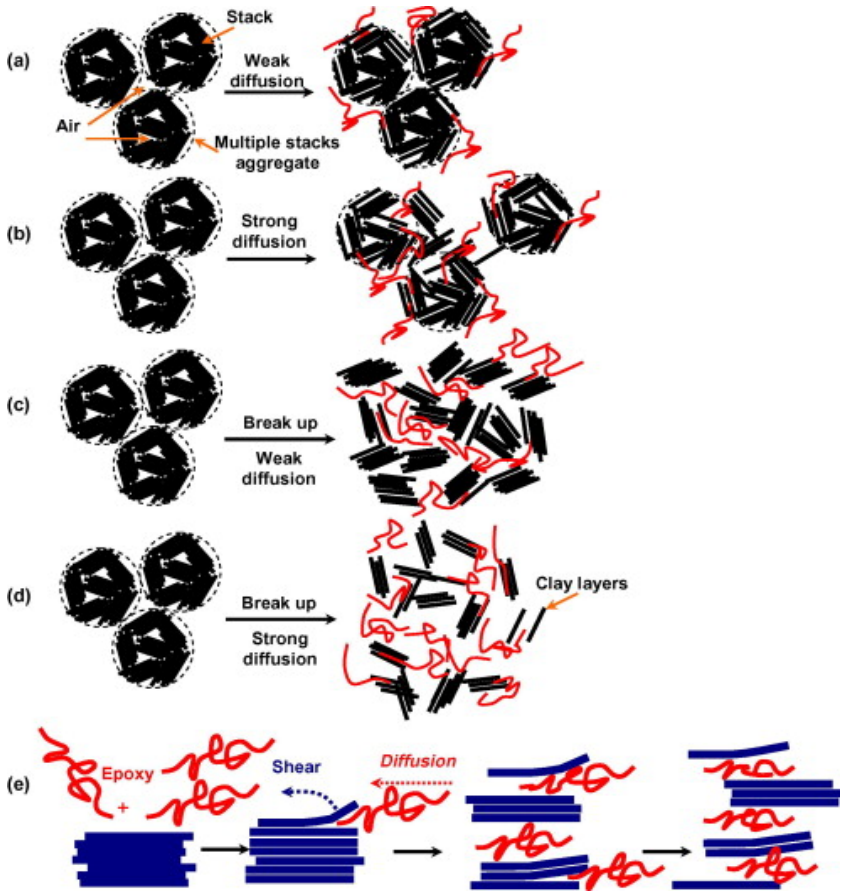


Figure 4.22 : Schematic representation of the functionalization process of clay

Figures 4.23, 4.24 and 4.25 show the Raman spectroscopy obtained for the 1g clay : 1g silane, 1g clay : 2g silane and 1g clay : 5g silane samples. The Raman spectra obtained shows that the 1g clay : 2g silane treatment caused the most amount of deformation to the clay particles. The significant bands for the 1g clay : 2g silane are bands at 145 cm^{-1}, 261 cm^{-1}, 483 cm^{-1}, 703 cm^{-1}, 946 cm^{-1} and 1055 cm^{-1}. The intensity of these bands at the points mentioned above are considerably greater than what was obtained for the other two samples. Treatment of 1g clay with 5g of silane did not produce a significant change to the Raman spectroscopy as shown in Figure 4.25, the same can be seen with the 1g clay : 1g silane treatment shown in Figure 4.23.

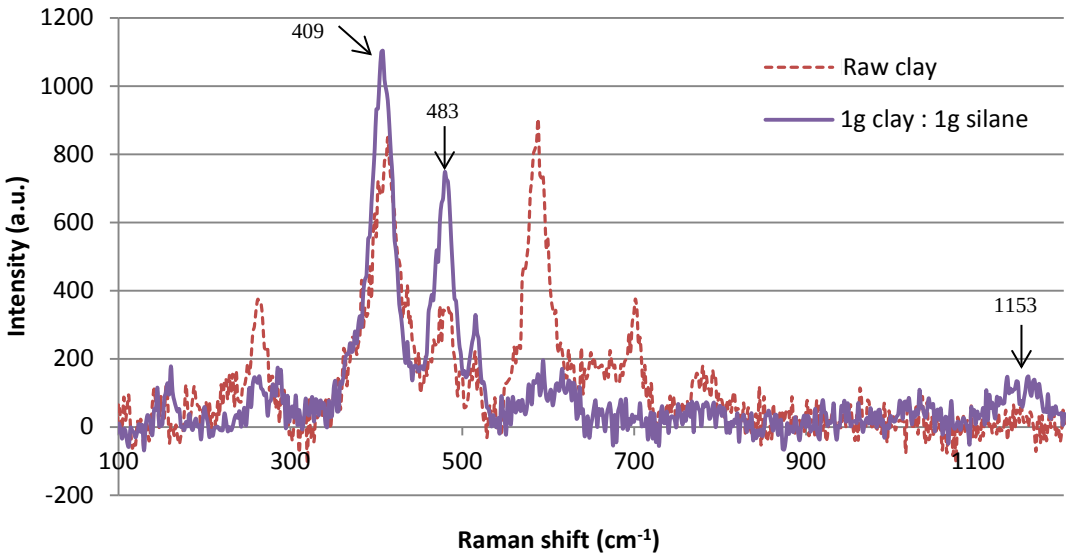


Figure 4.23 : Raman spectroscopy of 1g clay : 1g silane

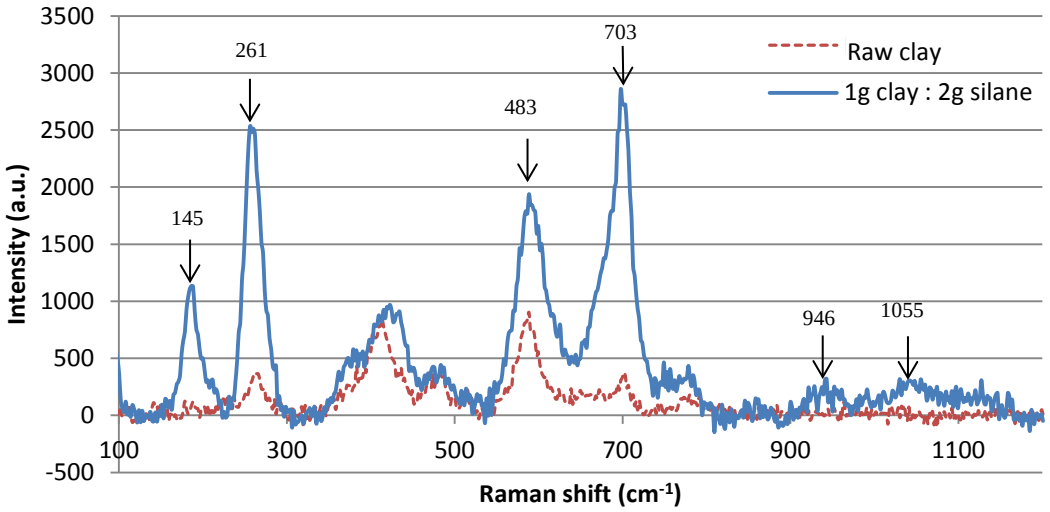


Figure 4.24 : Raman spectroscopy of 1g clay : 2g silane

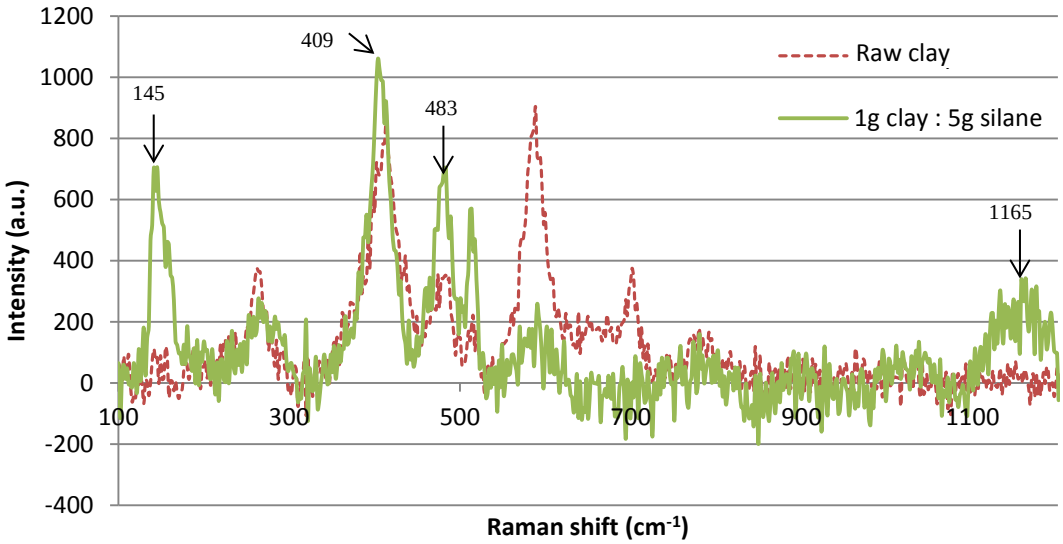


Figure 4.25 : Raman spectroscopy of 1g clay : 5g silane

When conducting analysis of the Raman spectroscopy of zeolites, Yu et al. [52] found that a band at around 490 cm^{-1} is due to the bending vibration of the 4-membered rings (Si-O-Al). They also found that bands around 700 cm^{-1} are due to the T-O symmetric stretching modes whereas bands around 950-1100 cm^{-1} are due to the T-O asymmetric stretching motions. Bands in the region between 220-280 cm^{-1} are due to the bending modes of 8 membered rings of the zeolite.

Yu et al. [52] also noted that it is difficult to obtain Raman spectra of clay because of the problems with signal to noise ratios and the Raman spectra for clay is often obscured by a broad florescence background. The 1g clay : 5g silane sample shows a band at 145 cm^{-1} which is due to the signal to noise ratio obtained from this sample. They also mentioned that clays are characterised by the molecular ratio (Si: Al ratio), which affects the band position and band intensity of the Raman spectra.

Due to the amount of distortion created at the same bands found by Yu et al. [52] it was concluded that the most amount of defects were introduced after the 1g clay : 2g silane treatment and thus was the treatment used for the clay functionalization.

Figure 4.26, 4.27 and 4.28 shows the FTIR plots of clay. In Figure 4.26 the treatment of the clay with 1g of silane had minimal effect on the result as the plot looks very similar to that of raw clay which indicates that no modification of the surface had taken place. With a 2g treatment of the clay, modification of the clay particles occurred at a few points such as between 600 – 800 cm^{-1}, 1000 cm^{-1} and at 2380 cm^{-1} as shown in Figure 4.27. A 5g treatment of clay resulted in a reduction of the properties of the clay at the points mentioned above as indicated in Figure 4.28.

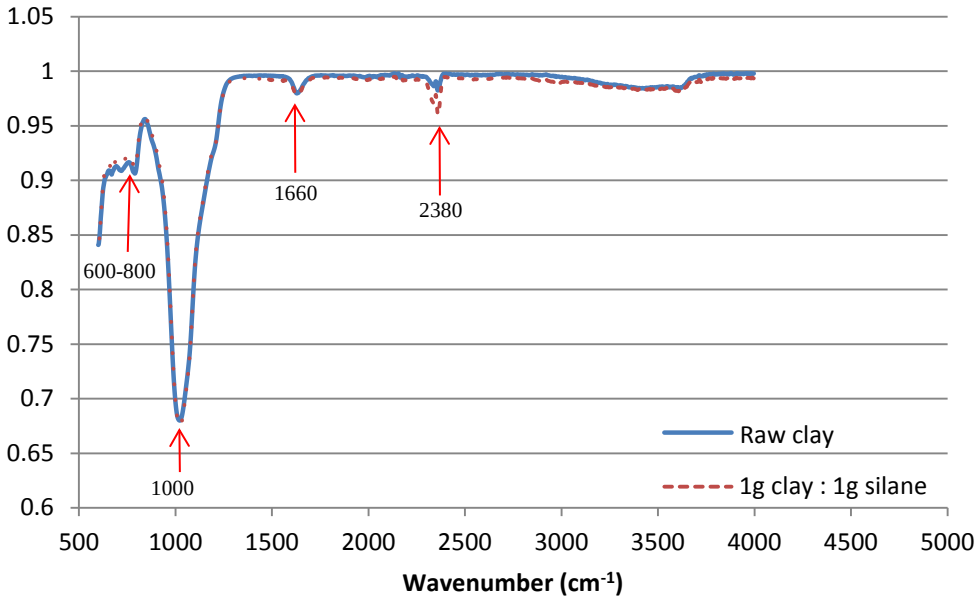


Figure 4.26 : FTIR Spectroscopy of 1g clay : 1g silane

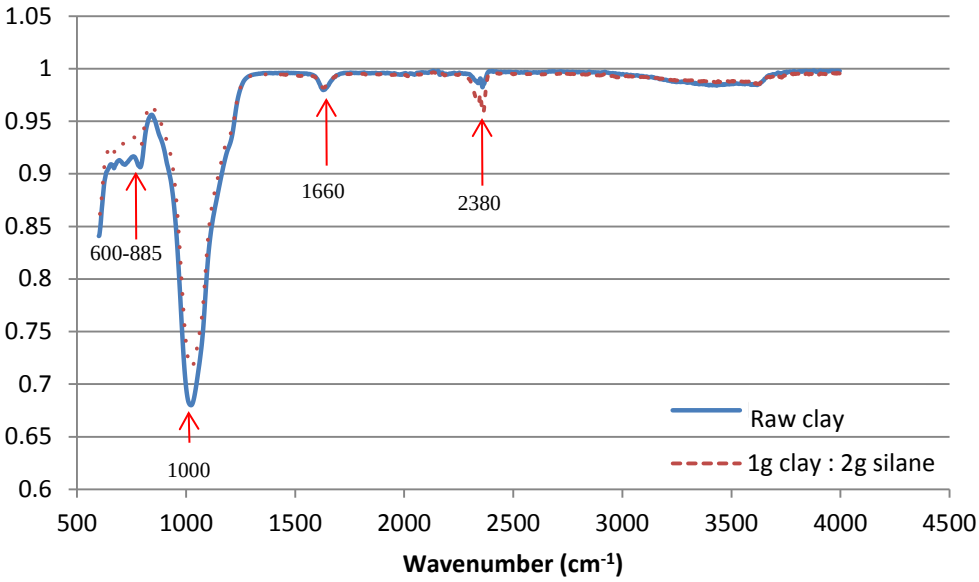


Figure 4.27 : FTIR Spectroscopy of 1g clay : 2g silane

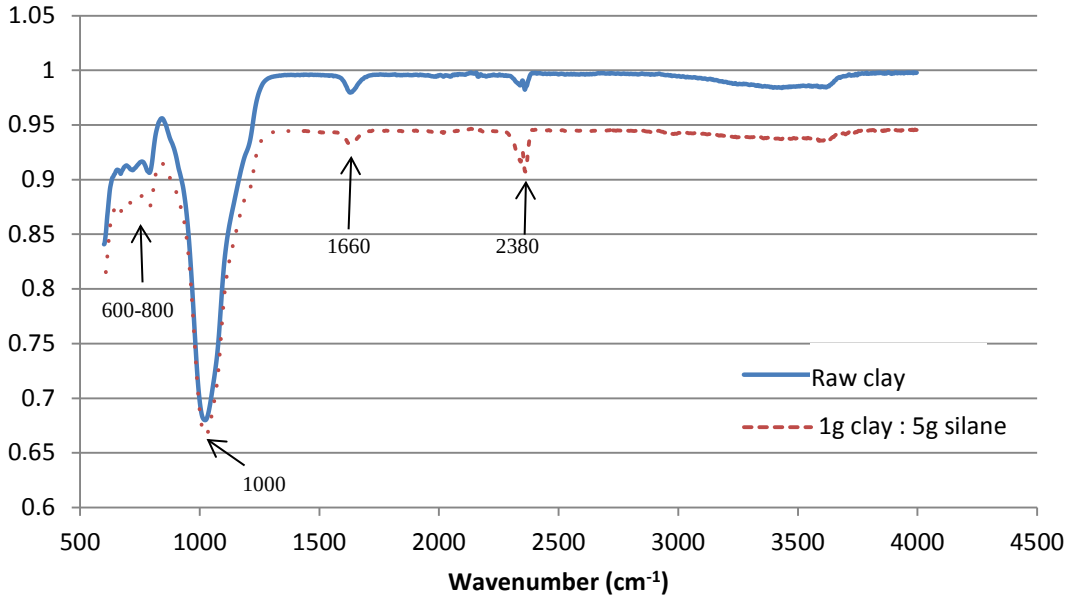


Figure 4.28 : FTIR Spectroscopy of 1g clay : 5g silane

Shanmugharaj et al. [40] researched the FTIR spectrum of clay and found a peak at 1630 cm^{-1} due to the OH stretching and bending vibrations of the adsorbed water. Peaks over the range from 1000 – 1200 cm^{-1} are due to the Si-O stretching of the silicates present in the clay with bending vibrations of the Al, OH and Mg found usually occurring between 800 - 916 cm^{-1} [40]. Based on the results obtained it can be noted that the treated clay does show a reaction to the treatment at 1000 cm^{-1} indicating the Si-O stretching of the clay silicates had taken place. Figure 4.27 does show a large amount of change in the 600-885 cm^{-1} region showing the bending vibrations of Al, OH and Mg. Peaks could also be seen at the 1660 cm^{-1} wavenumbers on both specimens but these were not amplified in comparison to raw clay.

Due to the positive modifications that had taken place on the clay using the 2g silane treatment on both the Raman and the FTIR analysis it was decided that this would be the treatment method to be used for the clay.

4.3 Particulate composites

4.3.1 CNT composites

Fabrication of CNT composites were not conducted due to recent work on these composites being done by Muthu et al. [59] and a post graduate student of the authors supervisor, Dendere [62]. They studied the effect on the mechanical properties of composites with the addition of CNT reinforcement particles. They discovered that a 0.5% addition of CNT improved the mechanical properties of the composites in the tensile, bending and impact tests conducted in comparison to the plain matrix.

4.3.2 Glass composites

Glass composite materials were fabricated using epoxy with 0.1%, 0.5% and 2% weight fractions of glass. These composite materials were subjected to tensile, flexural and impact tests to determine the benefits of the glass reinforcement within the composite. Figure 4.29 shows the tensile strength of the glass composites in comparison to plain epoxy. It can be seen that an addition of glass to epoxy does increase its tensile properties with the highest tensile strength obtained with a 0.5% weight fraction of glass. When the weight fraction is increased to 2%, a drop in the tensile properties can be seen.

An SEM image of the 0.5% glass specimen can be seen in Figure 4.30 which shows a good dispersion of glass in the matrix as there is no agglomeration of the particles. This indicates that the interfacial adhesion between the matrix and the fibres is good. A reduction in the tensile strength with the 2% weight fraction of glass was due to the agglomeration of glass particles as shown in Figure 4.31. This caused improper bonding between the matrix and the reinforcement which resulted in weak spots forming where the glass particles agglomerated.

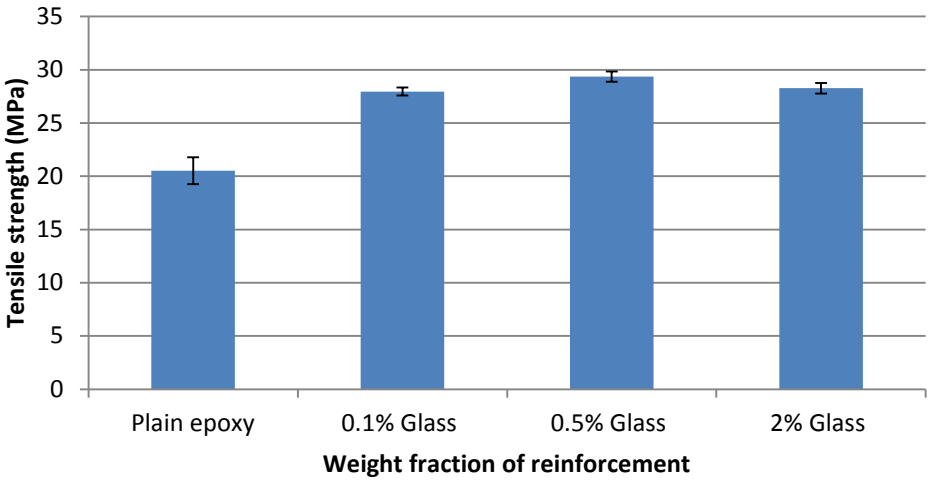


Figure 4.29 : Tensile strength of glass composite specimens

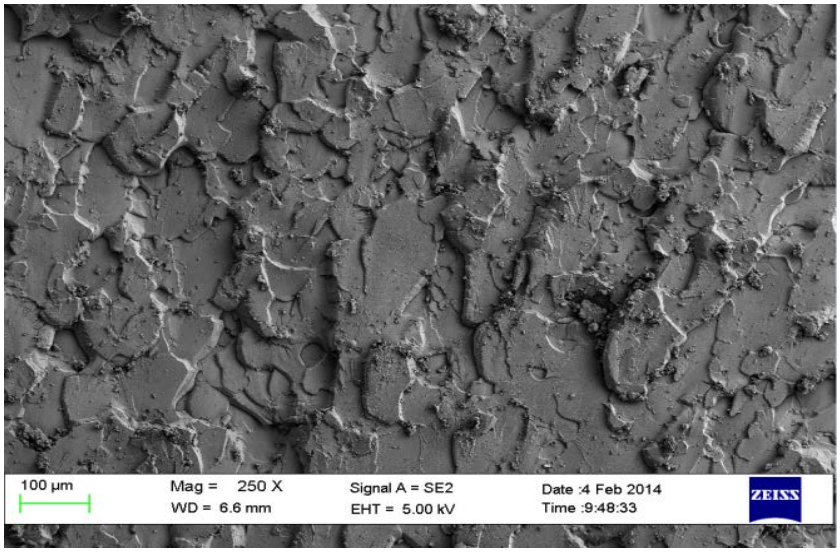


Figure 4.30 : SEM image of the 0.5% glass tensile specimen

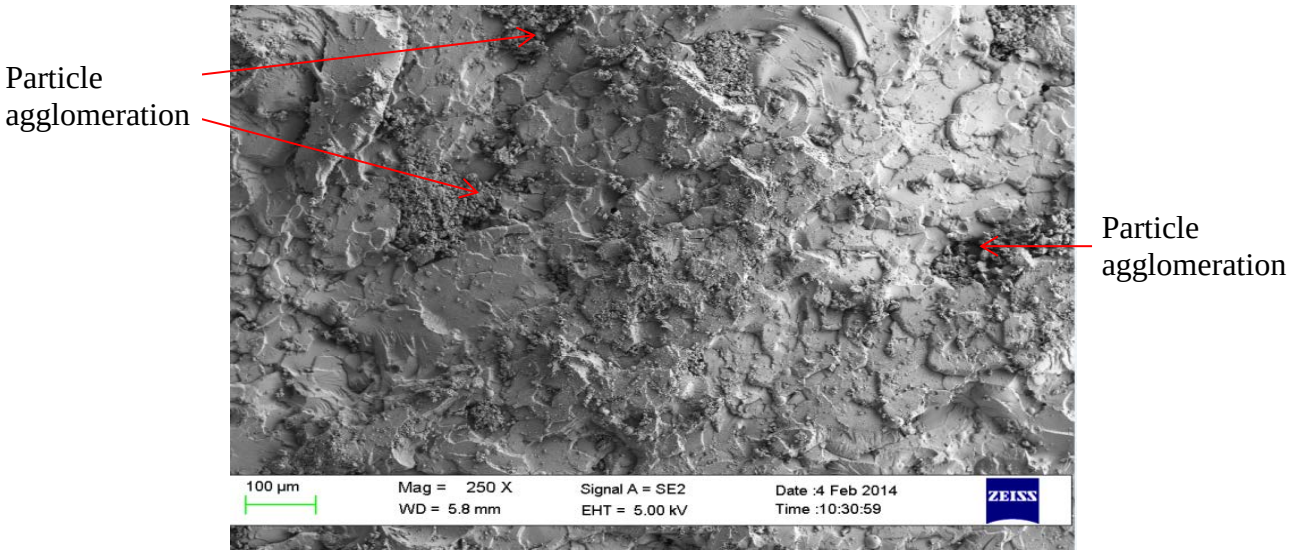


Figure 4.31 : SEM image of the 2% glass tensile specimen

Figure 4.32 shows the elastic modulus obtained for the glass composites. The 0.5% glass composite showed the highest elastic modulus amongst the glass composites. A 2% weight fraction of glass caused a reduction in the modulus of the glass specimen due to the particle agglomerations found in the specimen as shown in Figure 4.31.

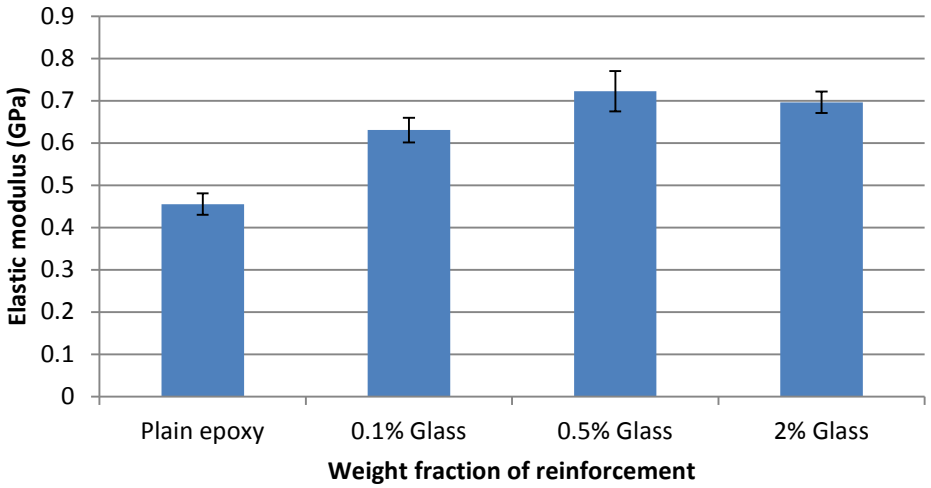


Figure 4.32 : Elastic modulus of glass composite specimens

Figure 4.33 shows the flexural stress of the glass specimens. A 0.5% weight fraction of glass produced the highest flexural strength amongst the glass composites with a 2% addition of glass causing a reduction in the properties due

to the particle agglomeration that can be seen in Figure 4.34. The 0.5% glass composite showed a 40% increase in comparison to plain epoxy.

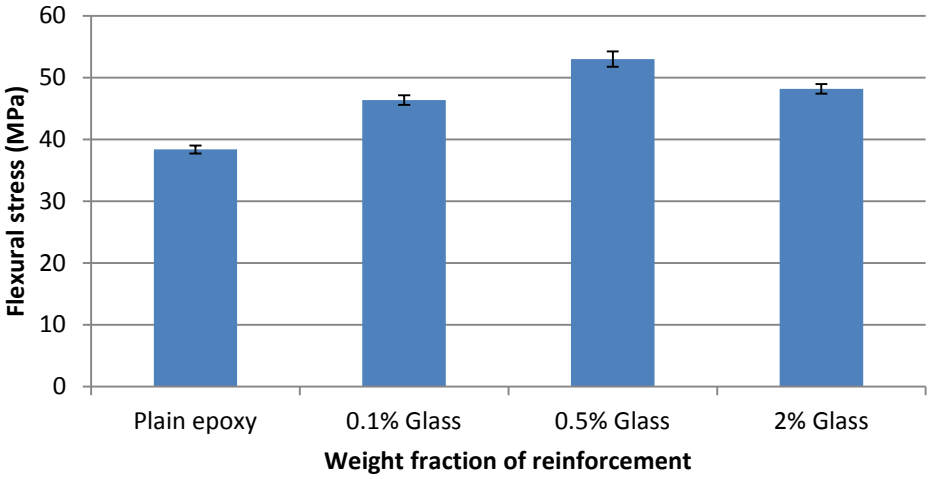


Figure 4.33 : Flexural strength of glass specimens

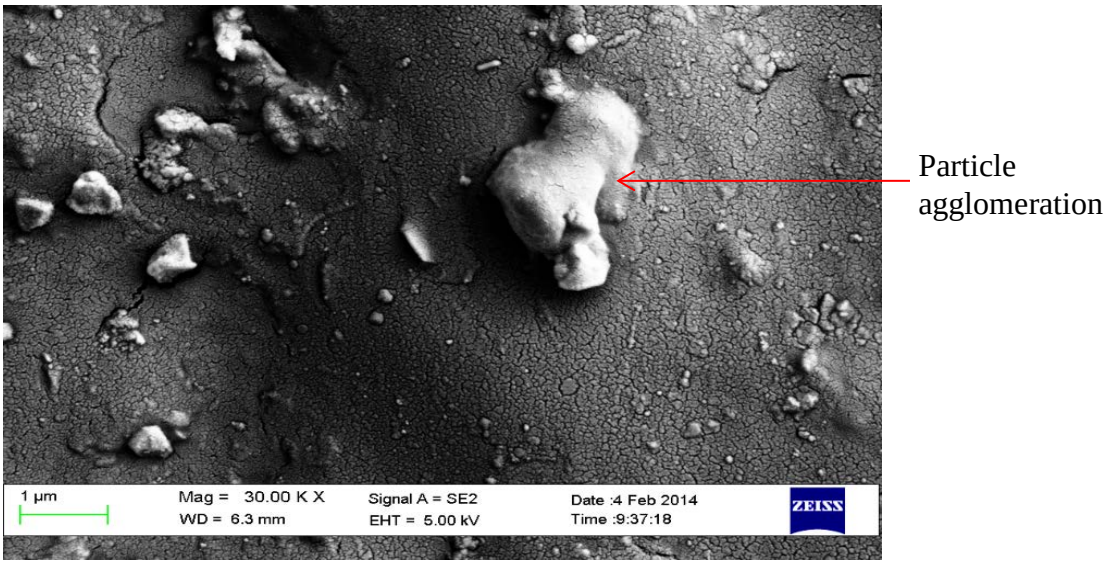


Figure 4.34 : SEM image of the 2% glass flexural specimen

The tangent modulus for the glass composites shown in Figure 4.35, shows that as the weight fraction of glass reinforcement increased so did the modulus. The 2% weight fraction of glass produced the highest modulus of 304 MPa. This result shows that the stress to strain ratio in bending increased with the reinforcement addition.

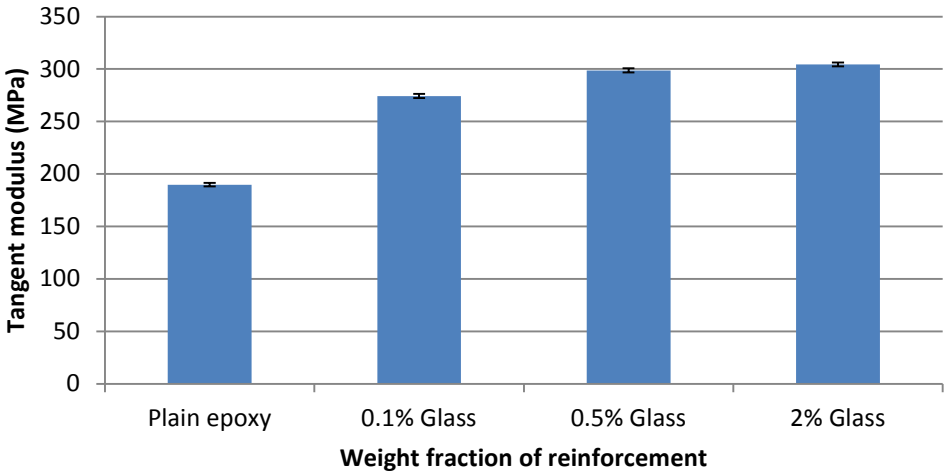


Figure 4.35 : Tangent modulus of glass specimens

Figure 4.36 shows the fracture toughness of the glass composite specimens. A 0.5% weight fraction of glass shows the highest fracture toughness for the glass composites with a value of 0.000803 MPa√m which is a 61% increase in comparison to plain epoxy. The reduction in properties of the 2% glass impact specimen is due to the particle agglomeration, as can be seen in Figures 4.31 and 4.34.

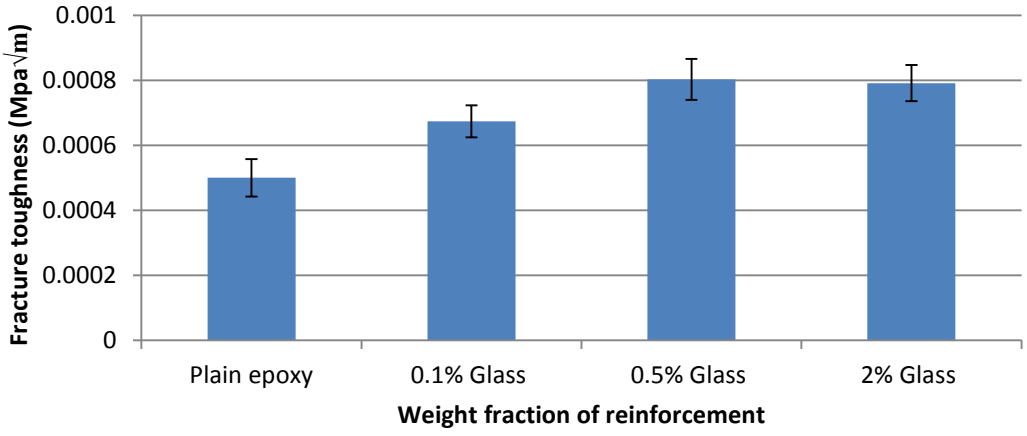


Figure 4.36 : Fracture toughness of glass specimens

4.3.3 Clay composites

Clay composite materials were fabricated using epoxy with 0.1%, 0.5% and 2% weight fractions of clay. These composite materials were subjected to tensile, flexural and impact tests to determine the benefits of the clay reinforcement in the composite. Figure 4.37 shows that a 0.5% weight fraction of clay produced the highest tensile strength amongst the clay composites which is 29 MPa, this however is 38% greater than plain epoxy. Figure 4.38 shows an SEM image of the 0.5% clay composite which shows good interfacial adhesion between the epoxy and clay particles which resulted in good tensile properties of the specimen. The good interfacial adhesion between the matrix and the clay reinforcement is due to the functionalization treatment conducted on the clay which proved to be successful.

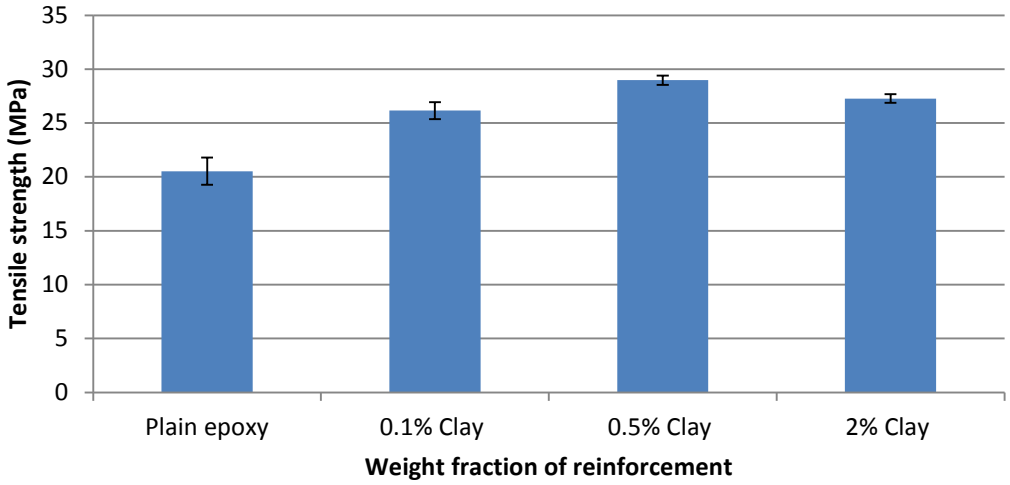


Figure 4.37 : Tensile strength of clay composite specimens

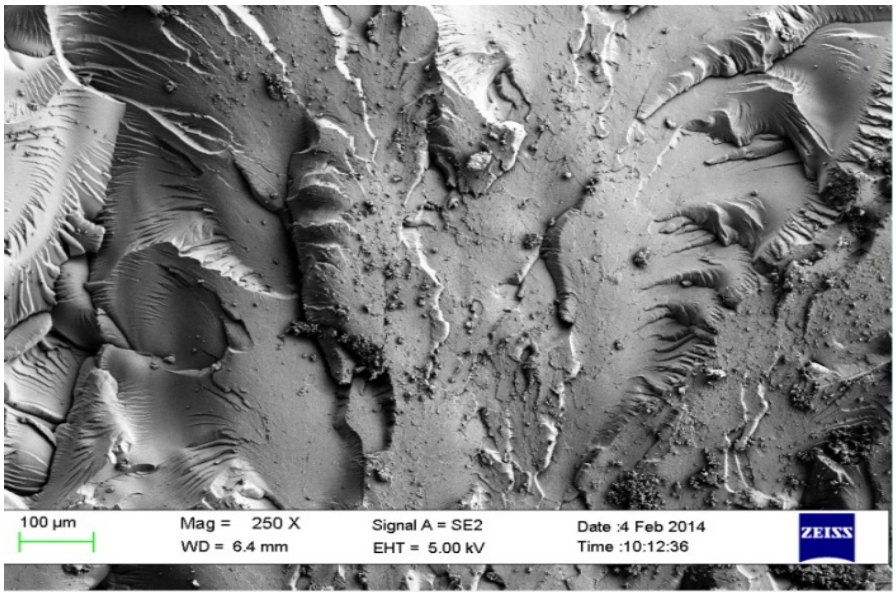


Figure 4.38 : SEM image of the 0.5% clay tensile specimen

Figure 4.39 shows the elastic modulus obtained for the clay composites. A 0.1% weight fraction of clay generated an increase in the modulus in comparison to the plain epoxy composite by 32%. As the weight fraction of clay increased so did the elastic modulus up to the 2% weight fraction of clay.

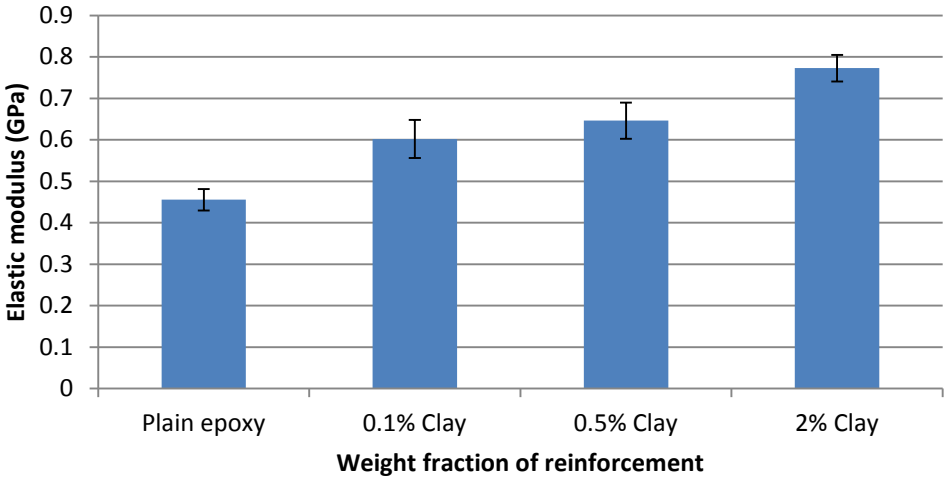


Figure 4.39 : Elastic modulus of clay composite specimens

Figure 4.40 shows the flexural strength obtained for the clay composites. It can be seen that a 0.5% weight fraction of clay exhibited the highest flexural strength of 60 MPa which is a 57% increase in comparison to plain epoxy. Figure 4.41 is

an SEM image of the 0.5% clay specimen showing good interfacial adhesion between the matrix and the reinforcement which resulted in good mechanical properties being obtained.

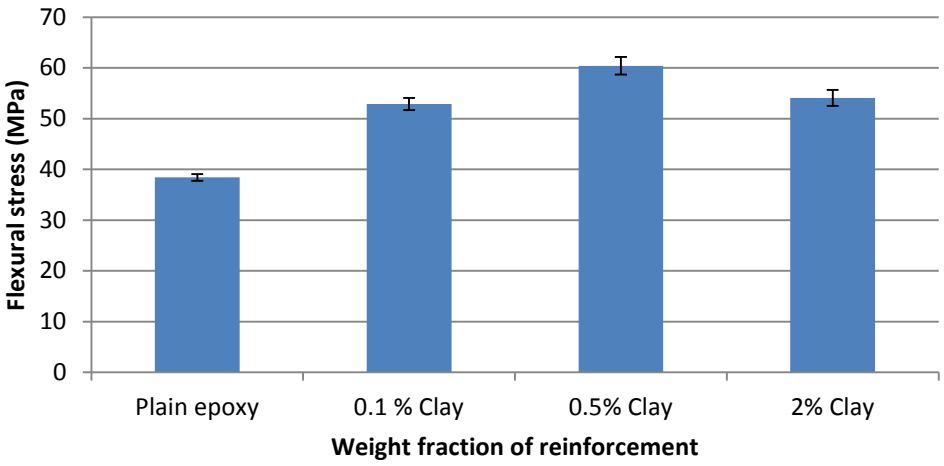


Figure 4.40 : Flexural strength of clay specimens

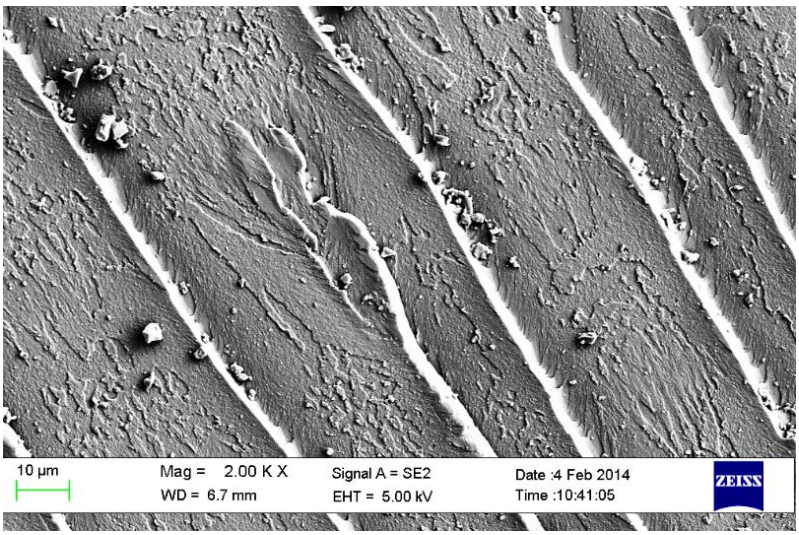


Figure 4.41 : SEM image of the 0.5% clay flexural specimen

Figure 4.42 shows the tangent modulus obtained for the clay specimens. The modulus increased with the increasing weight fraction of clay showing that the stress-strain ratio increased with the weight fraction.

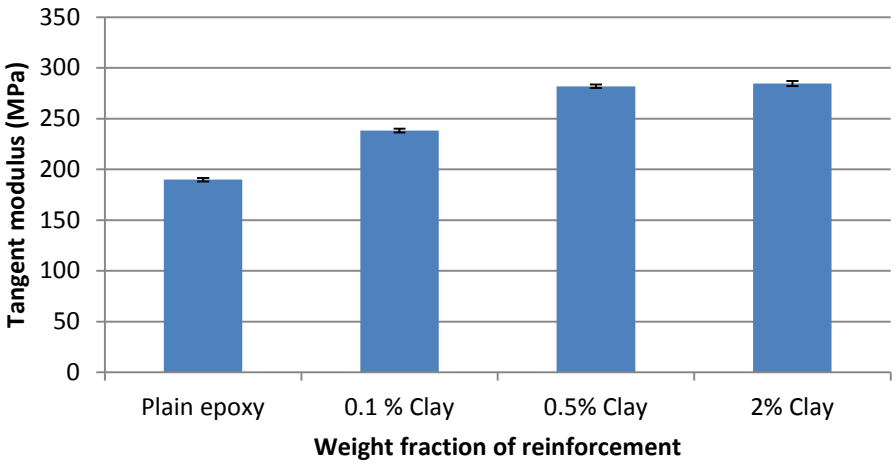


Figure 4.42 : Tangent modulus of clay specimens

The fracture toughness shown for the clay composites in Figure 4.43, is higher in comparison to the plain epoxy composites. A 0.5% weight fraction of clay produced the highest fracture toughness for these composites but then decreased upon a 2% addition of clay.

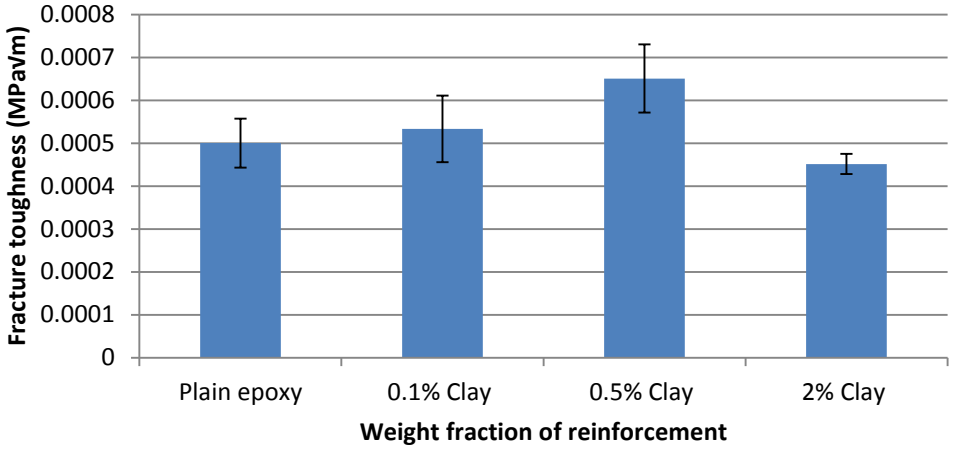


Figure 4.43 : Fracture toughness of clay specimens

Figure 4.44 shows the impact surface of the 2% clay surface showing that the clay particles dispersed well into the epoxy matrix. At a high magnification, 24.87k times, particle agglomeration could not been seen on the surface of the specimen. This shows that the functionalization treatment was indeed successful and indicates that the specimen failed due to the load applied and not due to interface or bonding issues.

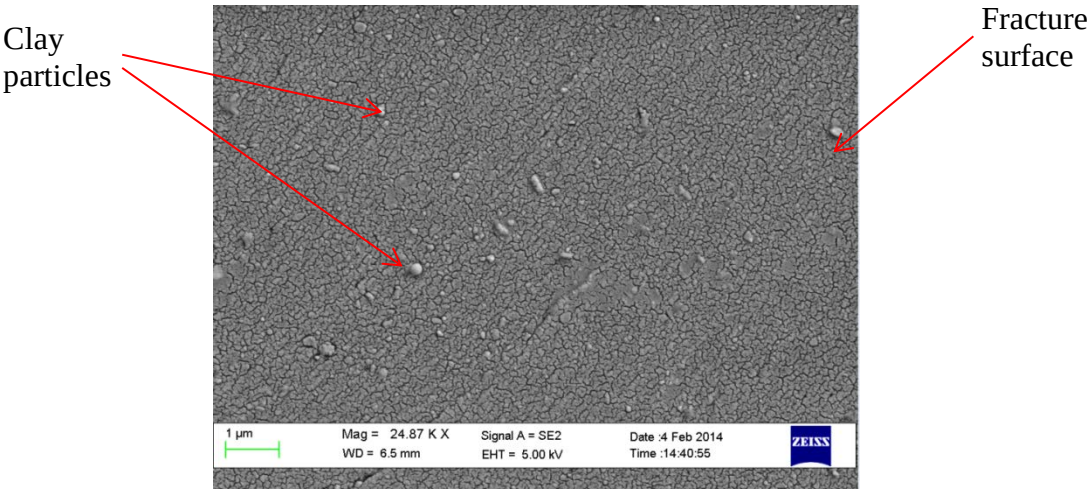


Figure 4.44 : SEM image of the 2% clay impact specimens

4.4 Hybrid composites

Hybrid composites were fabricated using the optimum volume fraction of coir fibre obtained from the epoxy-coir composites. Three different types of hybrid composites were fabricated being hybrid-CNT, hybrid-clay and hybrid-glass composites. The weight fractions used for these composites were 0.1%, 0.5%, 1.5% and 2% for the CNT composites, 0.1%, 1.5%, 2%, 4%, 5% and 6% for the clay composites and 0.1%, 1.5%, 2%, 4%, 8% and 12% for the glass composites. The above mentioned composites were subjected to tensile, flexural and impact tests to determine which composite exhibits the best properties.

4.4.1 Hybrid CNT composites

The tensile strength for the hybrid-CNT composites can be seen in Figure 4.45, which indicates that the tensile strength increased with the weight fraction of CNT until the 2% weight fraction where the tensile strength decreased. The epoxy-

1.5% CNT composite showed the best tensile strength amongst the CNT composites tested, with a tensile strength of 41 MPa which is a 49% increase in comparison to the epoxy-15% coir composites. The hybrid-2% CNT composite had a reduction in the tensile strength from the 1.5% CNT weight fraction by 9%.

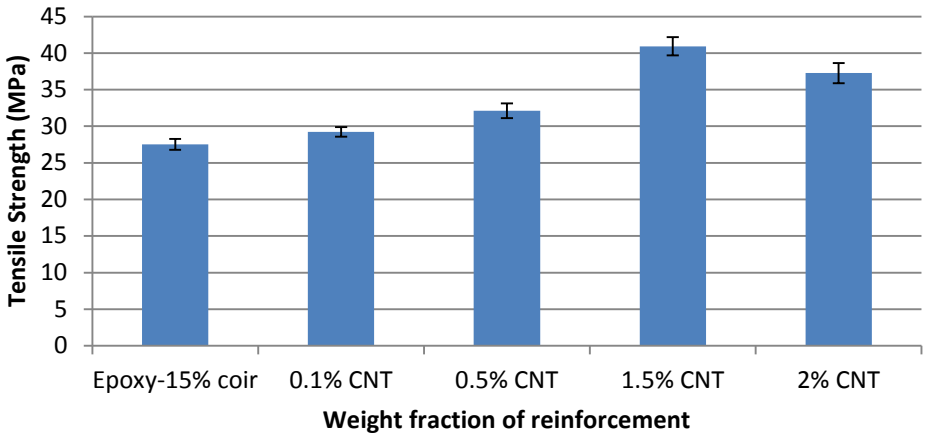


Figure 4.45 : Tensile strength of hybrid-CNT composite specimens

Figure 4.46 shows the elastic modulus of the hybrid-CNT composites which shows an increase in the modulus of the specimens as the weight fraction increased up to 2% which generated a value of 1.33 GPa. The modulus of the hybrid-2% CNT composite increased the modulus by 96% in comparison to the epoxy-15% coir composite showing that the stress to strain relationship increased with the weight fraction of CNT.

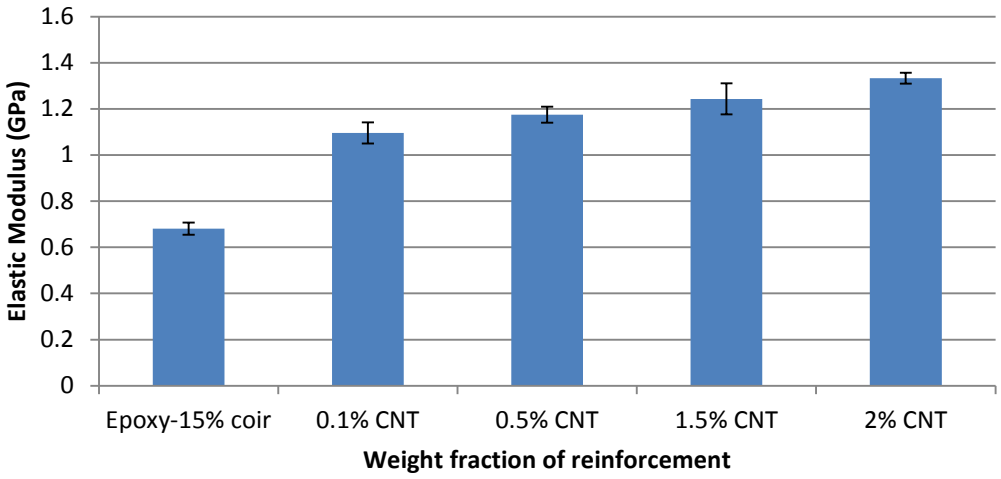


Figure 4.46 : Elastic modulus of hybrid-CNT composite specimens

Figure 4.47 shows an SEM image of the hybrid-1.5% CNT tensile specimen. The specimen does not show any agglomeration of particles which indicates that dispersion of the MWCNT particles in the matrix was good, the powdery substance shown on the image is coir fibre which was not blown out properly upon preparation of the specimen. With the MWCNT particles being dispersed easily into the matrix it indicates that the functionalization of the CNT particles was successful as the particles bonded to the matrix and dispersed well. The specimen also shows breakage of the fibre at the matrix interface which indicates good interfacial adhesion between the matrix and the fibres showing that the load is distributed well from the matrix to the fibre. Due to the dispersion of the MWCNT being good the specimen produced good tensile strength and modulus. Figure 4.48 shows an SEM image of the hybrid-2% CNT tensile specimen. The specimen shows a few reasons as to why the tensile strength reduced from the hybrid-1.5% CNT specimen. Fibre pull out can be seen showing that the higher weight fraction of CNT used caused the bonding to be reduced as there had not been good bonding between the matrix and the reinforcements. There are also voids on the specimen shown in Figure 4.48 which also caused a reduction in the tensile strength.

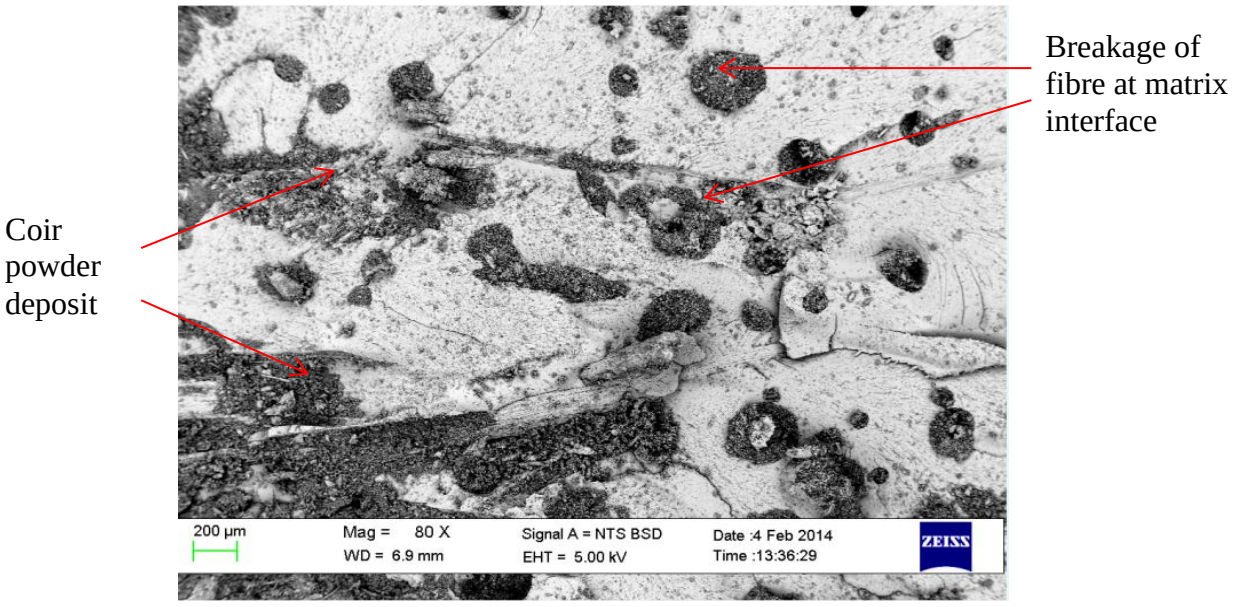


Figure 4.47 : SEM image of the hybrid-1.5% CNT tensile specimen

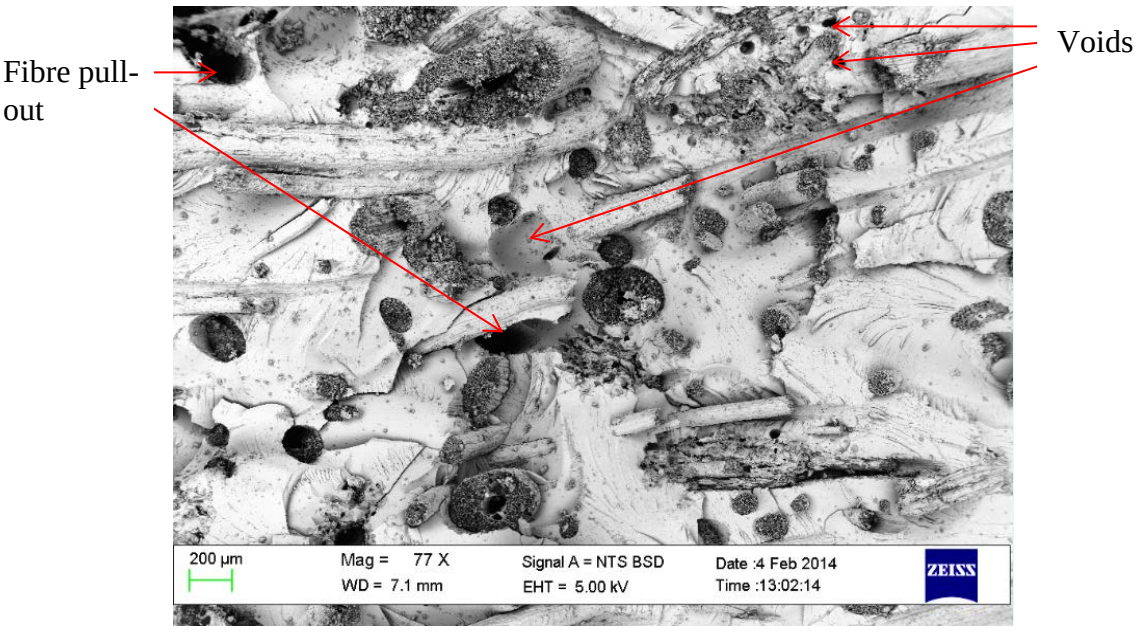


Figure 4.48 : SEM image of the hybrid-2% CNT tensile specimen

Figure 4.49 shows the results obtained from flexural testing of the hybrid-CNT composites which indicates that the flexural strength for the 1.5% weight fraction of CNT generated the highest value amongst all of the weight fractions of CNT tested. This specimen reached a value of 83 MPa which is a 52% increase in comparison to the epoxy-15% coir composite. A reduction in the flexural strength at the 2% weight fraction was observed which was due to the agglomeration of the

CNT at the higher weight fraction. The reduction in properties at a 2% weight fraction of CNT had also been observed by Dongsheng Mao [56] and Muthu et al. [52].

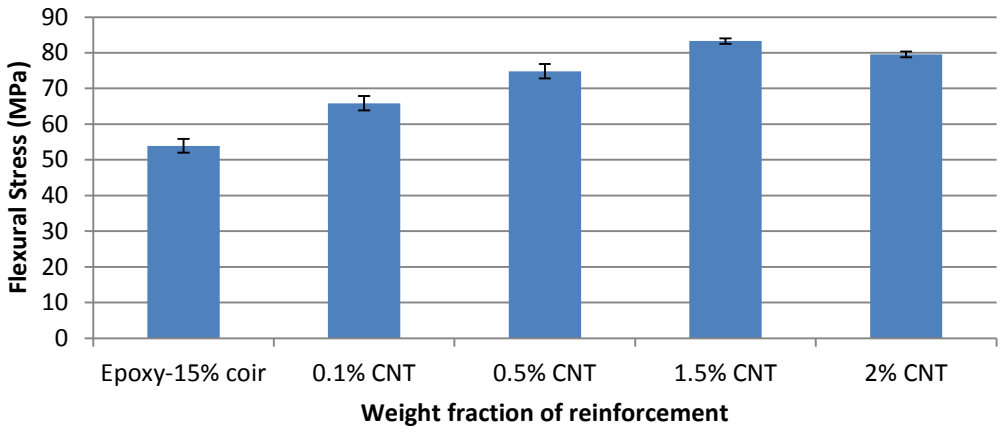


Figure 4.49 : Flexural strength of hybrid-CNT specimens

Figure 4.50 shows the tangent modulus for the hybrid-CNT composites and indicates that the tangent modulus increased as the weight fraction of the reinforcement increased up to the 1.5% weight fraction of CNT which showed a value of 387 MPa. The modulus of all the hybrid-CNT specimens showed to be greater than the epoxy-coir composite fabricated, even a 0.1% weight fraction of CNT showed a 10% increase in the modulus. A reduction in the modulus was seen with a 2% weight fraction of MWCNT by 3% in comparison to the 1.5% weight fraction indicating that the properties of the composite began to fail. This was due to the higher weight fraction of CNT used. Figure 4.51 shows an SEM image of the hybrid-1.5% CNT flexural specimen, no agglomeration can be seen which indicates that CNT dispersed well into the matrix indicating that functionalization of the particles was successful. Good interfacial bonding can be seen as some of the fibres broke at the matrix interface or on the fibres themselves due to the load applied. There is some evidence of fibre pull-out, but this showed that shorter fibres were pulled out due to the greater bond strength between the longer fibres and the matrix.

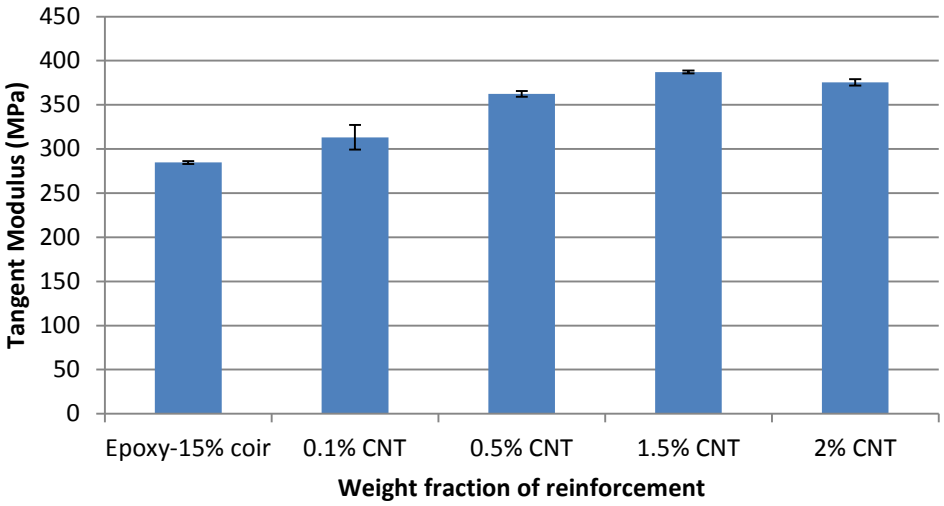


Figure 4.50 : Tangent modulus of hybrid-CNT specimens

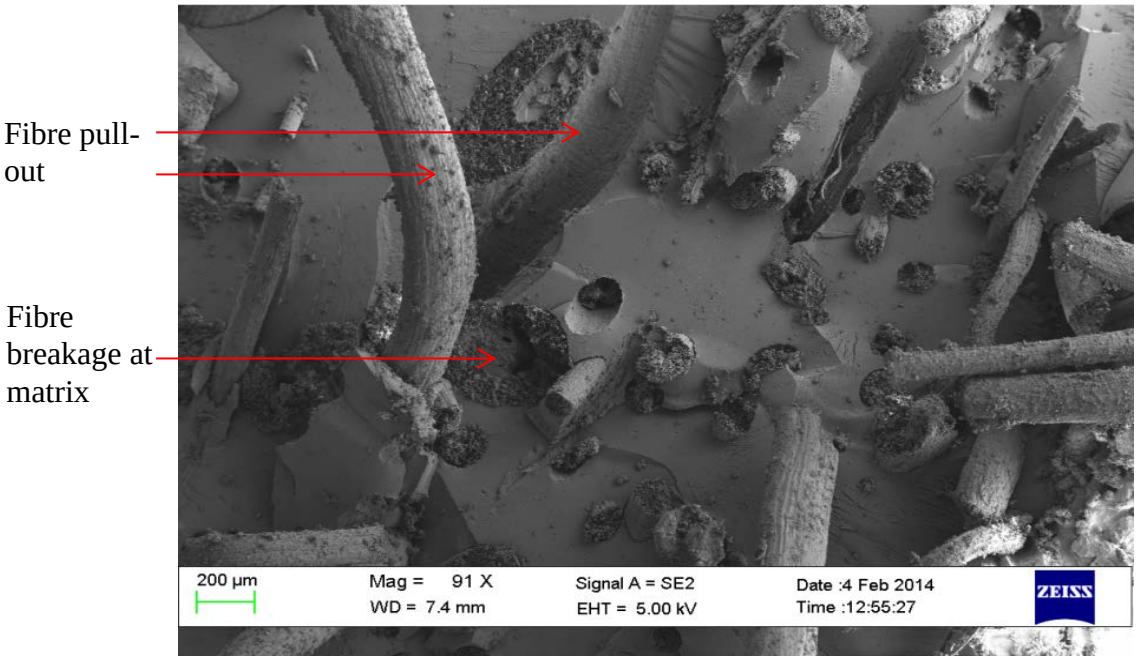


Figure 4.51 : SEM image of the hybrid-1.5% CNT flexural specimen

Figure 4.52 shows the fracture toughness for the hybrid-CNT composites. The fracture toughness increased over the weight fractions tested with the 1.5% weight fraction of CNT exhibiting the highest fracture toughness of 0.0011 MPa$\sqrt{m}$, which is greater that the fracture toughness obtained for the epoxy-15% coir composite by 23%. A 2% weight fraction of CNT had seen a reduction in the fracture toughness by 8% in comparison to the hybrid-1.5% CNT composite.

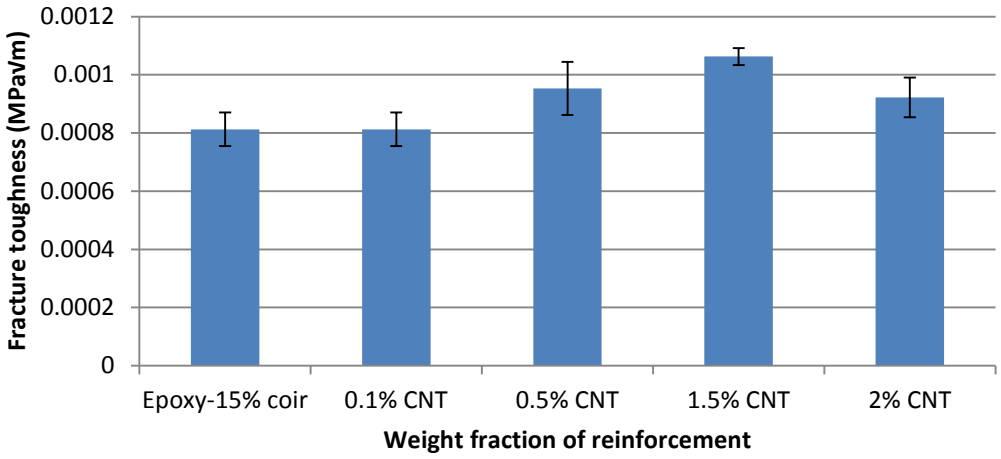


Figure 4.52 : Fracture toughness of hybrid-CNT specimens

Figure 4.53 shows an SEM image of a hybrid-0.5% CNT impact specimen. No agglomeration of the CNT particles can be seen showing that the dispersion of the CNT in the matrix is good. Breakage of the fibres can be seen at the matrix fibre interface which shows that good interfacial bonding had taken place.

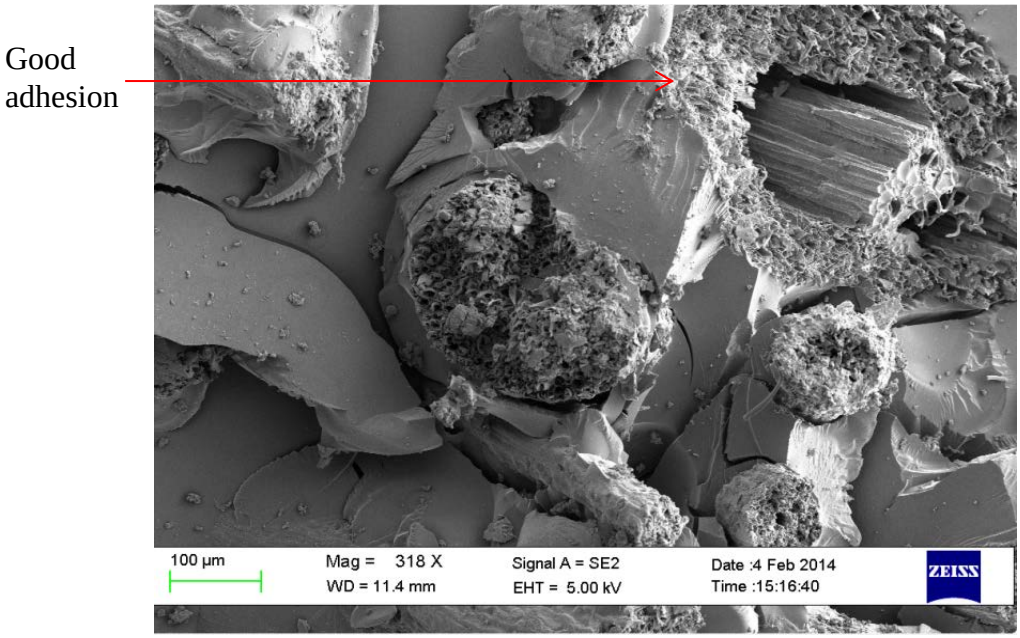


Figure 4.53 : SEM image of the hybrid-0.5% CNT impact specimen

All of the mechanical tests conducted indicate that the composite which exhibits the best properties among the CNT composites was the hybrid-1.5% CNT composite. A 2% weight fraction of CNT showed a reduction in the properties of the hybrid composites which was due to the agglomeration of the CNT particles which reduced the properties of the composite [21, 53, 56, 49]. The viscosity of the epoxy-CNT mixture was also high at the 2% weight fraction of CNT which generated voids in the specimen thus contributing to the reduction in its properties.

4.4.2 Hybrid-glass composites

Hybrid composites were fabricated using 0.1%, 1.5%, 2%, 4%, 8% and 12% weight fractions of glass and the optimum volume fraction of coir fibre being 15%. These specimens were subjected to tensile, flexural and impact tests to observe their properties.

Figure 4.54 shows the tensile strength for hybrid-glass composites. The 8% weight fraction of glass produced the highest tensile strength among these specimens being 39 MPa which is a 39% increase in comparison to the epoxy-15% coir composite which generated a tensile strength of 28 MPa. Figure 4.55 shows an SEM image for the hybrid-8% glass tensile composite. There are not many voids which could be seen indicating that there are not many weak points on the specimen. Large amounts of fibre pull out cannot be seen, however there is some evidence of short fibres being pull-out. This was due to the greater bond strength between the longer fibres and the matrix. Fibre breakage at the matrix fibre interface can be seen which shows that good interfacial bonding had taken place as well as good transfer of the load from the matrix to the fibres for the longer fibres. Dispersion of the glass spheres in the matrix was good as Figure 4.55 does not show particle agglomeration.

At a 12% weight fraction the tensile strength of the specimens decreased to a 17% lower value than the 8% weight fraction due to voids and particle agglomeration that could be seen on the specimen in Figure 4.56. The voids in the specimen

were formed due to the high weight fraction of glass used which resulted in a higher viscosity of the epoxy-glass mixture.

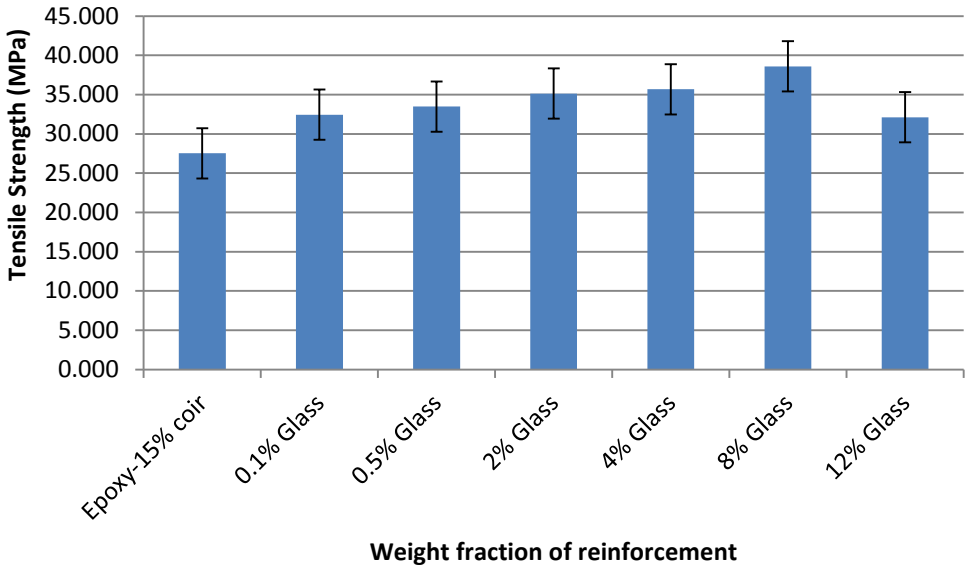


Figure 4.54 : Tensile strength of glass composite specimens

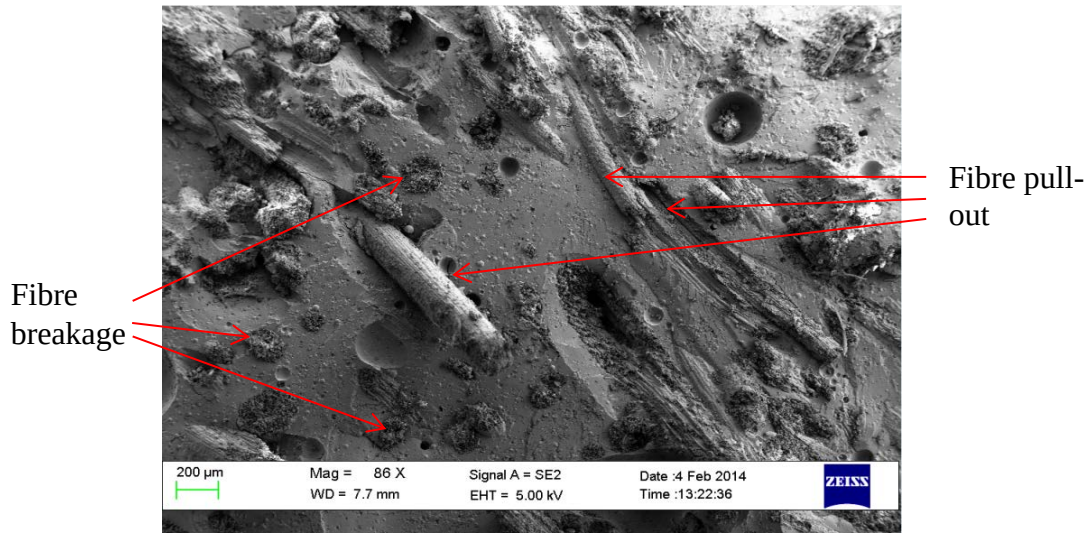


Figure 4.55 : SEM image of the hybrid-8% glass tensile specimen

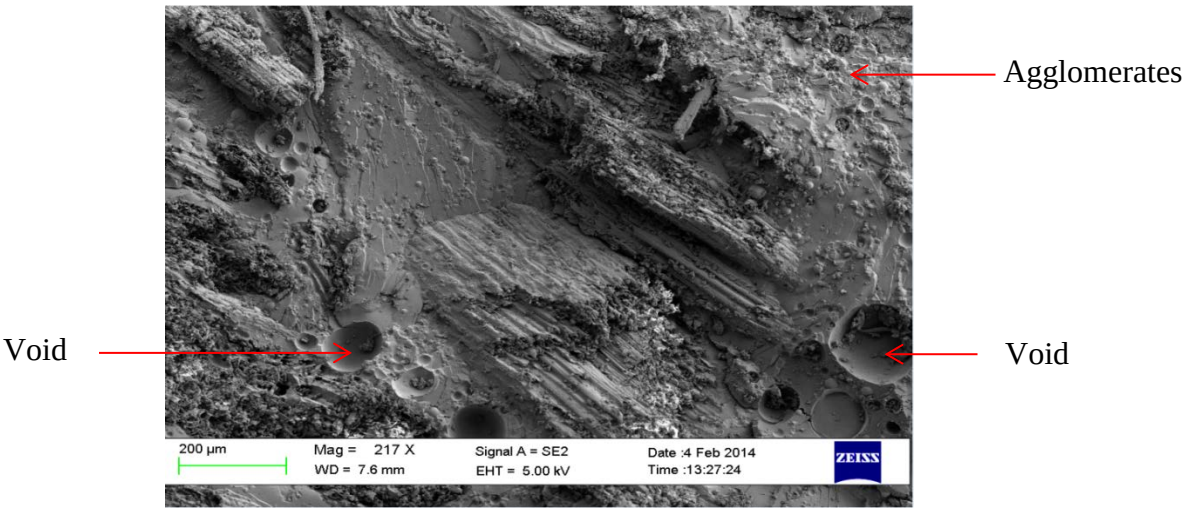


Figure 4.56 : SEM image of the hybrid-12% glass tensile specimen

The elastic modulus of glass composites can be seen in Figure 4.57. The 8% weight fraction of glass produced the highest modulus of 1.08 GPa amongst all of the glass specimens tested. This was a result of good bonding between the matrix and the reinforcements. The 12% weight fraction of glass resulted in a 22% reduction in the modulus of the specimen from the 8% weight fraction of glass, due to the agglomerations of the particles and the formation of voids shown in Figure 4.56.

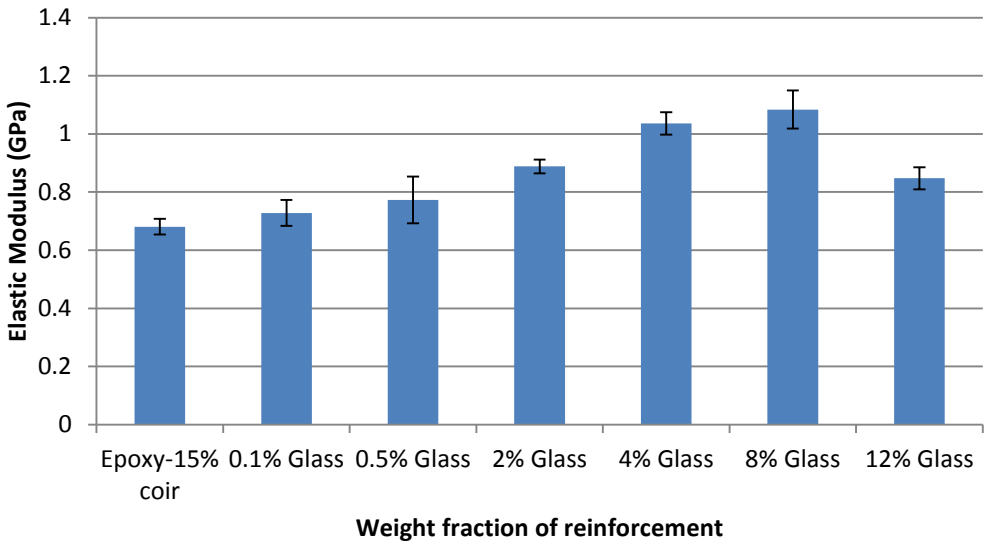


Figure 4.57 : Elastic modulus of hybrid-glass composite specimens

Flexural testing results for glass composites can be seen in Figure 4.58. The flexural strength increased amongst the hybrid composites until the 8% weight fraction of glass reinforcement. The hybrid-8% glass composite shows the highest flexural strength of 76 MPa, amongst the specimens tested which is a 73% and 100% increase in strength in comparison to the epoxy-15% coir and plain epoxy specimens respectively. Figure 4.59 shows an SEM image of the hybrid-8% glass composite, no agglomeration of the particles can be seen which shows that dispersion of the particles is good which increased the properties of the flexural specimen. The interfacial adhesion between the matrix and the reinforcements were good as shown in Figure 4.59 which also resulted in good mechanical properties. A 12% addition of glass reinforcement showed a 4% reduction in the flexural stress in comparison to the hybrid-8% glass composite due to particle agglomeration and fibre pull out as shown in Figure 4.60.

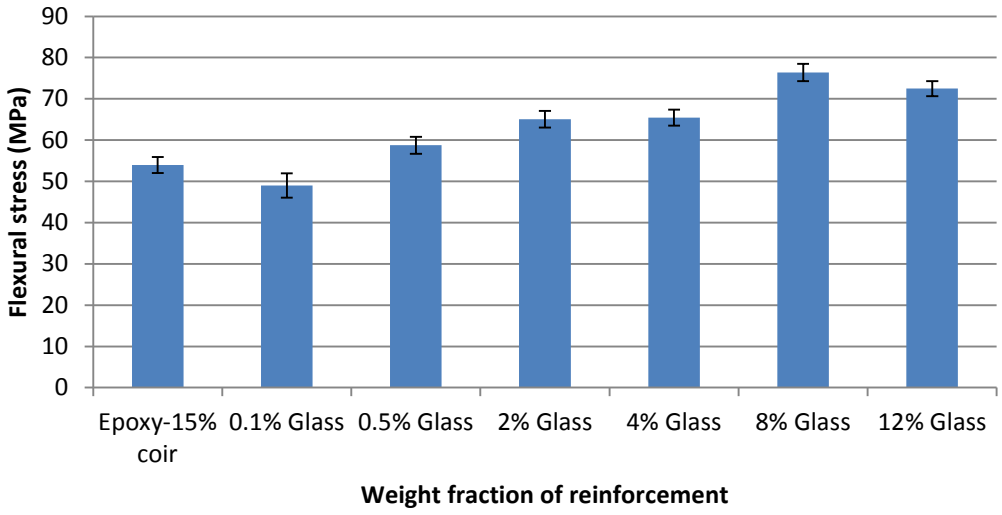


Figure 4.58 : Flexural strength of hybrid-glass specimens

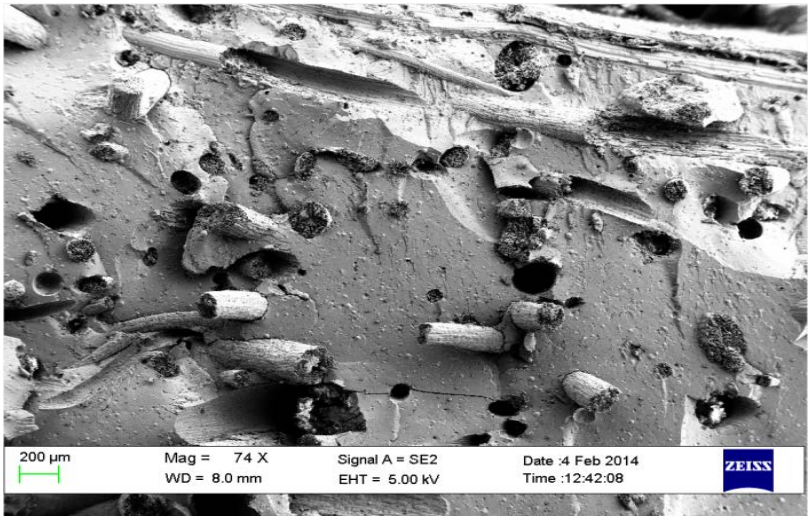


Figure 4.59 : SEM image of the hybrid-8% glass flexural specimen

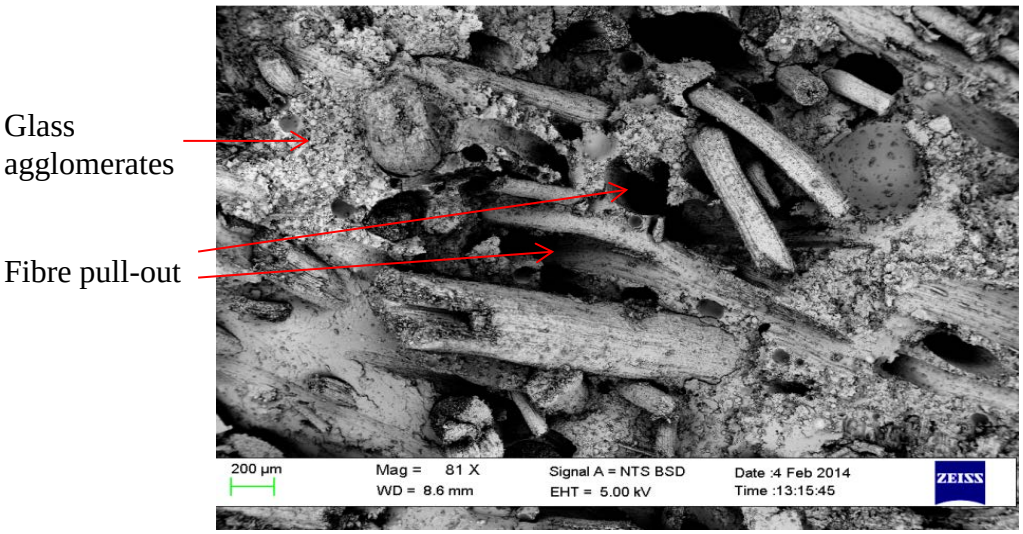


Figure 4.60 : SEM image of a hybrid-12% glass flexural specimen

The tangent modulus for the glass composites can be seen in Figure 4.61. The tangent modulus for the hybrid-glass composites increased from the 0.1% weight fraction of glass to the 8% weight fraction of glass with the 8% weight fraction exhibiting the highest modulus of 383 MPa. There was a 3% reduction in the tangent modulus of the 12% glass specimen from the 8% glass specimen due to the large amount of particle agglomeration and fibre pull out.

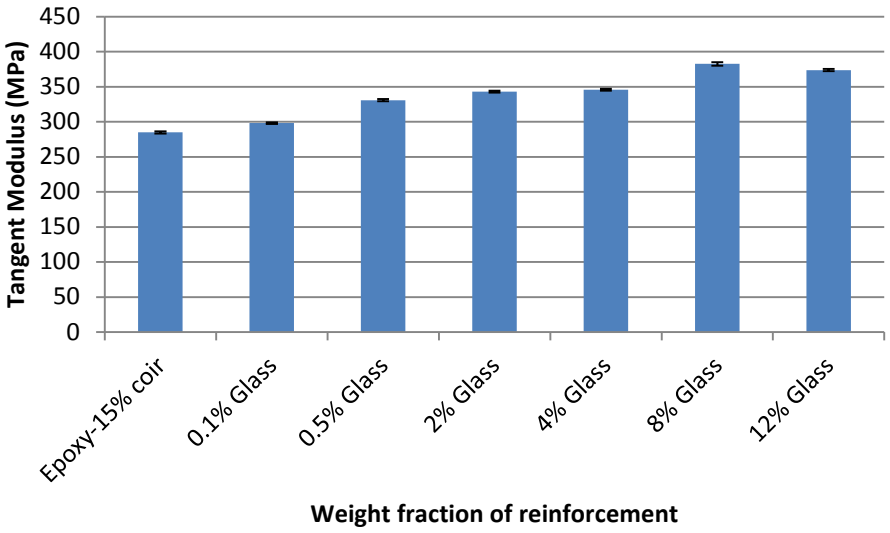


Figure 4.61 : Tangent modulus of hybrid-glass specimens

Figure 4.62 shows the fracture toughness of the hybrid-glass composites. The hybrid-0.1% glass composite exhibited the highest fracture toughness amongst all of the specimens tested with a value of 0.000929 MPa√m. The fracture toughness then decreased as the weight fraction of glass increased. A 0.1% weight fraction of glass increased the fracture toughness of the hybrid composite by 14% and 86% in comparison to the epoxy-15% coir and plain epoxy composites respectively. The 8% weight fraction of glass which generated the best properties in the tensile and flexural hybrid specimen tests showed a decrease in the fracture toughness by 10% in comparison to the epoxy-15% coir composite. This shows that as the weight fraction of reinforcement increased the tensile and flexural properties increased but the composite became brittle due to the higher weight fraction of glass used.

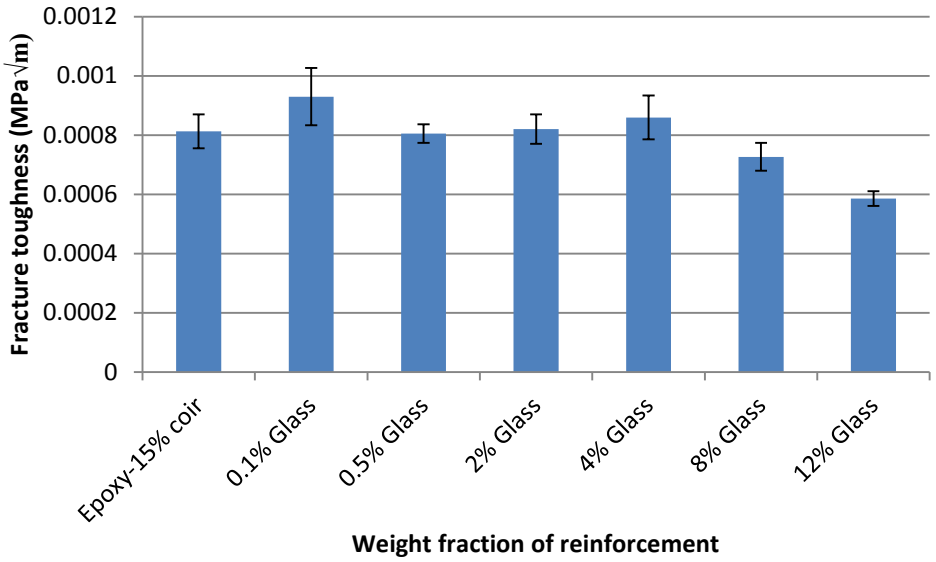


Figure 4.62 : Fracture toughness of hybrid-glass specimens

Tensile and flexural testing of the hybrid-glass composites resulted in the hybrid-8% glass composite exhibiting the best properties and was selected as the best hybrid composite fabricated with glass reinforcements. However impact testing of this composite resulted in less impact energy in comparison to the epoxy-15% coir composite. This result often does occur in composite materials where some properties are enhanced more than others. The decrease in the impact properties of the 8% glass composites is due to the high weight fraction of glass used which made the composite brittle but still possessing good tensile and flexural properties.

4.4.3 Hybrid-clay composites

Hybrid composites were fabricated for 0.1%, 1.5%, 2%, 4%, 5% and 6% weight fractions of clay and the optimum volume of coir fibre being 15%. These specimens were subjected to tensile, flexural and impact tests to observe their properties.

Figure 4.63 shows the tensile strength of clay composites. The tensile strength of the hybrid composite increased until the 4% weight fraction of clay which exhibited the highest tensile strength of 34 MPa. This was a 24% increase in tensile strength in comparison to the epoxy-15% coir composite. A 5% weight

fraction of clay produced a tensile strength of 29 MPa for the hybrid composite which is a 15% reduction in strength in comparison to the hybrid-4% clay composite.

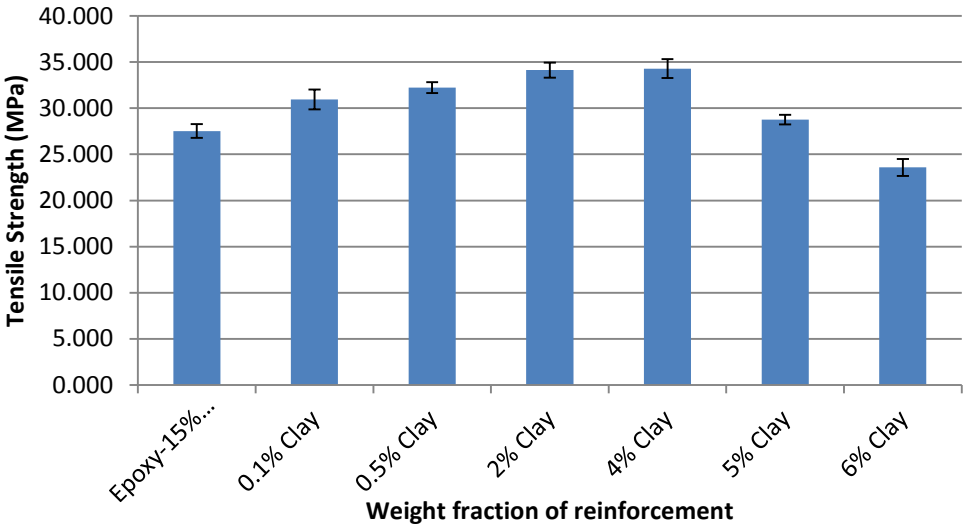


Figure 4.63 : Tensile strength of hybrid-clay composite specimens

Figure 4.64 shows an SEM image of the hybrid-4% clay tensile specimen. This specimen produced the highest tensile strength amongst the hybrid-clay composites. The specimen does not show any agglomeration of particles which indicates that dispersion of the clay particles in the matrix is good. With the clay particles being dispersed easily into the matrix it indicates that the functionalization of the clay particles was successful as the particles bonded to the matrix and dispersed well. The specimen also shows breakage of the fibre at the matrix interface which indicates good interfacial adhesion between the matrix and the fibres showing that the load is distributed well from the matrix to the fibre.

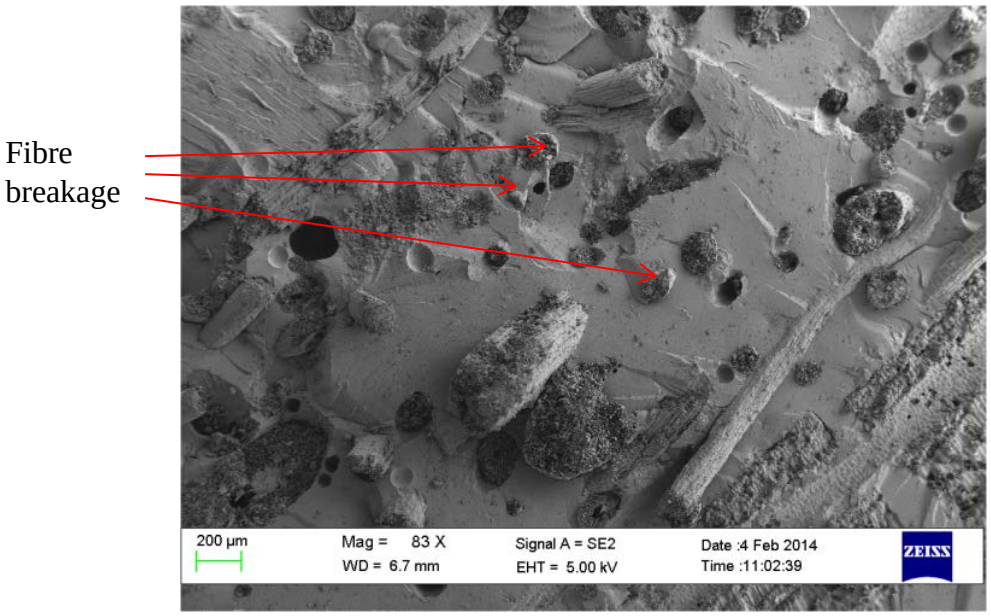


Figure 4.64 : SEM image of the hybrid-4% clay tensile specimen

Figure 4.65 shows an SEM image of the hybrid-5% clay specimen. In comparison to Figure 4.64 a fair amount of voids and particle agglomerations can be seen. The particle agglomeration is due to the higher weight fraction of clay used. Due to these factors the tensile properties of the composite specimen was reduced.

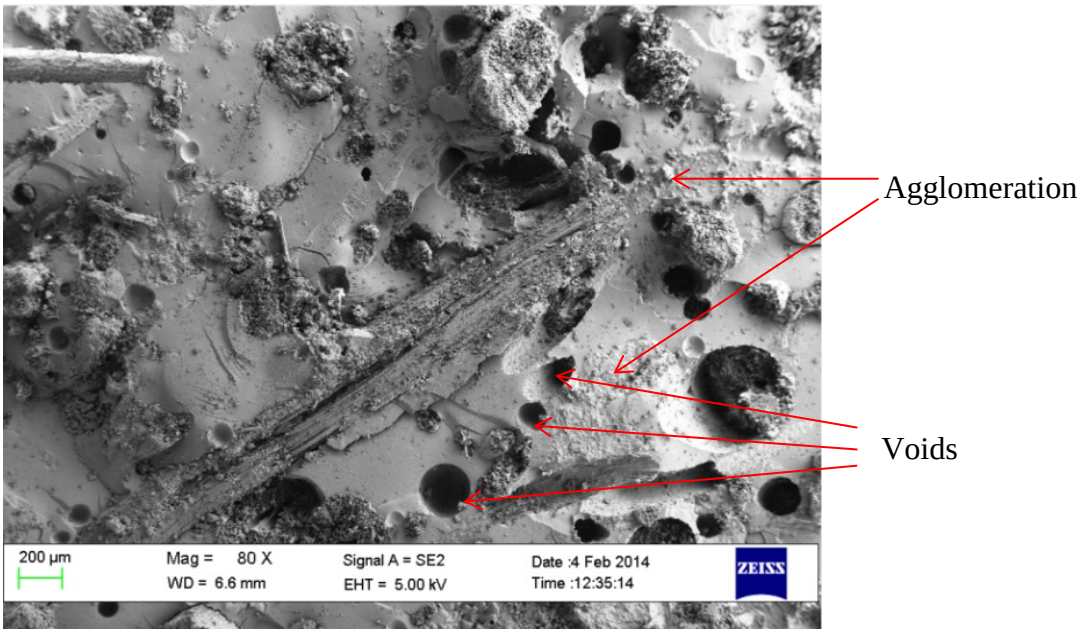


Figure 4.65 : SEM image of the hybrid-5% clay tensile specimen

Figure 4.66 shows the elastic modulus for the clay composites. The elastic modulus increased as the weight fraction of the clay increased. Although the 4% weight fraction of clay produced the highest tensile strength for the hybrid-clay composites, Figure 4.66 shows that the highest modulus generated was for the hybrid-5% clay composite being 1.014 GPa. This was a 49% increase in modulus in comparison to the epoxy-15% coir composite which indicates that the hybrid composite is stiffer than the epoxy-15% coir composite. At the 6% weight fraction of clay the elastic modulus decreased showing that the stress to strain ratio is decreasing.

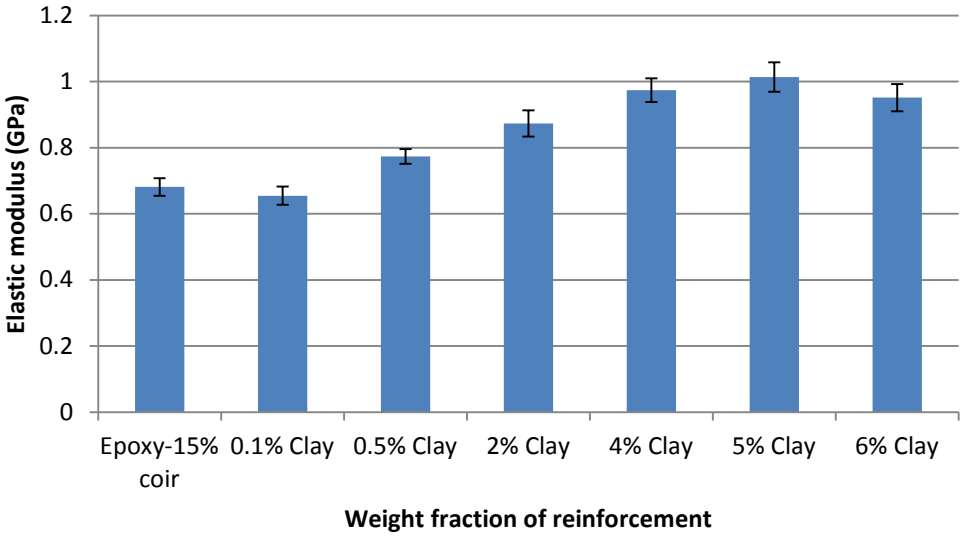


Figure 4.66 : Elastic modulus of clay composite specimens

Figure 4.67 shows the flexural strength for the hybrid-clay composites with a 4% reinforcement of clay generated the highest flexural strength of 75 MPa. This was a 38% increase in the flexural strength in comparison to the epoxy-15% coir composite. Both the 5% and 6% hybrid-clay composites show a decrease of 12% and 16% respectively in the flexural strength in comparison to the hybrid-4% clay composite. Figure 4.68 shows an SEM image of the hybrid-5% clay composite showing fibre pull out which indicates weak interfacial bonding which caused a reduction in the flexural strength of the composite.

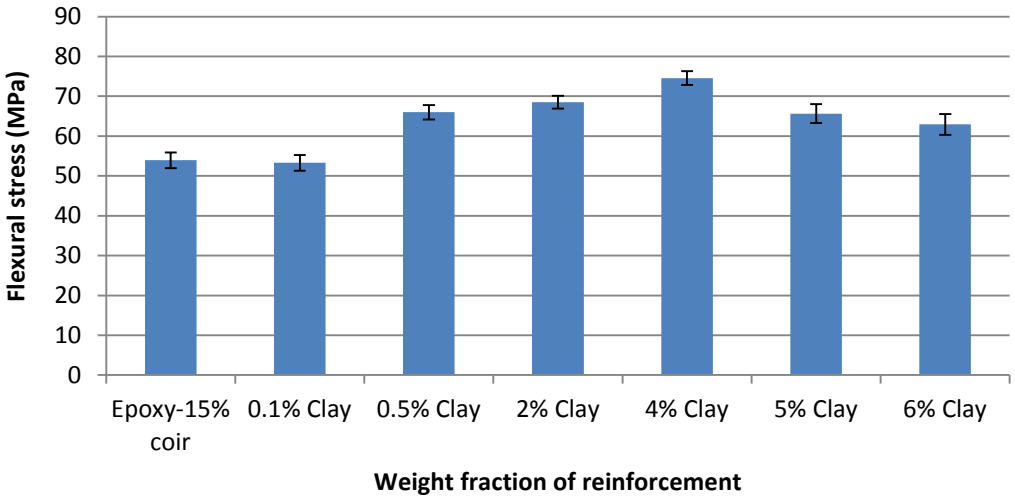


Figure 4.67 : Flexural strength of clay specimens

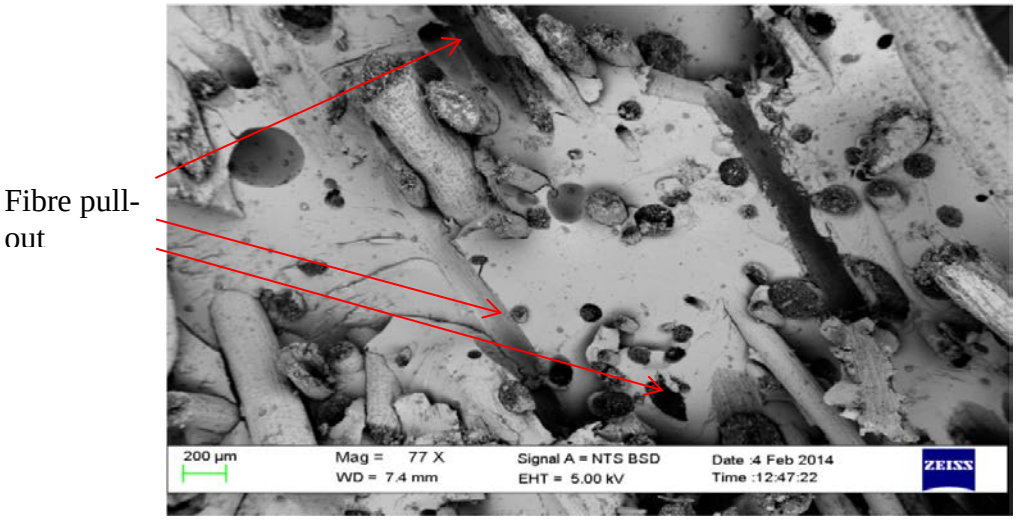


Figure 4.68 : SEM image of the hybrid-5% clay flexural specimen

Figure 4.69 shows the tangent modulus for the clay composites and indicates that the modulus increased from the 0.1% weight fraction of clay to the 6% weight fraction for the hybrid composites. The hybrid-6% clay composite produced the highest tangent modulus from the entire range of specimens tested with a 37% increase from the epoxy-15% coir composites. This shows that the ratio of stress to strain increased for these specimens and thus increased the bending stiffness.

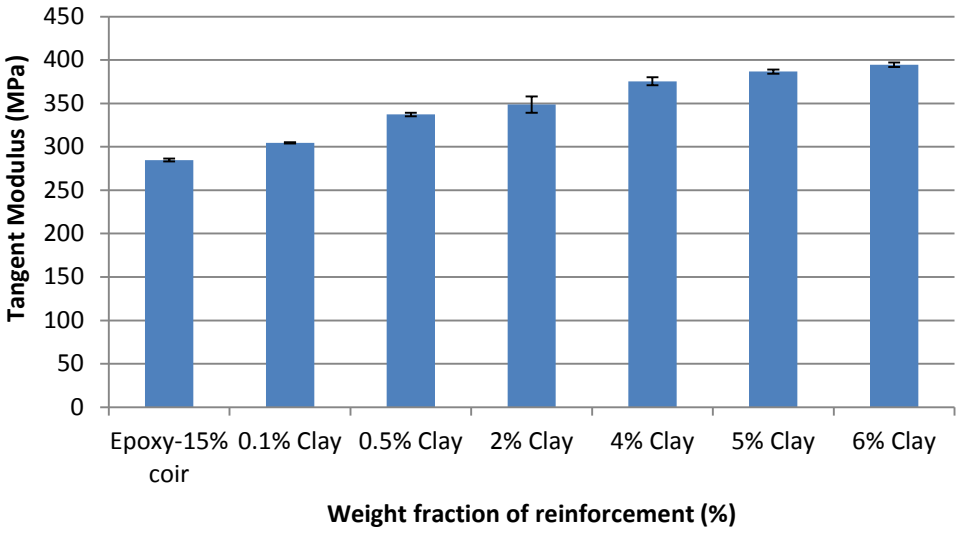


Figure 4.69 : Tangent modulus of clay specimens

Impact testing for the hybrid-clay specimens indicates that the fracture toughness was the highest for the 0.1% weight fraction of clay shown in Figure 4.70 which was a 22% increase in comparison to the epoxy-15% coir composite which showed a value of 0.0008125 MPa√m. As the weight fraction of clay increased in the hybrid composite the fracture toughness decreased with a 2% weight fraction of clay resulting in a reduction in fracture toughness as compared to the epoxy-15% coir composite.

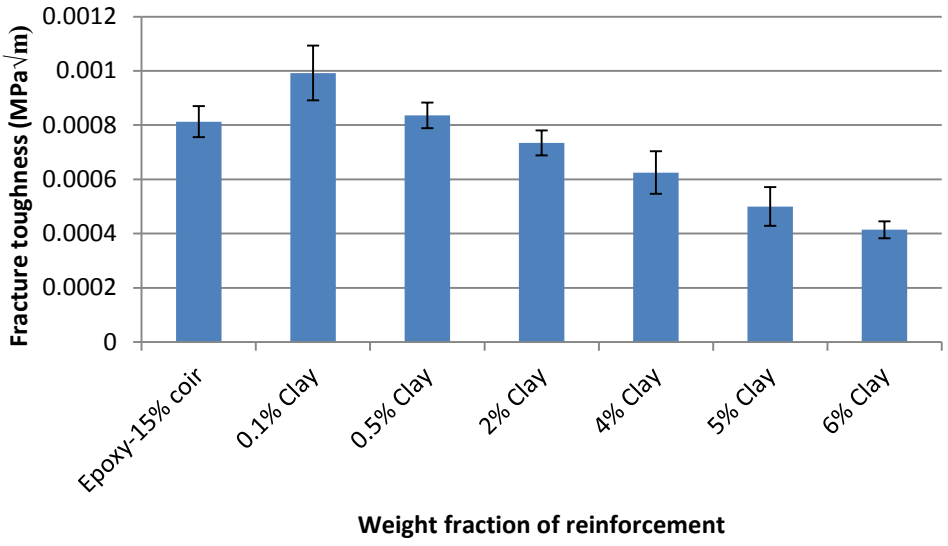


Figure 4.70 : Fracture toughness of hybrid-clay specimens

Figure 4.71 shows an SEM image of the hybrid-0.1% clay impact specimen which generated the highest fracture toughness amongst the clay composites. The distribution of the coir fibre looks good. The specimen does not show much signs of agglomeration or fibre pull out indicating that the interfacial bonding between the particles is good hence the specimen showed good fracture toughness.

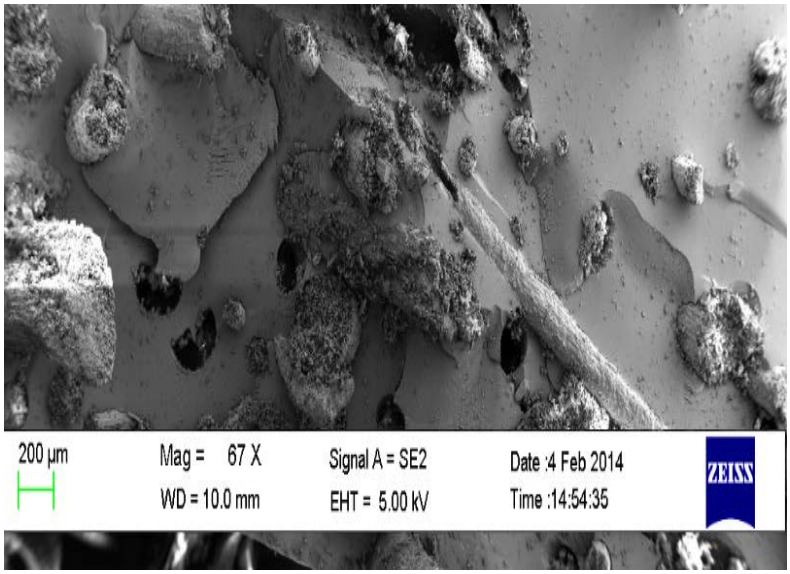


Figure 4.71 : SEM image of the hybrid-0.1% clay impact specimen

An SEM image was taken for the hybrid-4% clay impact specimen, Figure 4.72. The picture shows fibre pull out which impacted on the strength of the composite.

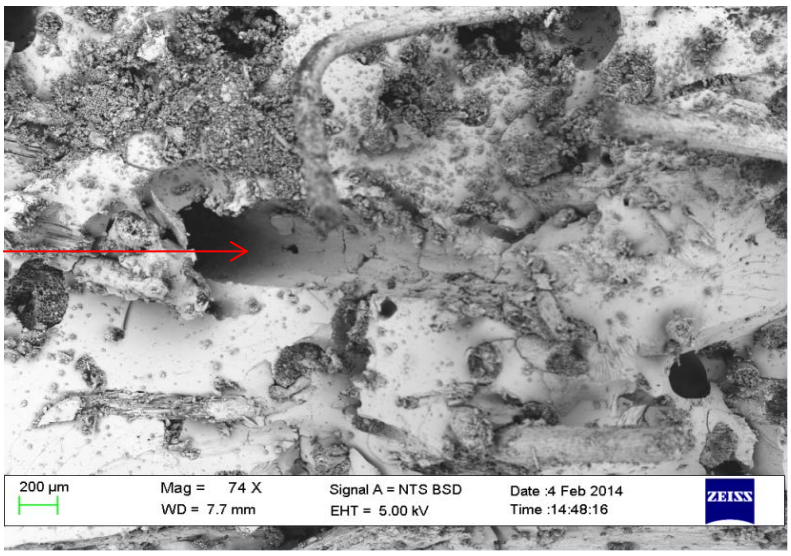


Figure 4.72 : SEM image of the hybrid-4% clay impact specimen

Tensile and flexural testing of hybrid-clay composites resulted in the 4% weight fraction of clay exhibiting the best tensile and flexural strength. The impact energy of this composite dropped to below that of the epoxy-15% coir composite but as mentioned for the hybrid-glass composites, not all properties of a composite can be enhanced simultaneously. With the increase in the tensile and flexural strength of the hybrid-4% clay composite it is selected as the best clay composite.

4.5 Summary

To determine which reinforcement generated the best mechanical properties from the composites a summary of the specimens which generated the best properties from each type of reinforcement, CNT, clay and glass was compiled and compared. It can be seen in the sub-sections above that the hybrid composites produced better mechanical properties than the particulate composites.

A summary of the specimens producing the highest tensile strength with the different reinforcements used can be seen in Figure 4.73. The hybrid-1.5% CNT composite generated the highest tensile strength followed by the hybrid-8% glass composite and then the hybrid-4% clay composite which resulted in a 6% and 16% higher tensile strength respectively.

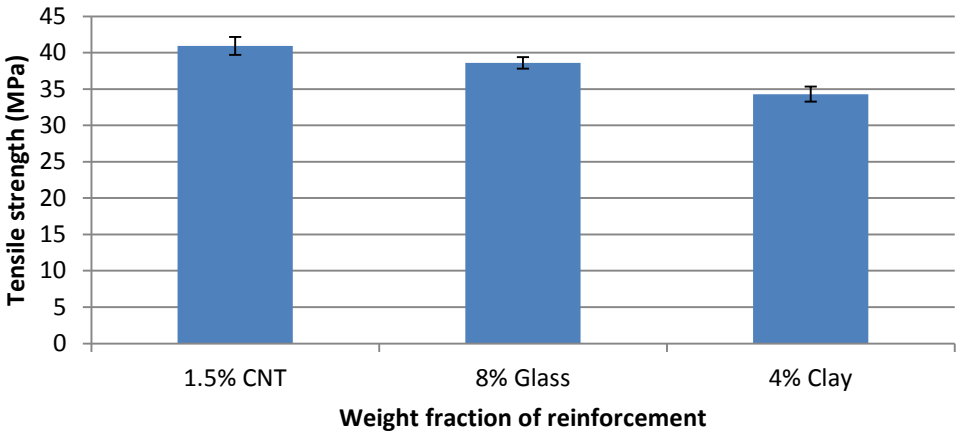


Figure 4.73 : Tensile strength of hybrid-composite specimens

A summary of the elastic modulus results for the composites which generated the best modulus among the different reinforcements can be seen in Figure 4.74. The hybrid-1.5% CNT composite produced the best modulus amongst all of the specimens with a 13% increase over the hybrid-8% glass specimens and an 18% increase over the hybrid-5% clay specimens respectively.

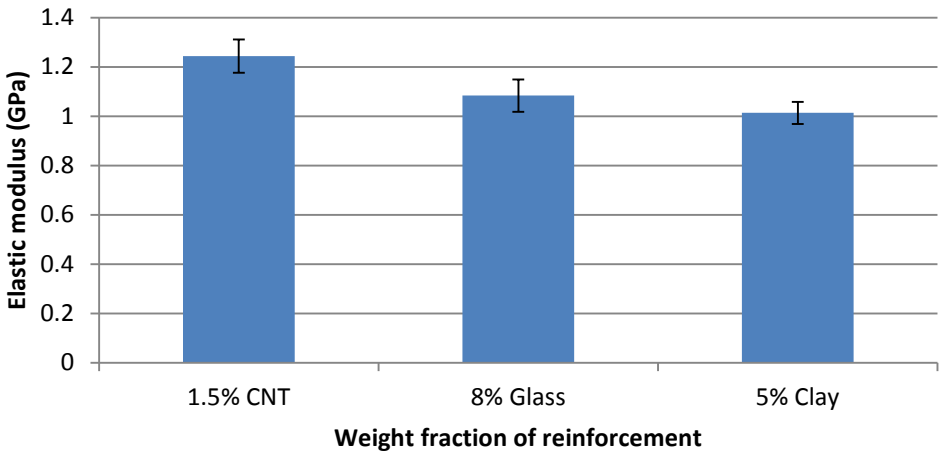


Figure 4.74 : Elastic modulus of hybrid-composite specimens

Figure 4.75 shows the flexural strength obtained for the composite materials which exhibited the best properties amongst the different reinforcements used. Both the flexural strength as well as the tangent modulus shown in Figure 4.76, indicates that the highest flexural properties are with the hybrid-CNT composites than the hybrid-glass and hybrid-clay composites. The flexural strength for the hybrid-1.5% CNT proved to be 8% greater than the hybrid-8% glass composite and 10% greater than the hybrid-4% clay composite.

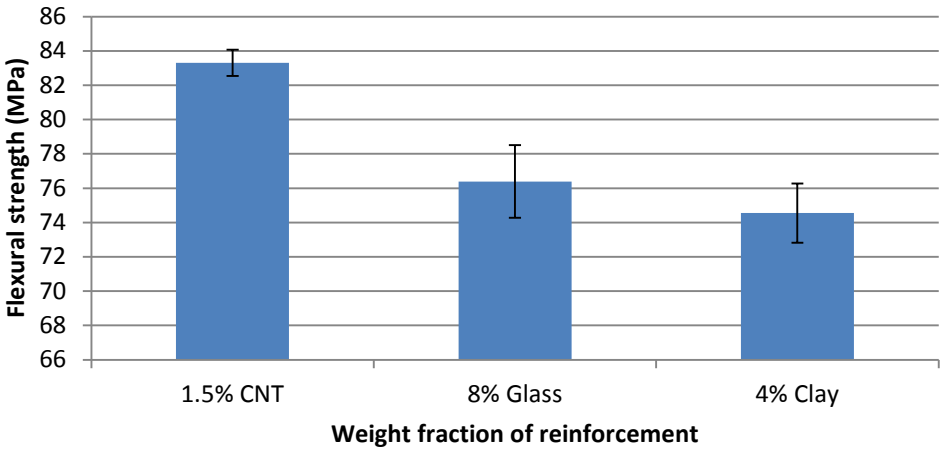


Figure 4.75 : Flexural strength of hybrid-composites

The hybrid-1.5% CNT composite generated a 1% increase in the modulus over the hybrid-8% glass composites and a 3% increase over the hybrid-4% clay composites.

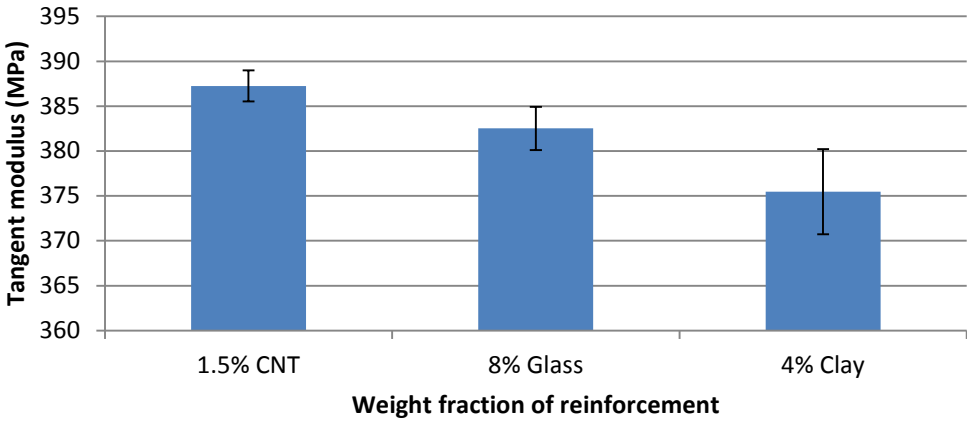


Figure 4.76 : Tangent modulus of hybrid-composites

A combination of the best composite specimens for the fracture toughness was combined in Figure 4.77. Here it can be seen that the hybrid-CNT composite produced the highest fracture toughness which indicates that it remains the strongest under impact testing. The 0.1% hybrid-clay composite produced a higher fracture toughness than the hybrid-0.1% glass composites by 1%. Due to glass being more brittle than clay it had been thought that this margin would be greater than 1% but it shows that the glass composites are capable of generating

hybrid composites which have good impact strengths in comparison to those of clay.

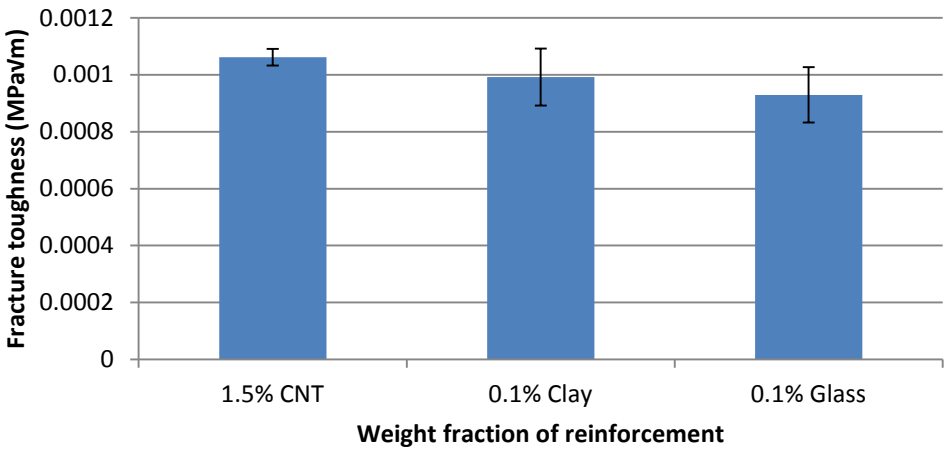


Figure 4.77 : Fracture toughness of hybrid-composites

It can thus be seen that the best hybrid composite produced was the hybrid-1.5% CNT composite due to the fact that it produced the best test results amongst the tests conducted.

It was noted that the hybrid-clay and hybrid-glass composites generated an average of a 10% increase in the properties as compared to the epoxy-clay and epoxy-glass composites. This indicates that hybrid composites generate better properties than the particulate composite materials.

5 CONCLUSION AND RECOMMENDATIONS

With the growing interest in hybrid composites the current researcher has made good observations regarding the fabrication and properties of hybrid composites. The use of the VRTM process had initially proved to be a very tricky as there were a lot of issues and problems which needed to be solved before test specimens could be fabricated. Each type of reinforcement type required a slight alteration to the process in order to fabricate good specimens. For the epoxy-coir composites the 15% weight fraction of the composite generated the best mechanical properties. With not much reference material available for hybrid-coir composites the researcher conducted testing on epoxy-glass and epoxy-clay specimens to justify the current research with research conducted by other researchers and found that the mechanical properties proved to be the best using a 0.5% weight fraction of reinforcement. The mechanical testing results indicate that the most suitable hybrid composite using coir fibre is by using a 1.5% weight fraction of CNT. This composite provided superior results in the tensile, flexural and impact testing of the specimens. The optimum weight fractions of glass and clay being 8% and 4% respectively did come close to the properties obtained from the hybrid-CNT composite.

A recommendation would be to improve the mat fabrication process as it is felt that a more continuous distributed mat may produce better mechanical properties. This however would need to be confirmed by conducting suitable research. Another interesting suggestion would be to break up the additional reinforcements in sections such as to conduct tests using CNT and graphite and nanoclay and clay just to observe what effect the nano particles would have on the mechanical properties of the composites in comparison to micro sized particles.

REFERENCES

1. P. Wambua, J. Ivens and I. Verpoest : Natural fibres: can they replace glass in fibre reinforced plastics? , Composites Science and Technology 63 (2003) 1259-1264

2. C. Zweben, M. Kutz : Composite materials, Mechanical Engineers Handbook: Materials and Mechanical Design, Volume 1, Third Edition; John Wiley and Sons, Inc.

3. D. Hall (1981) : An Introduction to Composite Materials; Cambridge University Press

4. G. Cicala, G. Cristaldi, G. Recca, G. Ziegman, A. El-Sabbagh, M. Dickert : Properties and Performances of various hybrid glass/ natural fibre composites for curved pipes, Materials and Design 30 (2009) 2538-2542

5. J. Yao, Y. Hu and W. Lu : A wood replacement material of sandwich structure using coir fibre mats and fibreglass fabrics as core layer, Bio-resources 7(1), 663-674

6. H. Alamri, I. M. Low : Effect of water absorption on the mechanical properties of nanoclay filled cellulose fibre reinforced hybrid nanocomposite, Composites Part A: Applied Science and Manufacturing Volume 44, January 2013, 23-31

7. M. M. Thwe, K. Liao : Durability of bamboo-glass fiber reinforced polymer matrix hybrid composites, Composites Science and Technology 63 (2003) 375-387

8. V. G. Geethamma, K. T. Mathew, R. Lakshminarayanan and S. Thomas : Composite of short coir fibres and natural rubber: effect of chemical modification, loading and orientation of fibre, Polymer Vol. 39 No. 6-7 (1998), 1483-1491

9. M. F. Ashby, D. R. H Jones (1999) : Engineering Materials Volume II – Microstructures, Processing, Design, 2nd Edition; Butterworth-Heinemann; Woburn, MA

10. F. Kreth, D. Goswami (2005) : Handbook of Mechanical Engineering 2nd ed., CRC Press LLC

11. M. Kutz (2006) : Mechanical Engineers Handbook 3rd ed, Vol 1 of 4 - Materials and Mechanical Design, Wiley

12. C. A. Harper (1999) : Modern Plastics Handbook; Magraw Hill;

13. N. E. Zander : Epoxy Nano-Reinforced Composite Systems, Army Research Laboratory, Aberdeen Proving Ground, MD 21005-5069, ARL-CR-601, February 2008 Dynamic Science

14. L. Cui, Y. Wang, W. Xiu, W. Wang, L. Xu, X. Xu, Y. Meng, L. Li, J. Gao, L. Chen, H. Geng : Effect of functionalization of multi-walled carbon nanotube on the curing behaviour and mechanical property of multi-walled carbon nanotube/ epoxy composites, Materials and Design 49 (2013) 279-284

15. Y. X. Zhou, P. X. Wu, Z. Y. Cheng, J. Ingram, S. Jeelani : Improvement in electrical, thermal and mechanical properties of epoxy by filling carbon nanotubes, express Polymer Letters Vol.2, No.1(2008) 40-48

6 X. Liang, K. Ibrahim, Z. Wu : XANES study of multiwalled carbon nanotubes modified by HNO3 vapour; Materials letters 72 (2012) 131-133

17. G. Kretsis : A review of the tensile, compressive, flexural and shear properties of hybrid fibre reinforced plastics, Composites, Volume 18, No. 1, January (1987), 13‑23

18. G. Liu, H. Zhang, X. Yang, Y. Wang : Facile synthesis of silica/polymer hybrid microspheres and hollow polymer microspheres, Polymer 48 (2007) 5896-5904

19. R. C. L. Dutra, B. G. Soares, E. A. Campos, J. L. G. Silva : Hybrid composites based on polypropylene and carbon fiber and epoxy matrix, Polymer 41 (2000) 3841–3849

20. M. J. John, R. D. Anandjiwala and L. A. Pothen (2007) : Hybrid Composites in 'Natural Fiber Reinforced Polymer Composites' Edited by Sabu Thomas and Laly A. Pothen, Old City Publishing

21. J. Shen, W. Huang, L. Wu, Y. Hu, M. Ye : The reinforcement role of different amino-functionalized multi-walled carbon nanotubes in epoxy nanocomposites, Composites Science and Technology 67 (2007) 3041-3050

22. S. Harish, D. Peter Michael, A. Bensely, D. Mohanlal, A. Rajadurai : Mechanical property evaluation of natural fibre coir composites, Materials Characterization 60 (2009) 44-49

23. S. V. Joshi, L. T. Drzal, A. K. Mohanty, S. Arora : Are natural fiber composites environmentally superior to glass fiber reinforced composites?, Composites: Part A 35 (2004) 371-376

24. G. Cicala, G. Cristaldi, G. Recca, G. Ziegmann, A. El-Sabbagh, M. Dickert : Properties and performance of various hybrid glass/ natural fibre composites for curved pipes, Materials and Design 30 (2009) 2538-2542

25. M. Z. Rong, M. Q. Zhang, Y. Liub, G. C. Yang, H. M. Zeng: The effect of fiber treatment on the mechanical properties of unidirectional sisal-reinforced epoxy composites, Composites Science and Technology 61 (2001) 1437–1447

26. K. G. Satyanarayana, K. Sukumaran, P. S. Mukherjee, C. Pavithran and S. G. K. Pillai : Natural fibre-Polymer Composites, Cement and Concrete Composites 12 (1990) 117-136

27. N. Defoirdt, S. Biswas, L. de Vriese, Q. N. Tran, J. van Acker, Q. Ahsan, L. Gorbatikh, A. van Vuure, I. Verpoest : Assessment of the tensile properties of coir, bamboo and jute fibre, Composites, Part A 41 (2010) 588-595

28. M. M. Rahman, M. A. Khan : Surface treatment of coir (cocos nucifera) fibres and its influence on the fibres physico-mechanical properties, Composites Science and Technology 67 (2007) 2369-2376

29. W. Wei, G. Huang : Characterization and utilization of natural coconut fibres composites, Materials and Design, Volume 30, Issue 7, August 2009, 2741-2744

30. J. Rout, M. Misra, S. S. Tripathy, S. K. Nayak, A. K. Mohanty : The influence of fibre treatment on the performance of Coir-polyester composites, Composites Science and Technology, Volume 61, Issue 9, July 2001, 1303-1310

31. M. Ali : Coconut fibre: A versatile material and its applications in engineering, Journal of Civil Engineering and Construction Technology Vol. 2(9), (2011), 189-197

32. S. N. Patankar, A. Das, Y. A. Kranov : Interface Engineering via compatibilization in HDPE composite reinforced with Sodium borosilicate hollow glass microspheres, Composites: Part A 40 (2009) 897-903

33. Z. Mitroova, N. Tomasovicova, G. Lancz, J. Kovac, I. Vavra, P. Kopcansky : Preparation and characterization of carbon nanotubes functionalized by magnetite nanoparticles, 2010 Nanocon, 12.-14.10.2010, Olomouc, Czech Republic, EU

34. R. Yudianti, H. O. Sudirman, Y. Saito, T. Iwata and J. Azuma : Analysis of functional group sited on Multi-wall Carbon Nanotube surface, The Open Materials Science Journal, 2011, 5, 242-247

35. W. Zou, Z. Du, Y. Liu, X. Yang, H. Li, C. Zhang : Functionalization of MWNT's using polyacryloyl chloride and the properties of CNT-epoxy matrix nanocomposites, Composites Science and Technology, Volume 68, Issues 15-16, December 2008, Pages 3259-3264

36. S. H. Kim, W. Lee, B. S. Kim, J. M. Park, J. K. Park : Assessment of state of dispersion for epoxy/CNT nanocomposites, 301-1201, Seoul National University, Seoul 151-742, Korea.

37. P. R. Shukla, S. Wang, H. M. Ang, M. O. Tade : Synthesis, characterisation and adsorption evaluation of carbon-natural-zeolite composites, Advanced Powder Technology 20 (2009) 245-250

38. A. D. Gianni, E. Amerio, O. Monticelli, R. Bongiovanni : Preparation of polymer/clay mineral nanocomposites via dispersion of silylated montmorillonite in a UV curable epoxy matrix, Applied Clay Science 42 (2008) 116-124

39. A. A. Silva, K. Dahmouche, B. G. Soares : Nanostructure and dynamic mechanical properties of silane-functionalized montmorillonite / epoxy nanocomposites : Applied Clay Science 54 (2011) 151-158

40. F. Chiu, H. Yen, C. Chen : Phase morphology and physical properties of PP/ HDPE/ organoclay (nano) composites with and without a maleated EPDM as a compatibilizer, Polymer Testing 29 (2010) 706-716

41. F. I. Romli, A. N. Alias, A. S. M. Rafie, D. Laila, A. A. Majid : Factorial study on the tensile strength of a Coir Fibre-reinforced Epoxy Composite, AASRI Procedia, Volume 3, (2012), 242-247

42. A. M. Shanmugharaj, K. Y. Rhee, S. H. Ryu : Influence of dispersing medium on grafting of aminopropyltriethoxysilane in composite and its physical characteristics, Journal of Physics and Chemistry of Solids (2008) 1375-1378

43. N. Phonthammachai, X. Li, S. Wong, H. Chia, W. W. Tjiu : Fabrication of CFRP from high performance clay/epoxy nanocomposite : Preparation, conditions, thermal-mechanical properties and interlaminar fracture characteristics, Composites: Part A 42 (2011) 881-887

44. J. H. Park, H. M. Lee, I. Chin, H. J. Choi, H. K. Kim, W. G. Kang : Intercalated polypropylene/ clay nanocomposite and its physical characteristics, Journal of Physics and Chemistry of Solids (2008) 1375-1378

45. Y. Xu, S. van Hoa : Mechanical properties of carbon fibre reinforced epoxy / clay nanocomposites, Composites Science and Technology 68 (2008) 854-861

46. T. D. Ngo, M. T. Ton-That, S. V. Hoa. K. C. Cole : Effect of temperature, duration and speed of premixing on the dispersion of clay/ epoxy nanocomposites, Composites Science and Technology 69 (2009) 1831-1840

47. T. P. Mohan, K. Kanny : Water barrier properties of nanoclay filled sisal fibre reinforced epoxy composites, Composites Part A: Applied Science and Manufacturing (2011) 385-393

48. M. Ho, C. Lam, K. Lau, D. H. L. Ng, D. Hui : Mechanical properties of epoxy-based composites using nanoclays, Composite structures, Volume 75 (2006) 415-421

49. M. Silani, S. Ziaei-Rad, M. Esfahanian, V. B. C. Tan : On the experimental and numerical investigation of clay/epoxy nanocomposite, Composite Structures 94 (2012) 3142-3148

50. H. He, Q. Tao, J. Zhu, P. Yuan, W. Shen, S. Yang : Silylation of clay mineral surfaces, Applied Clay Science Volume 71 (2013) 15-20

51. A. Yasmin, J. J. Luo, J. L. Abot, I. M. Daniel : Mechanical and thermal behaviour of clay/ epoxy nanocomposites, Composites Science and Technology 66 (2006) 2415-2422

52. Y. Yu, G. Xiong, C. Li, F. Xiao : Characterization of aluminosilicate zeolites by UV Raman spectroscopy; Microporous and Mesoporous Materials 46 (2001) 23-34

53. P. A. Schroeder : Infrared Spectroscopy in Clay Science: IN CME Workshop Lectures, Vol. 11, Teaching Clay Science, A. Rule and S. Guggenheim, eds., The Clay Mineral Society, Aurora, CO, 181-206 (2002)

54. J. Madejova, P. Komadel : Baseline studies of the Clay Minerals Society Source Clays: Infrared Methods, Clays and Clay Minerals, Vol. 49, No. 5, (2001), 410-432

55. F. A. Abuilaiwi, T. Laoui, M. Al-Harthi, and M. A. Atieh : Modification and functionalization of Multi-walled Carbon Nanotube (MWCNT) via Fischer Esterification, The Arabian Journal for Science and Engineering, Volume 35, Number 1C (2010), 37-48

56. D. Mao : Improving mechanical properties of Nanocomposites using Carbon Nanotubes, Society for the Advancement of Material and Process Engineering (2009)

57. J. Seetharamappa, S. Yellappa, and F. D'Souza : Carbon Nanotubes – Next generation of Electronic materials, The Electrochemical Society interface (Summer 2006), the chalkboard

58. M. R. Mansor, S. M. Sapuan, E. S. Zainudin, A. A. Nuraini, and A. Hambali : Stiffness Prediction of Hybrid Kenaf/Glass Fiber Reinforced Polypropylene Composites using Rule of Mixtures (ROM) and Rule of Hybrid Mixtures (RoHM), Journal of Polymer Materials Volume 30, No.3 (2013), 321-334

59. S. D. Jacob Muthu, R. Paskaramoorthy : Double-wall Carbon Nanotube-reinforced Polyester Nanocomposites: Improved Dispersion and Mechanical properties, Polymer composites Volume 33, Issue 6 (2012), 866–871

60. A. G. Osorio, I. C. L. Silveira, V. L. Bueno, C. P. Bergmann : H_2SO_4/ HNO_3/HCL – Functionalization and its effect on dispersion of carbon nanotubes in aqueous media, Applied Surface Science 255 (2008) 2485-2489

61. C. M. Damian, A. M. Pandele, H. Iovu: Ethylenediamine Functionalization effect on the Thermo-mechanical properties of epoxy Nanocomposites reinforced with Multiwall Carbon Nanotubes, U.P.B. Sci. Bull., Series B, Vol. 72, Issue 3, 2010

62. C. Dendere : Mechanical Characterization of GRP and Nano-strengthened GRP Hybrid Composite using Experimental Methods. Johannesburg, South Africa: University of Witwatersrand, (2013)

63. M. A. Almaadeed, M. Ouederni, P. N. Khanam : Effect of chain structure on the properties of glass/ fibre/ Polyethylene Composites, Materials and Design (2012)

64. N. Venkateshwaran, A. Elayaperumal, G. K. Sathiya: Prediction of tensile properties of hybrid-natural fibre composites, Composites: Part B 43 (2012) 793-796

65. D. R. Mulinari, C.A.R.P. Baptista, J. V. C. Souza, H. J. C. Voorwald : Mechanical Properties of Coconut Fibres Reinforced Polyester Composites; Procedia Engineering 10 (2011) 2074-2079

66. H. Gu : Tensile behaviours of the coir fibre and related composites after NaOH treatment, Materials and Design 30 (2009) 3931-3934

67. N. Ezekiel, B. Ndazi, C. Nyahumwa, S. Karlsson : Effect of temperature and durations of heating on coir fibres, Industrial Crops and Products – IND Crops Products, vol. 33, no. 3, pp. 638-643, 2011

68. I. Tavman, V. Cecen, I. Ozdemir, A. Turgut, I. Krupa, M. Omastova, I. Novak : Preparation and characterization of highly electrically and thermally conductive polymeric nanocomposites, Archives of Material Science and Engineering, Volume 40, Issue 2, December 2009, Pages 84-88

69. O. Valentino, M. Sarno, N. G. Rainone, M. R. Nobile, P. Ciambelli, H. C. Neitzert, G. P. Simon : Influence of the polymer structure and nanotube concentration on the conductivity and rheological properties of polyethylene/ CNT composites, Physica E 40 (2008) 2440-2445

70. A. Allaoui, S. Bai, H. M. Cheng, J. B. Bai : Mechanical and electrical properties of a MWNT/ epoxy composite, Composite Science and Technology 62 (2002) 1993-1998

71. R. Y. Sato-Berru, E. V. Basiuk and J. M. Saniger : Application of principle component analysis to discriminate the Raman spectra of functionalized multi-walled carbon nanotubes, Journal of Raman Spectroscopy, J. Raman Spectroscopy. 2006; 37: 1302-1306

Appendix A – Sample testing specimens

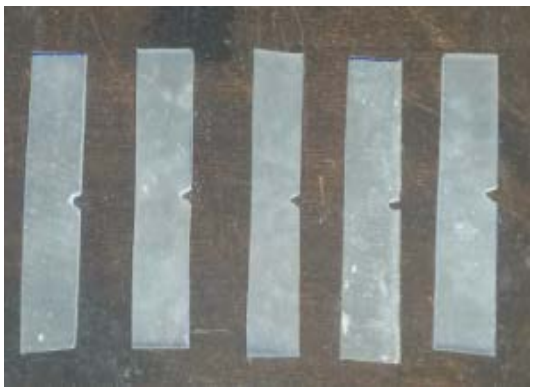
Plain epoxy



Tensile specimen



Flexural specimen



Impact specimen

Epoxy Coir Specimens



Tensile specimen

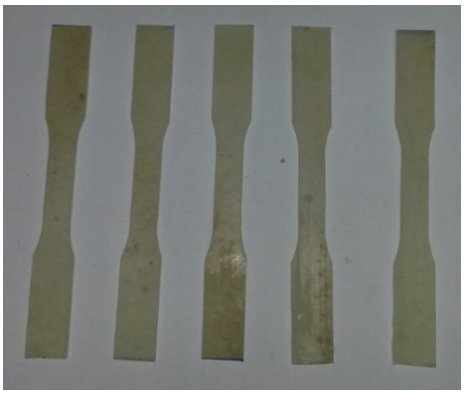


Flexural specimen

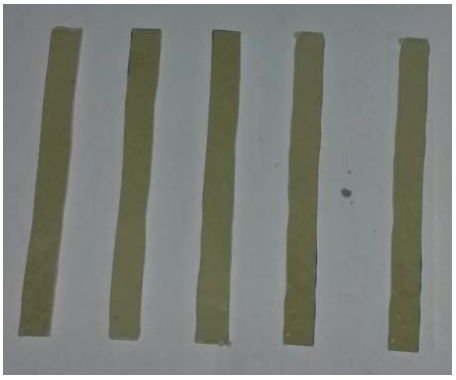


Impact specimen

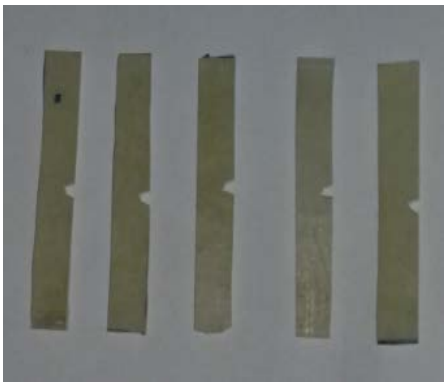
Clay Specimens



Tensile specimen

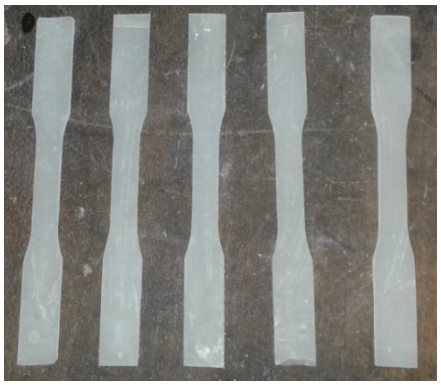


Flexural specimen

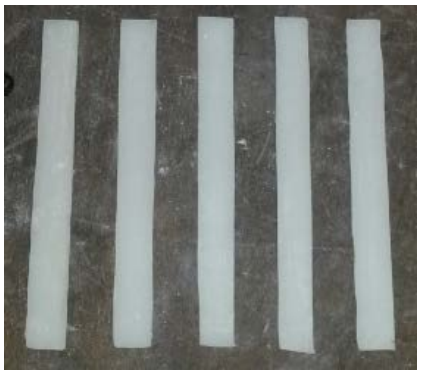


Impact specimen

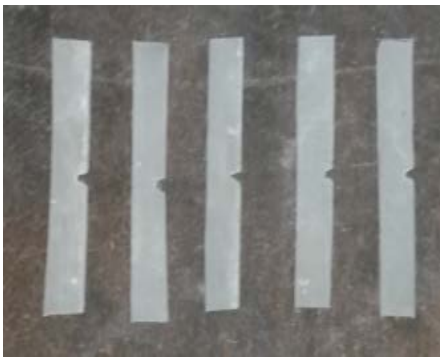
Glass Specimens



Tensile specimen



Flexural specimen

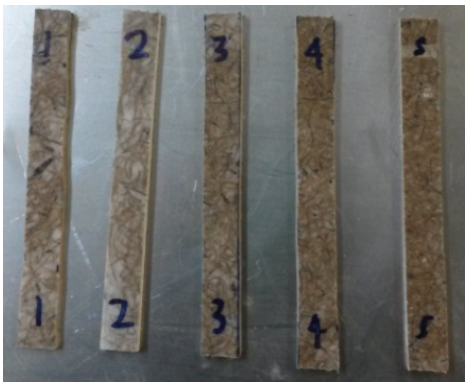


Impact specimen

Epoxy-Coir Fibre-Glass



Tensile specimen



Flexural specimen



Impact specimen

Epoxy-Coir Fibre-Clay



Tensile specimen

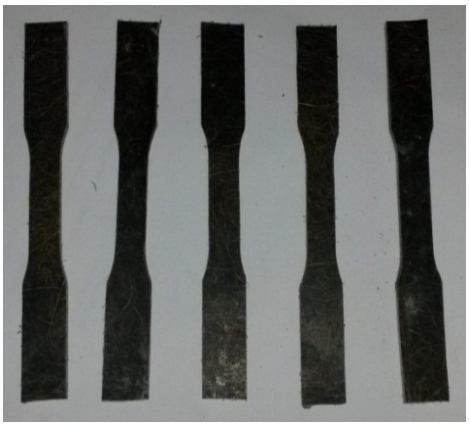


Flexural specimen

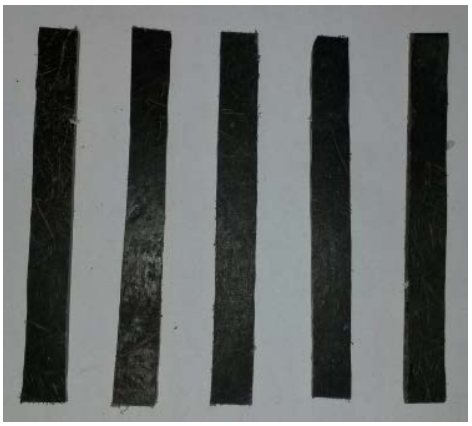


Impact specimen

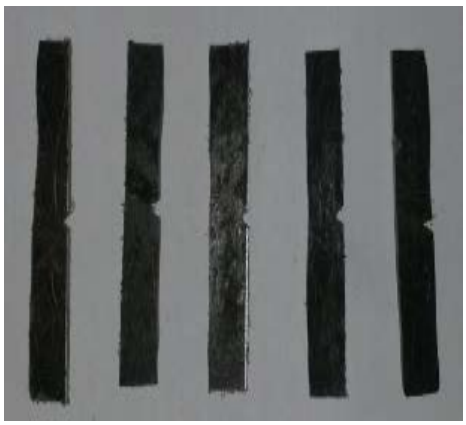
Epoxy-Coir Fibre-CNT



Tensile specimen



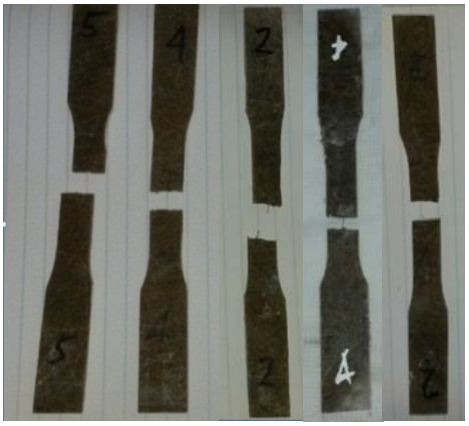
Flexural specimen



Impact specimen

Appendix B – Sample fractured specimens

Epoxy Coir Specimens



Tensile specimen

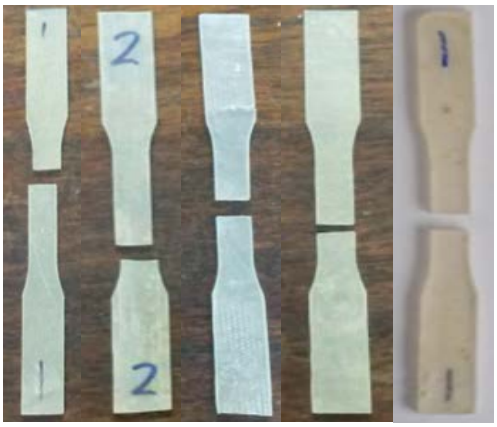


Flexural specimen

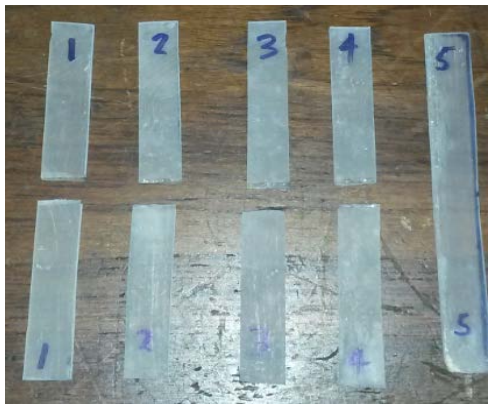


Impact specimen

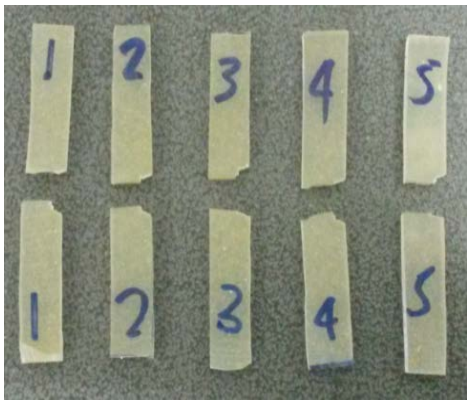
Clay Specimens



Tensile specimen

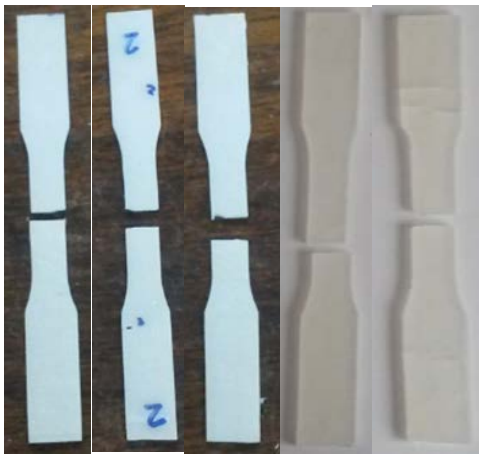


Flexural specimen

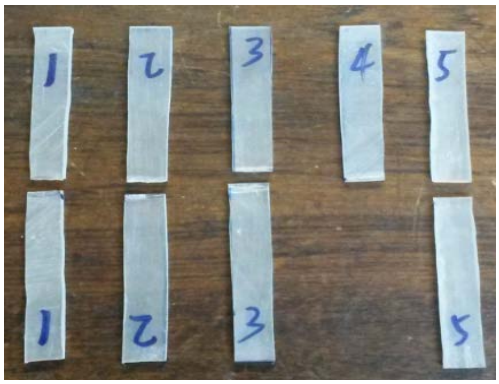


Impact specimen

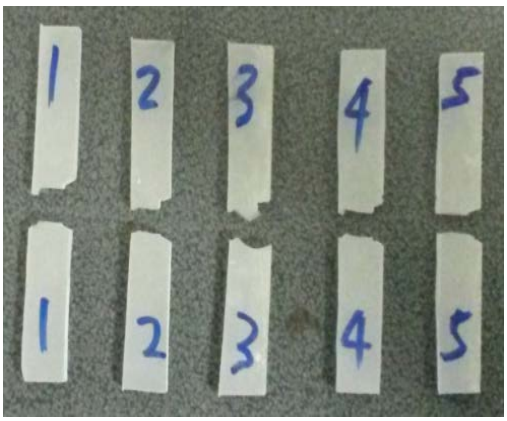
Glass Specimens



Tensile specimen



Flexural specimen

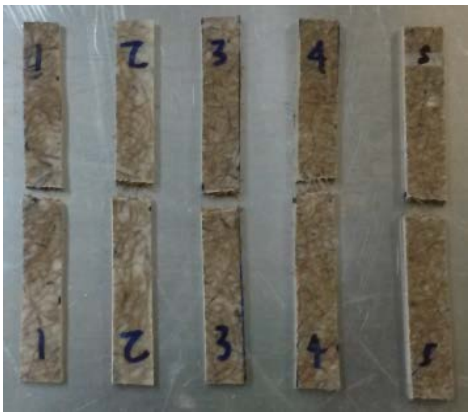


Impact specimen

Epoxy-Coir Fibre-Glass



Tensile specimen



Flexural specimen



Impact specimen

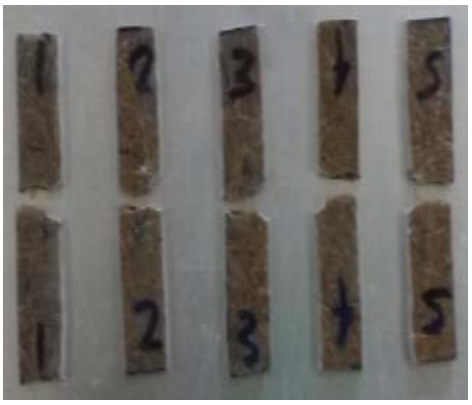
Epoxy-Coir Fibre-Clay



Tensile specimen

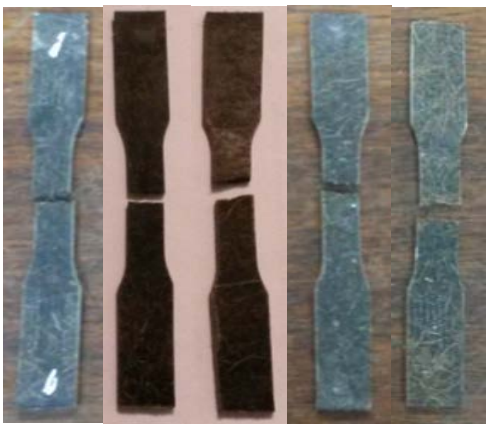


Flexural specimen

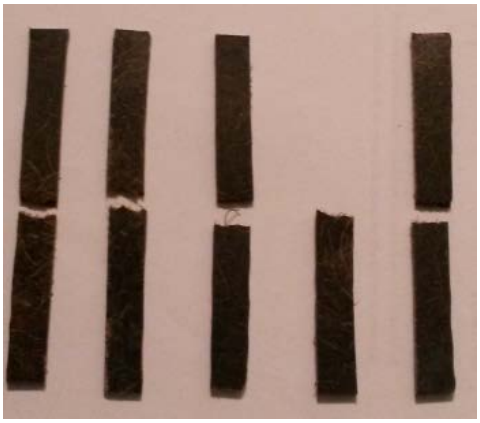


Impact specimen

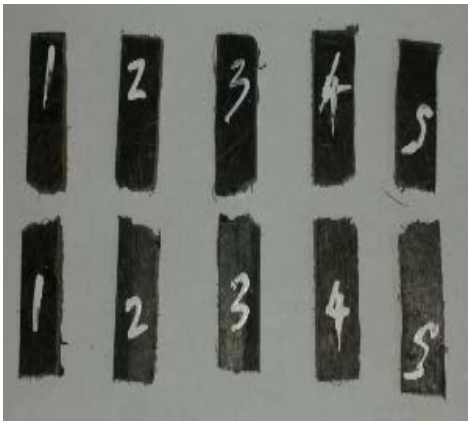
Epoxy-Coir Fibre-CNT



Tensile specimen



Flexural specimen



Impact specimen

Appendix C – Results of mechanical testing

Summary of specimen results

	Tensile Strength (MPa)	Elastic/ Youngs Modulus (GPa)	Flexural Strength (MPa)	Flexural Modulus (MPa)	Fracture Toughness (MPa√m)
Plain Epoxy					
Specimen 1	21.92	0.45	39.13	188.26	0.00047
Specimen 2	19.43	0.41	37.48	190.89	0.00055
Specimen 3	21.88	0.48	38.08	187.48	0.00043
Specimen 4	20.58	0.46	38.12	192.19	0.00059
Specimen 5	18.82	0.48	39.19	190.08	0.00047
Average	20.53	0.46	38.40	189.78	0.00050
Standard Deviation	1.26	0.03	0.66	1.71	0.00
Epoxy-7% Coir Composite					
Specimen 1	23.22	0.54	40.09	238.15	0.00078
Specimen 2	23.71	0.57	37.10	279.63	0.00059
Specimen 3	22.19	0.55	38.16	277.15	0.00078
Specimen 4	24.40	0.57	42.42	275.65	0.00078
Specimen 5	22.28	0.56	39.06	251.22	0.00078
Average	23.16	0.56	39.37	264.36	0.00074
Standard Deviation	0.85	0.01	1.82	16.64	0.00
Epoxy-10% Coir Composite					
Specimen 1	25.97	0.56	43.70	284.40	0.00090
Specimen 2	23.07	0.54	46.27	285.54	0.00078
Specimen 3	22.45	0.60	48.88	288.82	0.00066
Specimen 4	26.46	0.63	43.85	282.34	0.00074
Specimen 5	25.25	0.58	44.22	282.52	0.00078
Average	24.64	0.58	45.38	284.72	0.00077
Standard Deviation	1.60	0.03	1.98	2.37	0.00
Epoxy-15% Coir Composite					
Specimen 1	27.99	0.65	55.97	285.40	0.00086
Specimen 2	27.37	0.68	52.36	286.72	0.00078
Specimen 3	26.91	0.71	56.22	287.27	0.00090
Specimen 4	26.65	0.65	51.65	288.44	0.00074
Specimen 5	28.69	0.72	52.50	290.45	0.00078
Average	27.52	0.68	53.74	287.65	0.00081
Standard Deviation	0.74	0.03	1.95	1.70	0.00

Epoxy-20% Coir Composite					
Specimen 1	24.15	0.58	47.61	290.89	0.00078
Specimen 2	24.73	0.60	51.80	292.27	0.00074
Specimen 3	22.60	0.62	53.66	299.59	0.00078
Specimen 4	22.79	0.55	54.59	292.25	0.00082
Specimen 5	23.52	0.60	51.25	293.84	0.00070
Average	23.56	0.59	51.78	293.77	0.00077
Standard Deviation	0.80	0.03	2.41	3.06	0.00
Epoxy-0.1% Glass composite					
Specimen 1	28.01	0.66	45.64	271.48	0.00064
Specimen 2	27.30	0.62	47.31	273.50	0.00073
Specimen 3	28.29	0.66	45.80	275.46	0.00062
Specimen 4	27.90	0.60	47.39	277.48	0.00073
Specimen 5	28.31	0.60	45.81	273.48	0.00064
Average	27.96	0.63	46.39	274.28	0.00067
Standard Deviation	0.37	0.03	0.78	2.04	0.00
Epoxy-0.5% Glass composite					
Specimen 1	29.16	0.69	53.49	298.48	0.00088
Specimen 2	29.94	0.68	51.01	295.72	0.00073
Specimen 3	29.73	0.71	52.72	299.12	0.00076
Specimen 4	29.42	0.73	54.86	302.18	0.00088
Specimen 5	28.55	0.81	53.05	298.18	0.00076
Average	29.36	0.72	53.03	298.74	0.00080
Standard Deviation	0.48	0.05	1.25	2.07	0.00
Epoxy-2% Glass composite					
Specimen 1	28.57	0.70	47.34	302.16	0.00079
Specimen 2	27.45	0.65	48.46	305.49	0.00073
Specimen 3	28.12	0.73	47.85	305.32	0.00082
Specimen 4	28.92	0.69	47.76	302.05	0.00088
Specimen 5	28.31	0.70	49.58	306.85	0.00073
Average	28.28	0.70	48.20	304.37	0.00079
Standard Deviation	0.49	0.03	0.78	1.93	0.00
Epoxy-0.1% Clay composite					
Specimen 1	25.83	0.64	51.41	237.57	0.00044
Specimen 2	24.88	0.67	51.98	240.87	0.00044
Specimen 3	26.94	0.56	53.38	239.36	0.00062
Specimen 4	26.08	0.58	54.88	235.18	0.00059
Specimen 5	27.05	0.56	52.79	237.48	0.00059
Average	26.16	0.60	52.89	238.09	0.00053
Standard Deviation	0.79	0.05	1.20	1.92	0.00

Epoxy-0.5% Clay composite					
Specimen 1	29.29	0.62	57.29	279.32	0.00059
Specimen 2	28.43	0.58	59.78	283.81	0.00073
Specimen 3	29.52	0.66	61.78	282.42	0.00076
Specimen 4	28.53	0.68	61.07	283.02	0.00059
Specimen 5	29.10	0.70	62.08	280.48	0.00059
Average	28.97	0.65	60.40	281.81	0.00065
Standard Deviation	0.43	0.04	1.75	1.66	0.00
Epoxy-2% Clay composite					
Specimen 1	26.58	0.77	55.07	284.86	0.00050
Specimen 2	27.42	0.79	52.87	286.39	0.00044
Specimen 3	27.34	0.71	56.63	285.54	0.00044
Specimen 4	27.83	0.81	52.14	279.48	0.00044
Specimen 5	27.18	0.77	53.66	286.44	0.00044
Average	27.27	0.77	54.07	284.54	0.00045
Standard Deviation	0.41	0.03	1.61	2.60	0.00
Hybrid					
Hybrid-0.1% Clay composite					
Specimen 1	32.47	0.65	56.57	304.76	0.00098
Specimen 2	29.39	0.60	51.86	305.26	0.00098
Specimen 3	31.72	0.68	52.26	304.82	0.00098
Specimen 4	30.94	0.68	51.18	303.30	0.00086
Specimen 5	30.27	0.67	54.54	304.78	0.00117
Average	30.96	0.65	53.28	304.58	0.00099
Standard Deviation	1.08	0.03	1.99	0.67	0.00
Hybrid-0.5% Clay composite					
Specimen 1	31.45	0.80	65.03	339.58	0.00078
Specimen 2	33.19	0.78	66.31	334.52	0.00086
Specimen 3	32.44	0.73	64.58	339.41	0.00078
Specimen 4	31.85	0.78	69.30	337.48	0.00086
Specimen 5	32.23	0.77	64.67	335.35	0.00090
Average	32.23	0.77	65.98	337.27	0.00084
Standard Deviation	0.59	0.02	1.77	2.06	0.00
Hybrid-2% Clay composite					
Specimen 1	32.91	0.91	67.76	347.25	0.00078
Specimen 2	33.95	0.80	67.68	338.95	0.00070
Specimen 3	35.27	0.89	69.61	356.15	0.00074
Specimen 4	34.78	0.90	71.02	338.67	0.00078
Specimen 5	33.73	0.85	66.44	362.58	0.00066
Average	34.13	0.87	68.50	348.72	0.00073
Standard Deviation	0.83	0.04	1.62	9.44	0.00

Hybrid-4% Clay composite					
Specimen 1	32.58	0.98	71.82	372.26	0.00059
Specimen 2	35.75	0.91	76.98	368.58	0.00059
Specimen 3	34.17	1.00	74.84	379.75	0.00059
Specimen 4	34.53	0.95	75.42	375.29	0.00059
Specimen 5	34.47	1.01	73.67	381.48	0.00078
Average	34.30	0.97	74.55	375.47	0.00063
Standard Deviation	1.02	0.04	1.73	4.74	0.00
Hybrid-5% Clay composite					
Specimen 1	28.21	0.98	66.10	388.54	0.00043
Specimen 2	29.54	1.01	68.86	385.78	0.00059
Specimen 3	28.48	1.10	63.94	382.48	0.00059
Specimen 4	28.34	0.97	67.16	387.48	0.00047
Specimen 5	29.23	1.00	62.17	389.29	0.00043
Average	28.76	1.01	65.64	386.71	0.00050
Standard Deviation	0.53	0.04	2.36	2.42	0.00
Hybrid-6% Clay composite					
Specimen 1	22.71	0.93	65.04	395.67	0.00043
Specimen 2	23.38	0.92	59.42	389.48	0.00039
Specimen 3	25.27	1.03	60.76	397.35	0.00039
Specimen 4	22.87	0.92	66.58	394.84	0.00039
Specimen 5	23.68	0.97	62.80	395.28	0.00047
Average	23.58	0.95	62.92	394.52	0.00041
Standard Deviation	0.91	0.04	2.64	2.66	0.00
Hybrid-0.1% Glass composite					
Specimen 1	31.29	0.68	51.69	298.59	0.00078
Specimen 2	33.60	0.71	52.87	297.35	0.00086
Specimen 3	31.54	0.71	46.86	297.87	0.00098
Specimen 4	33.12	0.81	44.97	299.87	0.00105
Specimen 5	32.68	0.73	48.60	296.15	0.00098
Average	32.44	0.73	49.00	297.97	0.00093
Standard Deviation	0.89	0.04	2.94	1.24	0.00
Hybrid-0.5% Glass composite					
Specimen 1	35.87	0.81	55.21	328.72	0.00082
Specimen 2	32.61	0.89	60.36	332.48	0.00078
Specimen 3	33.48	0.79	57.69	329.81	0.00086
Specimen 4	32.19	0.72	60.74	332.48	0.00078
Specimen 5	33.22	0.65	59.68	330.48	0.00078
Average	33.47	0.77	58.74	330.79	0.00080
Standard Deviation	1.28	0.08	2.05	1.49	0.00

Hybrid-2% Glass composite					
Specimen 1	33.79	0.90	67.31	342.48	0.00078
Specimen 2	35.85	0.87	61.59	343.47	0.00086
Specimen 3	36.06	0.89	66.66	340.15	0.00078
Specimen 4	35.47	0.92	65.57	344.76	0.00090
Specimen 5	34.48	0.85	64.24	343.78	0.00078
Average	35.13	0.89	65.08	342.93	0.00082
Standard Deviation	0.86	0.02	2.03	1.57	0.00
Hybrid-4% Glass composite					
Specimen 1	35.79	1.08	64.77	347.48	0.00090
Specimen 2	36.49	1.03	63.10	346.47	0.00078
Specimen 3	34.39	1.03	68.20	344.15	0.00098
Specimen 4	35.32	1.05	67.16	343.71	0.00086
Specimen 5	36.38	0.99	63.85	346.78	0.00078
Average	35.67	1.04	65.41	345.72	0.00086
Standard Deviation	0.77	0.03	1.95	1.50	0.00
Hybrid-8% Glass composite					
Specimen 1	39.84	1.09	73.01	378.79	0.00078
Specimen 2	38.58	1.11	77.72	380.58	0.00070
Specimen 3	37.72	1.00	76.39	383.58	0.00078
Specimen 4	39.03	1.03	79.32	384.75	0.00070
Specimen 5	37.78	1.19	75.50	384.87	0.00066
Average	38.59	1.08	76.39	382.51	0.00073
Standard Deviation	0.80	0.07	2.12	2.42	0.00
Hybrid-12% Glass composite					
Specimen 1	30.48	0.86	70.28	374.69	0.00059
Specimen 2	31.97	0.91	72.31	373.58	0.00063
Specimen 3	33.72	0.86	74.43	370.78	0.00059
Specimen 4	31.59	0.81	70.72	373.74	0.00059
Specimen 5	32.81	0.80	74.61	375.88	0.00055
Average	32.11	0.85	72.47	373.73	0.00059
Standard Deviation	1.10	0.04	1.81	1.69	0.00
Hybrid-0.1% CNT composite					
Specimen 1	28.32	1.43	68.70	287.52	0.00090
Specimen 2	28.99	1.04	62.69	311.45	0.00074
Specimen 3	28.98	1.32	65.26	318.69	0.00078
Specimen 4	29.68	0.81	67.18	328.47	0.00086
Specimen 5	30.22	0.89	65.50	319.65	0.00078
Average	29.24	1.10	65.86	313.16	0.00081
Standard Deviation	0.66	0.24	2.02	13.91	0.00

Hybrid-0.5% CNT composite					
Specimen 1	33.42	1.41	72.87	358.32	0.00105
Specimen 2	30.76	1.04	76.98	365.26	0.00098
Specimen 3	32.84	1.43	77.62	364.82	0.00078
Specimen 4	31.17	1.02	73.73	358.30	0.00098
Specimen 5	32.38	0.97	72.99	364.78	0.00098
Average	32.12	1.17	74.84	362.30	0.00095
Standard Deviation	1.00	0.20	2.04	3.26	0.00
Hybrid-1.5% CNT composite					
Specimen 1	42.46	1.27	84.14	385.48	0.00109
Specimen 2	39.37	1.21	82.66	387.83	0.00109
Specimen 3	39.64	1.13	82.36	389.87	0.00105
Specimen 4	41.22	1.33	84.25	385.18	0.00102
Specimen 5	41.96	1.27	83.10	387.87	0.00105
Average	40.93	1.24	83.30	387.25	0.00106
Standard Deviation	1.23	0.07	0.77	1.73	0.00
Hybrid-2% CNT composite					
Specimen 1	39.83	1.34	80.15	378.49	0.00098
Specimen 2	36.98	1.30	79.86	372.46	0.00090
Specimen 3	35.68	1.36	79.48	379.77	0.00082
Specimen 4	37.27	1.35	77.98	370.05	0.00102
Specimen 5	36.55	1.31	80.27	375.76	0.00090
Average	37.26	1.33	79.55	375.31	0.00092
Standard Deviation	1.39	0.02	0.83	3.63	0.00